Pickering Emulsions for the emulsion stability and skin delivery of flavonoids using different oil types

Elisabeth Alice Dufton

Submitted in accordance with the requirements for the degree of Doctor of Philosophy.

The University of Leeds, School of Design.

December 2018

The candidate confirms that the work submitted is her own and that appropriate credit has been given where reference has been made to the work of others.

Acknowledgements

Greatest thanks to the support from the students and staff in the School of Design, Blackburn research group and Rayner research group at the University of Leeds.

I am indebted to the fantastic help and support from the Food Colloids Group from the School of Food and Nutrition at the University of Leeds; notebly the knowledgeable guidance from Prof. Brent Murray and the kindest help from Dr. Didem Sanver. Without them and the departmental support this research would not have been possible.

Special thanks to my supervisors Dr. Richard Blackburn, Prof. Chris Carr and lab technicians in the School of Design and their trust in my abilities and to be able to take on this research in a unique direction and providing new skills for the department.

This research would not have been possible without the support from the Clothworkers' Foundation, and I am forever grateful. Their interest and belief in my research from the beginning was wonderful encouragement.

PhD research inevitably has ups and downs; my family, friends and partner have been there for me in encouragement, emotional support and guidance - keeping my chin up when I needed it and always making me smile. Mark, Anita, Helen, Daniel, Xenia and Chelsea, thank you.

Abstract

Introduction

A Pickering emulsion (PE) is a particle stabilised emulsion. Due to the amphiphilic structure of some flavonoids, they can form good stable PE. The use of Pickering emulsions serve as a potential useful approach for improving the formulation solubility of flavonoids, as well as reducing skin irritancy for topical formulations by removing emulsifiers from cosmetic formulations. This research in this study is the first (to the authors knowledge) to investigate the skin release kinetics and permeation of the flavonoids incorporated into a Pickering emulsion. Changes to the barrier properties of porcine *Stratum corneum* (SC) *in vivo* were also evaluated by investigating lipid morphology changes of the stratum corneum *post hoc* after the application of the Pickering emulsion and skin permeation studies.

Oil in water (O/W) Pickering emulsions were made with three flavonoids differing in structure and physiochemical properties; rutin, isoquercetin and quercetin, each with 20 % w/w of oil. Three types of oil were used to make the Pickering emulsions; paraffin (hydrocarbon oil), almond and coconut (vegetable). Pickering emulsion were made with a jet homogeniser. PEs were evaluated for emulsion structure. Skin permeation release kinetics were established using split thickness porcine skin (intact stratum corneum and epidermis) in a Franz diffusion set up over 24 hours using an infinite dose technique. They were benchmarked against comparison controls, using mixtures of oil and flavonoid (omitting high pressure homogenisation), which did not form PEs. Flavonoids permeating through the skin membrane were identified by Reverse-Phase High Performance Liquid Chromatography (RP-HPLC). Various mathematical models from literature were used to describe the release kinetics of the flavonoids based on the permeation data. The morphology of the lipid chain packing in the SC was evaluated using Fourier Transfer Infrared (FT-IR) spectroscopy and subsequent analysis using a *Gaussian* curve fitting algorithm.

Results

Flavonoids were found to aggregate at the oil/water interface to form Pickering emulsions. From visual stability observations (low-high phase separation and creaming); rutin > isoquercetin > quercetin, and for oil types this order paraffin > almond ≥ coconut oil. High shear homogenisation is essential for Pickering emulsion formation, and PEs do not form spontaneously. Quercetin did not form a PE with coconut oil.

FT-IR results indicated a change in lipid morphology from the CH_2 symmetric stretching and the CH_2 scissoring bandwidths. A greater disruption in the extracellular matrix lipid packing was observed from the flavonoid suspensions and oil mixtures more than the Pickering emulsions, indicating that when the flavonoids are coating the oil in a Pickering emulsion, it reduces oil exposure to the SC lipids. In addition, a change in lipid morphology was seen between flavonoids; with the effect being in the order rutin > isoquercetin > quercetin.

For skin permeation assays, after 7 hours there was no difference between the amount of flavonoids released from the epidermis, regardless of flavonoid structure. At 24 hours there was significantly more rutin delivered from paraffin and almond oil suspension (control) than the corresponding Pickering Emulsion ($P < 0.05$) and significantly more isoquercetin was delivered from vegetable oils suspensions (control) than the corresponding Pickering Emulsion ($P < 0.05$). Quercetin from PEs was not released from the membrane, only from the suspension (control). When flavonoids are aggregated at the O/W interface in a PE it changes the release kinetics and SC/epidermal penetration due to flavonoids being held at the interface before emulsion collapse.From the % dose applied, flavonoids were delivered in the order isoquercetin > rutin for the PEs and quercetin > isoquercetin > rutin for non-emulsions. This follows the predicted permeability behaviour due to the physiochemical properties of those specific flavonoids.

Contents

Abbreviations

ATR-FT-IR: Attenuated Transform Reflectance Fourier Transform Infrared

CSLM – Confocal Scanning Laser Microscope

ECM - Extracellular matrix

HEX - Hexagonal

LIQ - Liquid Crystal

$LogP_{oct/aq}$: partition coefficient between octanol and water

OA - Oleic acid

OR - Orthorhombic

O/W : oil in water

PE : Pickering Emulsions

RP-HPLC : Reverse phase high performance liquid chromatography.

SC: Stratum corneum

Chapter 1 Literature Review

1.1 Introduction

Personal care skincare products are a complex mixture of ingredients, which need to be optimised for stability, solubility, viscosity, preservation, colour, smell, texture, emolliency, before any “functional” actives are added. The formulation as a whole will either hinder or promote skin delivery of active ingredients that have specific effects, *e.g.* a flavonoid compound can offer antioxidant and anti-ageing performance. Designing a formulation that will achieve optimal delivery of an active to the skin is highly topical in current cosmetic science research. A prerequisite to achieving this goal is obtaining knowledge of both the active compound that is intended for skin delivery and also the chemical interaction of the formula upon said delivery. Previous studies have shown that even the introduction of one additional ingredient, can impede the penetration of active ingredients through the skin (2). Findings such as this demonstrate how important it is to understand the chemistry of the entire formulation and interactions of all the components. One ingredient could make the difference to a product “working”, or not.

As well as enhancing the permeation of actives through the skin the formulation must also be stable and aesthetically pleasing to the end users. Wiechers *et al.* (2012) defined four important aspects that an optimal formulation should hence (3):

(i) contain a high enough concentration of the active to provide demonstrable therapeutic benefits;

(ii) solubilise the active to facilitate penetration;

(iii) contain penetration enhancers;

(iv) possess cosmetic product qualities such as smell, colour, and stability.

Another formulation property to consider has been highlighted by Abbot, who remarks that it is futile to deliver an active solubilised in water to the skin, as an inherent property of the skin is that it is water repellent, and therefore it is imperative to characterise a solute's aqueous solubility (4). Within the literature it is widely debated how best to deliver an active from a cosmetic (5, 6).

The rate limiting step to skin permeation is the stratum corneum (SC). Penetrating molecules have to overcome the SC lipid matrix before permeating into deeper or targeted skin layers.

1.2 Human Skin Structure

The skin is the largest organ of the human body and is highly exposed to environmental damages. It is composed of 3 main layers **Figure 1-1**; the hypodermis (subcutaneous fat), followed by the dermis, epidermis (including *stratum corneum*) (7).

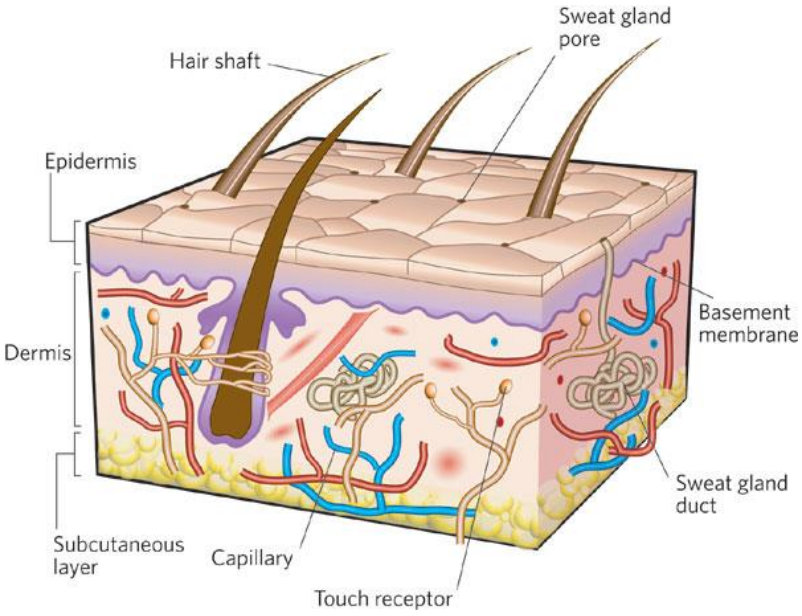

Figure 1-1 Structure of human skin, taken from MacNeil (2007) (8).

The viable dermis provides skin integrity with the extracellular matrix (ECM). The dermis also has appendages such as hair follicles and sebaceous glands; contains an array of proteins, nerve cells, lymph cells and also blood capillaries are present which provide nutrients and oxygen to the skin **(Figure 1-1**).

1.2.1 Viable Epidermis and the Stratum Corneum

The epidermis itself comprised of 4-5 layers (depending on anatomical site) consisting of: stratum basale (SB), stratum spinosum (SS), stratum granulosum (SG), stratum lucidum (on palms and soles of feet) and finally the stratum corneum (SC) – topmost layer of the skin (7), portrayed in **Figure 1-2**.

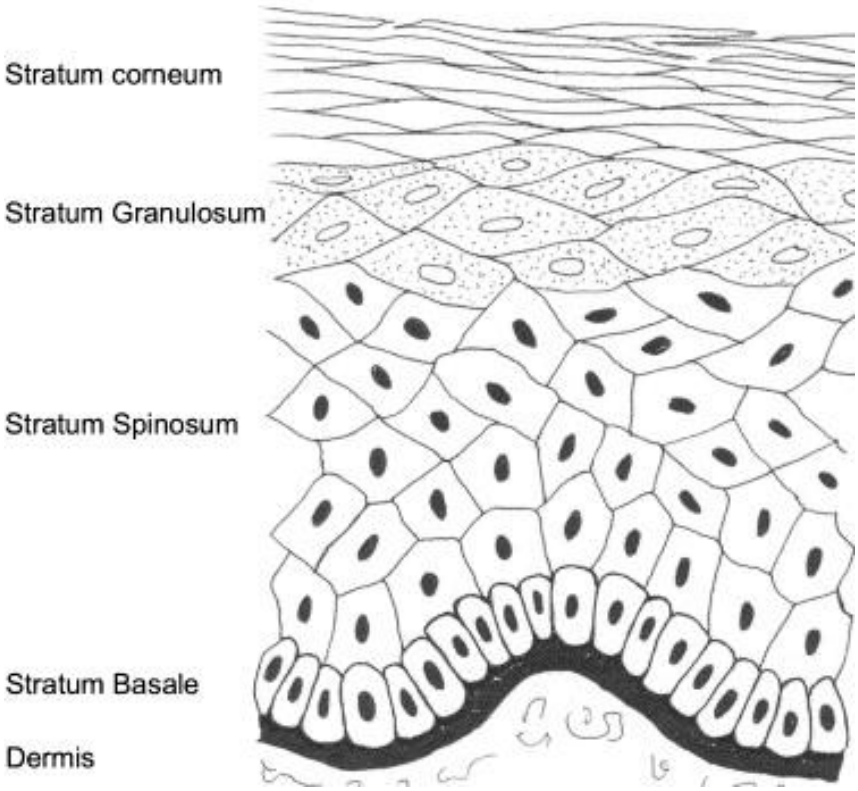

Figure 1-2 Detailed structure of the epidermis and its 4 layers (9).

The stratum basale is where keratinocyte cells are produced, before migrating up through the other overlayers of the epidermis. This layer is typically one cell layer thick and contains other cells such as melanocytes, which carry the pigment melanin, and also Langerhans cells, which fight infection. The next layer, the stratum spinosum is where keratinisation of the skin cells starts to take place (10).

The *Stratum corneum* is the protection barrier of the human body and main barrier to overcome for effective chemical penetration into the skin. The main constituents of the SC are typically 75-80 % protein, 5-15 % lipids and 5 -10 % unidentified material (dry weight) (11). The SC is comprised of 15-20 layers of flattened, dead corneocytes layered on top of one another and are best described in the popular term as a “brick and mortar” structure: the keratinocytes are the bricks and the mortar in a rich lipid matrix cementing the keratinocytes together. The corneocytes are arranged

approximately 75 nm apart and the corneocytes are also believed to be arranged in clusters of 12 cells (12). Long chained omega-hydroxyceramides are anchored to the corneocyte envelopes and these ceramides are responsible for the alignment and conformational order of the extracellular lipids (12).

This lipid matrix contains essential lipids such as cholesterol, ceramides and phospholipids, which help to maintain skin hydration and barrier function (7). As the SC is mainly composed of water-insoluble proteins and lipids, it is essentially water repellent. The lipid matrix is thought to be the main penetration pathway and the lipids in the stratum corneum are present in crystalline, gel and liquid crystalline forms at physiological temperature (11).

1.2.2 Skin Lipids

Ceramides are the main constituent of the *Stratum corneum* lipids, forming the extracellular matrix (ECM). Ceramides are long chained fatty acids (C_{22} – C_{30}) with small head groups containing at least two hydroxyl groups and an amide link (13). The amide linkage is to the amino group of a di- or tri-hydroxy sphingoid base (7). The nomenclature of the ceramides is based on their structural components and assignment of the structure is by letters. This nomenclature was developed by Motta *et al.* (1993), which superseded the previous structural identification of ceramides based on their mobility in thin layer chromatography (14, 15). Firstly, the sphingoid bases: *S* = sphingosine*, P* = phytosphingosine, *H* = 6-hydroxysphingosine. Fatty acids bound to the sphingoid base are identified by their hydroxylation; *N* = no hydroxylation, *O* = omega hydroxylated fatty acid and *A* – alpha-hydroxylated fatty acid. Lastly, the letter *E* represents the esterification of long chain fatty acids with unsaturated fatty acids, *e.g.* linoleic acid, which are attributed to the long chain *ω*-acyl ceramides.

There are currently fifteen ceramides identified in the human extracellular matrix, with the fatty acid portions of the ceramides ranging from C_{24}-C_{26} and the sphingoid base

ranging from C_{18}-C_{22} (16). **Figure 1-3** shows the ceramides found in porcine epidermis along with current nomenclature (7, 15).

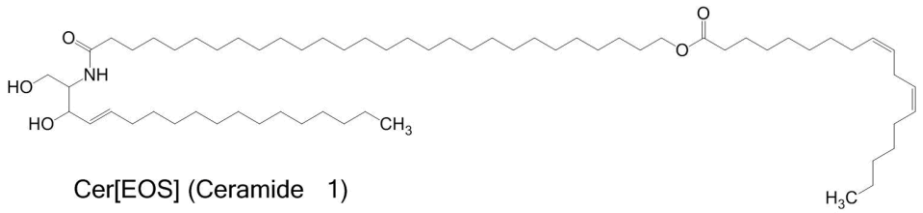

Cer[EOS] (Ceramide 1)

Cer[NS] (Ceramide 2)

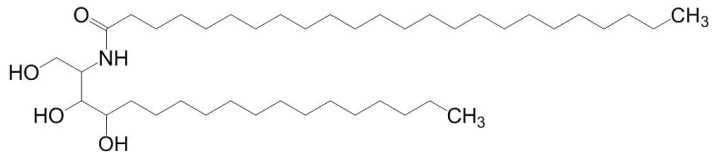

Cer[NP] (Ceramide 3)

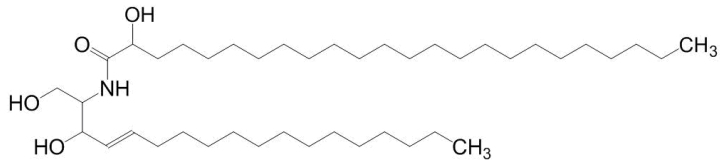

Cer[AS] (Ceramide 5)

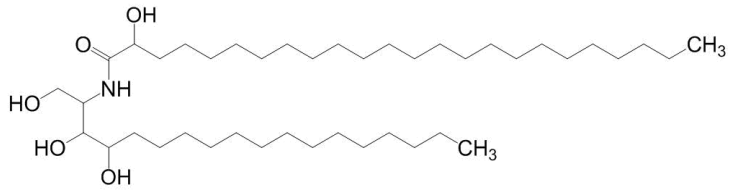

Cer[AP] (Ceramide 6)

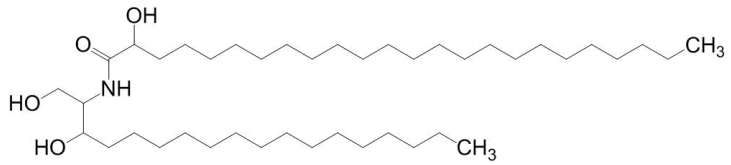

Cer[AdS]

Figure 1-3 Chemical structure of ceramides identified in porcine skin (7) with chemical nomenclature.

Ceramides make up ca. 20 % of the total lipid content of the *Stratum corneum* of pig ears, of which 0.02 % of ceramides are glucosylceramides; the main component of the latter being acylglucosylceramides esterified with linoleic acid. (17). Linoleic acid has been demonstrated as being an essential component for the water barrier properties of the *stratum corneum* (18). In human and porcine ear epidermis, long chain glycosphyingolipids and ceramides (C_{24}-C_{30}) and 2-hydroxy fatty acids with a melting point >75 ºC improve resistance in temperature change, UV exposure and oxidation of the SC domains and still provide a stable lipid phase (17). From the basement membrane of the epidermis to the *stratum corneum*, the chain length of the lipids increase, with chain lengths >C_{24} (19). Lipids are formed in the lamellar bodies in the spinous cells and continue to fill with lipids as they migrate into the granular layer of the epidermis (13).

Ceramides with chain lengths of $C_{30\text{-}34}$ and fatty acids with $C_{14\text{-}22}$ in length are covalently bound to the corneocyte envelope, and are thought to be responsible for the stability and tight lattice packing of the extracellular lipids (19).

The lipid lamella in the extracellular matrix is arranged in two alternating phases; long periodic phase (LPP) with a length of 13 nm and a short periodic phase (SPP) with a period length of 6 nm (7). When skin is hydrated, the SPP can expand from 5.8 nm to 6.8 nm (20). However, this was observed in mouse SC, therefore could be different for human and porcine skin. It is still debated and investigated in literature as to role specific ceramides play in skin permeation. Ceramide-I (CerEOS), the least polar ceramide, is unique to epidermal tissue (13).

There are strong interactions between the lipids attributed for the skin barrier function. There exists strong polar interactions (hydrogen bonds) between the polar head groups and non-polar bonds (Van der Waals) between the acyl chains (21, 22). These bonds are also modified by the presence and ratio of lipid components (22).The most impermeable barrier comes from when there exists a higher ratio of neutral lipids than

sphingolipids (19). Paired with trans epidermal water loss can give an indication to the overall barrier properties of the skin (23). Changes in the shape of lipid conformation in the skin can be caused by environmental factors, such as chemical and temperature change, which can be detected by FT-Raman spectroscopy. (11). The *stratum corneum* ceramides and fatty acids are significantly reduced in harsher weather environments (winter compared to summer months) (24).

1.2.3 Water within the *stratum corneum*

Different types of water exist in the SC; bound and free. Bound water describes water molecules hydrogen bonded within the intercellular lipids at the polar regions (25) and is attributed to skin elasticity (26). Bonded water in the lipid matrix contributes approximately 33.3 % of the total (27) which accounts for the polar regions.

1.2.4 Skin Lipid Packing

The organisation of the lipids within the SC conform to an organised ordered orthorhombic (OR) or hexagonal (HX) structure and disordered in liquid crystal (LC) structure, **Figure 1-4 (a)**. In the orthorhombic structure, the aliphatic chains of the lipids are packed closed together in an all-*trans* orientation, creating a crystal lattice conformation. In the hexagonal structure the all-*trans* aliphatic chains are tilted in the crystal plane, and have increased spaces between lipid chains, whereas the aliphatic chains in the liquid crystal structure have no lateral packing and are in a disordered conformation, **Figure 1-4 (b)** (1). The orientation of these lipids in defined structures is important in maintaining an efficient barrier. The structure of these lipids and lateral packing has been extensively studied using several techniques; X-ray diffraction, Fourier Transform Infrared (FT-IR) spectroscopy, Differential Thermal Calorimetry (DSC), ^{2}H Nuclear Magnetic Resonance (NMR) spectroscopy and electron spectroscopy (1, 28).

Infrared spectroscopy is a non-invasive, simple technique able to provide information on the lipid conformation of the *stratum corneum*. In infrared spectroscopy, a molecule absorbs energy from an infrared light source and that molecule converts that energy into vibrational energy. An isolated molecule absorbs energy at a well-defined frequency (29); the exact frequency in which vibrational energy is released indicates the strength of the bonds of that molecule (30). In FT-IR analysis the spectral region of 4000 – 1450 cm^{-1} is known as the group frequency region where stretching vibrations of diatomic groups predominate, *e.g.* hydroxy O-H stretching, while the band region 1450 – 600 cm^{-1} is known as the fingerprint region as it is a complex combination of both stretching and bending vibrational patterns unique to individual molecules (30).

(a)

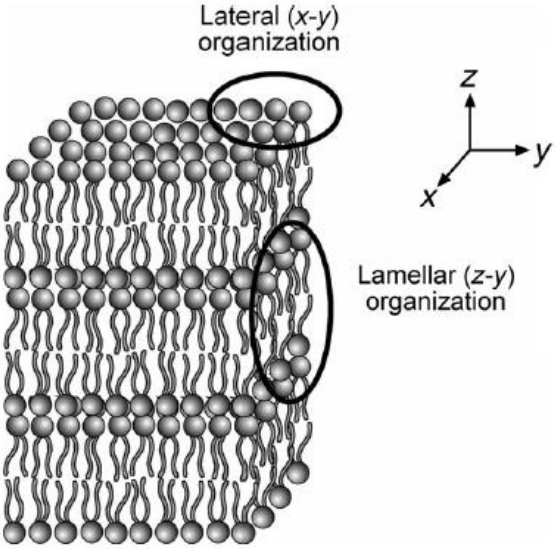

(b)

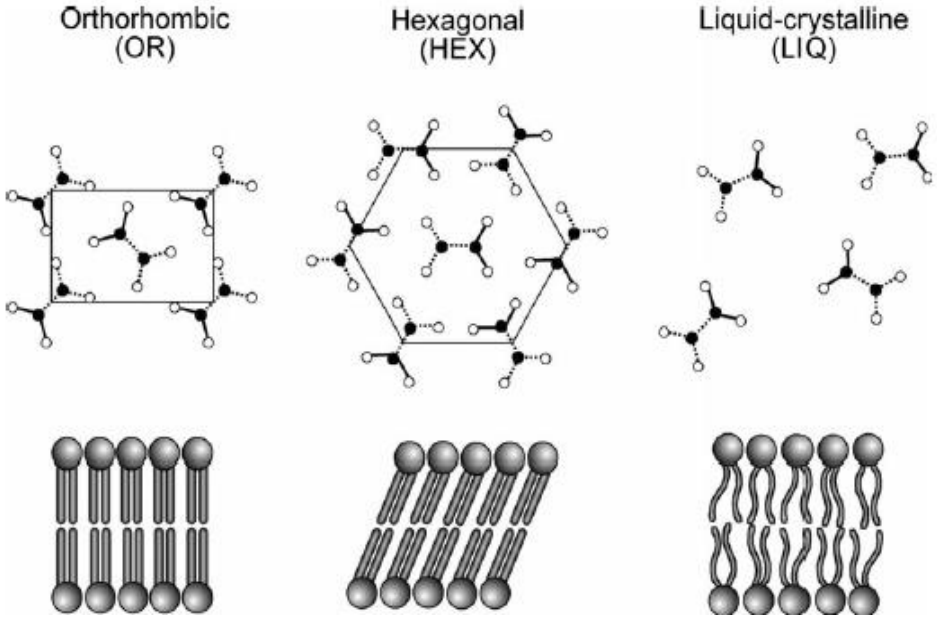

Figure 1-4 Lipid chain conformation in the extracellular matrix of the *stratum corneum*: (a) lateral packing and lamellar organisation, (b) chain conformation in an orthorhombic, hexagonal and liquid crystal conformation. Taken from Boncheva *et al.* 2008 (1)

IR spectroscopy data can be used to characterise the structure and lateral packing of these lipids. Boncheva *et al.* (2008) identified the lipid conformation and lateral packing by the bandwidth of the CH_2 symmetric stretching; increased rotations of the aliphatic chains in transition from OR⟶HX and in increasing disorder of the aliphatic chains in the transition from HX⟶LC conformation led to broadening of this band and shifted to a higher wavenumber (1).

The lipids exhibit an orthhombic structure at a skin temperature of 30 - 32 ºC (28). Phase transitions from OR-HEX-LIQ using Fourier Transform-Infrared Spectroscopy have been observed for lipid models in response to temperature increase (12, 31). The equimolar lipid mixtures form orthorhombic and hexagonal chain packing under physiological conditions (pH 5.5 and 30-35 ºC) and is greatly dependent on the hydration of the ceramides – a decrease in hydration results in a tightly packed orthorhombic phase. The lipids at the surface of the SC have medium barrier properties in the hexagonal conformation, however the lipid morphology becomes more orthorhombic in the deeper layers of the SC (28). At a depth of 4-8 µm (20 – 40 %) into the SC, the *trans*-chain conformation and lateral packing of the lipids are at a maximum and then decrease with increasing depth to the stratum granulosum layer (32)..

1.2.5 Damage to the skin

Free radicals and reactive oxygen species (ROS) are responsible for damage to the skin including skin cancer. The superoxide anion ($O_2^{-\bullet}$), peroxide, hydroxyl radical ($OH^{\bullet}$), hydroxyl ion, and singlet oxygen ($^1O_2$) are the most common ROS (32). Free radicals are highly reactive because they have an incomplete outer electron shell and therefore have an affinity to either donate or obtain electrons from another species in order to achieve greater stability. From within the cell $O_2^{-\bullet}$ and H_2O_2 are generated through natural metabolism when glucose is synthesised from adenosine triphosphate (ATP) (32). ROS can also be generated in the skin by external factors such as

cigarette smoke, pollution and ultra-violet radiation, the latter has been recognised as having the highest contributor to skin damage (33). UV radiation causes excitation of molecules and converts molecular oxygen into the superoxide anion, $O_2^{-\bullet}$ (34). The damage caused by UV radiation triggers inflammatory immune cells to release proteases and more ROS (35), thus the attack from ROS increased. Damage to the skin by ROS can be caused directly or indirectly by attacking DNA, proteins and lipids.

1.2.6 Protecting the skin with antioxidants

Natural antioxidant compounds have an important role to play in preventing skin damage. Antioxidants are a class or organic compounds that can quench these free radicals and thus prevent attack on biological macromolecules. The skin has naturally occurring antioxidants such as vitamin C, E and ubiquinone that are present to defend the biological macromolecules from the constant onslaught of reactive oxygen species and free radical attack. However, with increasing age, these naturally occurring molecules are depleted from the skin and therefore the defence to ROS attack is lowered.

It has been shown that topical antioxidants can help in the prevention from ROS attack on the skin. Synthetic antioxidants do exist, however plants provide a plentiful source of naturally occurring antioxidant compounds known as flavonoids. Flavonoids have potent antioxidant activity and a diet rich in fruit and vegetables sees these compounds being delivered to the human body.

1.3 Flavonoids

Plant extracts contain high levels of antioxidant phenolic compounds which have been linked to reducing the risk of heart diseases, cancer and skin disorders (32, 36-38). They can be classified based on their structure, with the majority being identified as "flavonoids". All flavonoids share a common structure of two 6-membered rings (A and B) joined by a central pyran ring (C) and are further differentiated based on the presence and position of additional hydroxyl, methyl and/or sugar moieties on the three rings, **Figure 1-5**

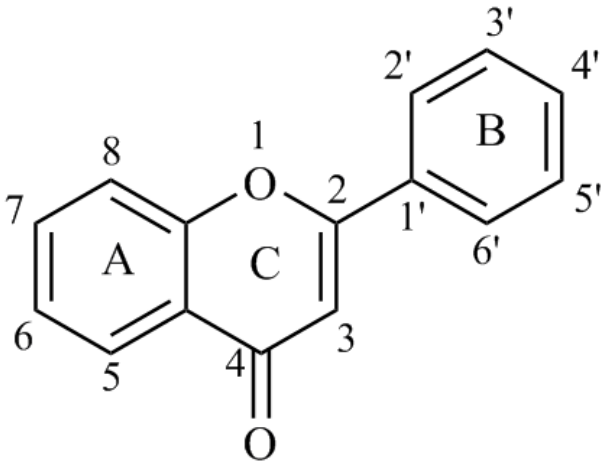

Figure 1-5 Basic structure of a flavonoid compound

Phenolic compounds have a multi-functional purpose in cosmetic products and can be regarded as an anti-ageing active with proven antioxidant, anti-collagenase, anti-elastase and anti-hyaluronidase properties (39)

The structure activity relationship of phenolic compounds has been widely studied (40-42). According to Vagánek *et al.* a compound should have the following features to be a good antioxidant: (i) a catechol (*ortho*-dihydroxy) group present on the B ring enabling electron delocalisation; (ii) a double bond between the C2=C3 conjugated to a carbonyl group on C4 in the C ring which allows for electron delocalisation from the B ring; and (iii) the presence of hydroxyl groups at the C3 and C5 providing hydrogen

bonds to the carbonyl group on C4 (42). These features are pictured in **Figure 1-6**. The activity of phenolics has been linked to the ease in which they can donate a hydrogen atom to neutralise the free radical (43). Glycosylation of the 3-OH greatly reduces the antioxidant activity of 3-hydroxyflavones (44) as it loses the ability to donate a hydrogen atom, which is a mechanism for quenching free-radicals or forming a hydrogen bond with the carbonyl at C4.

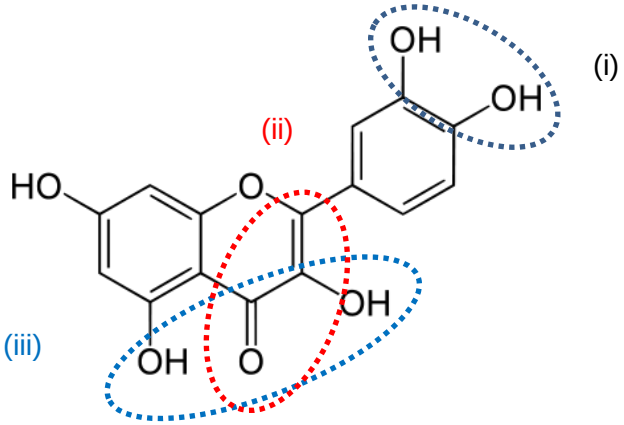

Figure 1-6 Quercetin, a 3-hydroxy flavonol. An example of a flavonoid with the three main features for a good antioxidant (i) a catechol moiety on the B ring, (ii) a double bond between C2 and C3 and a carbonyl at C4 and (iii) hydroxyl groups at the C3 and C5 positions.

The chemical structure is not alone responsible for the observed antioxidant activity of a compound. The medium in which the antioxidant is present (polar/non-polar) and pH can have an effect on the activity (44). If the pH of the medium in which the phenolic compound is in is higher than that of the first p*K*a of hydroxyl group, the antioxidant activity is lowered because that moiety has lost the ability to donate a hydrogen atom to quench the free radical. An example of this behaviour is *trans*-resveratrol in which the 4'hydroxy group has been identified as the most significant group in its antioxidant activity (45). *Trans*-resveratrol has 3 ionisation states and the 4'-OH is the most acidic. If the pH of the medium is higher than that of the first p*K*a (8.8) the activity of *trans*-resveratrol will be greatly reduced (45).

One of the most widely studied flavonoids are rutin and quercetin (46). Rutin is a glycoside of the flavonol quercetin with rutinose, quercetin-3-O-rutinoside. Rutin has many beneficial properties which make it a good active for personal care such as antioxidant activity and anti-inflammatory (46). Both rutin and isoquercetin are the most abundant glycosides of quercetin and can undergo enzymatic degradation into the aglycone quercetin within the intestinal tract (46) (47).

1.3.1 Flavonoids and skin permeation

The solubility and the partition coefficient of an active ingredient must be thoroughly understood in order to achieve effective percutaneous penetration, otherwise the active will preferentially stay in formulation and delivery into the skin will be ineffective.

Das and Kalita (2014) have recently conducted a study on the enhancement of percutaneous penetration of rutin. By creating a complex of rutin with phospholipids they demonstrated that the aqueous solubility and the hydrophilicity of rutin was increased, therefore facilitating an increase in skin penetration (48). Their argument for this behaviour was that rutin is very hydrophobic and to enhance skin delivery, it must be made more water soluble (hydrophilic).

In a flavonoid structure (section **1.3**) the hydroxyl groups can influence the overall hydrophilic nature of the molecule, and aromatic rings can similarly influence the hydrophobic nature and thus can be deemed amphiphilic molecules (49). Being both hydrophilic and hydrophobic in nature, some flavonoids, *e.g.* rutin, are reported to act as emulsion stabilisers resulting in aggregation at the oil/water interface, leading to the formation of Pickering emulsions (49). The pKa of the flavonoid will also influence the skin permeation.. Below the pKa, molecules will be protonated and least water soluble, above the pKa molecules will be ionised and water solubility increased (50).

1.3.2 Analysis of Flavonoids using Reverse Phase – High Performance Liquid Chromatography

Flavonoid compounds can be characterised and quantified using reverse phase high performance liquid chromatography (RP-HPLC) using an instrumental system based on a C-18 non-polar solid phase (stationary phase) and an aqueous phase (mobile phase). The elution programme for the mobile phase typically utilises a two-step gradient profile, starting with a high proportion of the polar component and gradually increasing the non-polar component. Typical solvents used are water (polar) and

acetonitrile (non-polar). The pH of the water is typically acidified to prevent the ionisation of phenolic compound. Through the use of known standards and developing an understanding of the structure/retention behaviour of the flavonoid compounds on a RP-HPLC column a detailed elution profile of mixtures of flavonoids can be established. It is known that phenolic compounds that contain hydroxyl groups that will form hydrogen bonds and interact with the mobile phase and will elute first in the polar mobile phase as they have a higher affinity for this phase. Likewise flavonoids with hydrophobic groups e.g. methyl or aromatic rings will prefer the non-polar stationary phase and elute slower. When detecting phenolic compounds by RP-HPLC, the aqueous phase is often acidified to be lower than the p*Ka* of the phenolic molecules; of which rutin, isoquercetin and quercetin p*Ka* are around 6 (51). This ensures protonation of the molecule and increases its polarity, which allows for clear flavonoid separation on the polar C-18 column.

1.4 Formula Ingredients

The following section outlines other ingredients that are used in personal care formulations which can alter the barrier properties of the *Stratum corneum*, therefore affecting the skin penetration of the chosen actives.

1.4.1 Permeation Enhancers

Permeation enhancers are chemicals that are added to a formulation for the purpose of facilitating the enhancement of an actives skin penetration by modification of the *Stratum corneum* (SC) lipids in the extracellular matrix (ECM) (28). This is done by the permeation enhancer disrupting the internal lipid packing of the ECM, either by fluidisation, disorganisation or extraction of the lipids and possibly by affecting the tight epidermal junction (28). Permeation enhancers work by affecting the interactions of the polar head groups and the non-polar alkyl chains of the ceramides in the lipid matrix (52).

The most common permeation enhancers used for lipid barrier disruption for topical formulations for percutaneous penetration of actives include; propylene glycol, ethoxydiglycol, fatty acids such as oleic acid, terpenes, azone, ethanol, dimethyl sulfoxide (DMSO), and surfactants (28). Oleic acid and propylene glycol have no restrictions on EU cosmetic directive, whereas ethoxydiglycol is restricted to 2.6 % *w*/w (53).

Penetration enhancing chemicals are the most favourable method of increasing the skin permeation of actives because they can be added to the formula relatively easily and these ingredients modify the skin barrier as soon as the formula is topically applied. However, the application of permeation enhancers in “effective” concentrations is not used in personal care products as they can cause skin irritation and permeate molecules to the dermis which are out the scope of the legislative

definition of a personal care product. These enhancers are preferentially used for topical medicinal products.

1.4.2 Surfactants and Emulsifiers

Surfactant are molecules which offer amphiphilic properties due to the chemical structure of a polar (hydrophilic) head group and a non-polar (lipophilic) tail) and its ability to adsorb at the interface between polar and non-polar media. Surfactant are molecules which offer amphiphilic properties due to the chemical structure of a polar (hydrophilic) head group and a non-polar (lipophilic) tail) and its ability to adsorb at the interface between polar and non-polar media. Surfactants are widely used and are important in personal care formulations as they provide a variety of functions based on their structure; emulsifiers, detergents, lubricants, softeners, wetting agents, levelling agents, dispersants, solubilises, foaming agents and disinfectants (54). An additional function is that surfactants can be utilised as a permeation enhancer ingredient and to aid percutaneous delivery of actives (28, 55). The structural size of the hydrophilic or lipophilic portions of the molecule determines its surfactant behaviour and is characterised by its hydrophilic-lipophilic balance (HLB) value and if charged or uncharged (54). Surfactants are classed based on their hydrophilic head charge; anionic (negative), cationic (positive), amphoteric (variable charge) and non-ionic (no charge) which also determines their function in formulations. In aqueous detergent formulations such as shampoo and body washes, when applied surfactants form micelles around lipid or oil-based dirt and can be removed by rinsing. In emulsion formulations surfactants are known as emulsifiers and provide stability against phase separation and the formation of multiple phases. As surfactants solubilise non-polar material, they can deplete the lipids from the stratum corneum, or disrupt the lipid packing morphology. Studies have found that exposure to anionic surfactants such as sodium lauryl sulphate (SLS) and sodium carboxylates resulted in a depletion and morphology change in skin lipids (56, 57). The change in lipid morphology by the

surfactant was concluded as being the primary reason for an increase in permeation rate of actives across the skin (56). Once the use of surfactants was stopped, there was recovery of the lipid barrier of the skin (57).

Natural occurring surfactants such as lecithins, have been demonstrated to enhance the delivery of topical actives (58). They do so by interacting the stratum corneum lipid packing and occludes the skin surface, therefore increasing tissue hydration and consequently the permeation of actives.

1.4.3 Emollients - barrier repair ingredients.

Petrolatum-based ingredients including soft paraffin, paraffin oil and waxes are composed of multi-hydrocarbon chains (higher than C_{25} in length) which provide skin repairing properties because the chains are representable to the acyl chains of the ceramide lipids and can permeate into the SC easily (28). They are able to penetrate into the upper layers of the skin but not deeper tissues (28).

Typically biomimetic formulations use a topical application of a multi-lamellar lipid structure similar to stratum corneum lipids to improve the barrier function (59).

Included the group of barrier restoring chemicals are glycerol/glycerine, urea and petrolatum (28). However, urea and isopropanol hinder the formulation release of polyphenols such as rutin, whereas propylene glycol promotes the release (60).

1.4.4 Plant Oils

Natural oils derived from plant material are used in personal care for skin emollience and skin conditioning, as well as for marketing purposes. Two examples of oils that are abundantly used are almond and coconut oil. Almond oil is a light yellow, odourless oil containing high levels of oleic acid and liquid at room temperature (61). Coconut oil is semi-solid at room temperature with a distinct coconut aroma. Coconut oil falls into the category of lauric oils; characterised by their high levels of short and medium fatty acid chain lengths (C6-C14) (62). These medium chain fatty acids reach about 80 % of the

oil composition, whereas in non-lauric oils they are less than 2% and these fatty acids are also responsible for coconut oils having a sharp melting point around 32 ˚C (62). **Table I** displays the predominant fatty acid composition found in these two oils, which highlights that the composition between almond and coconut is different.

Table I Predominant fatty acid composition in (a) almond oil and (b) coconut oil. a(Pantzaris and Basiron 2002) (61) b(Roncero et al. 2016) (62)

(a)

Predominant fatty acids in almond oil	% mass	Chain length saturation
Oleic acid	57.5-78.[7a]	C18:1
Linoleic acid	12.0 – 33.9 [a]	C18:2
Palmitic acid	5.2 – 6.7 [a]	C16:0
Strearic acid	0.2 – 1.7 [a]	C18:0
Palmitoleic acid	0.3 – 0.6 [a]	C16:1

(b)

Predominant fatty acids in coconut oil	% mass	Chain length saturation
Lauric acid	45.1-50.3[b]	12:0
Myristic acid	16.8-20.6 [b]	14:0
Palmitic acid	7.7 – 10.2 [b]	16:0
Oleic acid	5.4 – 8.1 [b]	18:1
Capric acid	5.5 – 7.8 [b]	10:0

Fatty acids in the oil can have an effect on the barrier properties of the *Stratum corneum* which will be discussed further in the next section.

1.4.5 Fatty Acids

Unsaturated and saturated fatty acids have been shown to enhance the skin permeation of topically applied actives (63, 64).

Kandumalla *et al.(*1999) investigated the effect of saturated and unsaturated fatty acids as well as the effect of the acyl chain length on the permeation of melatonin across rat and porcine skin (63). For unsaturated fatty acids there existed a parabolic relationship between permeation rate (flux) and the acyl chain length for both animal skin models. The flux of melatonin was increased with increasing acyl chain length; C9 -C11 for rate skin and C9-C12 for porcine skin. However, as the acyl chain increased, the permeation rate decreased; C12-C14 for rat skin and C14 for porcine skin. These skin barrier disruption results have been related in **Figure 1.1-7** to Trans Epidermal Water Loss (TEWL). With unsaturated fatty acids, as the degree of unsaturation increased from 1 – 3, the flux of melatonin was increased for both rat and pig skin.

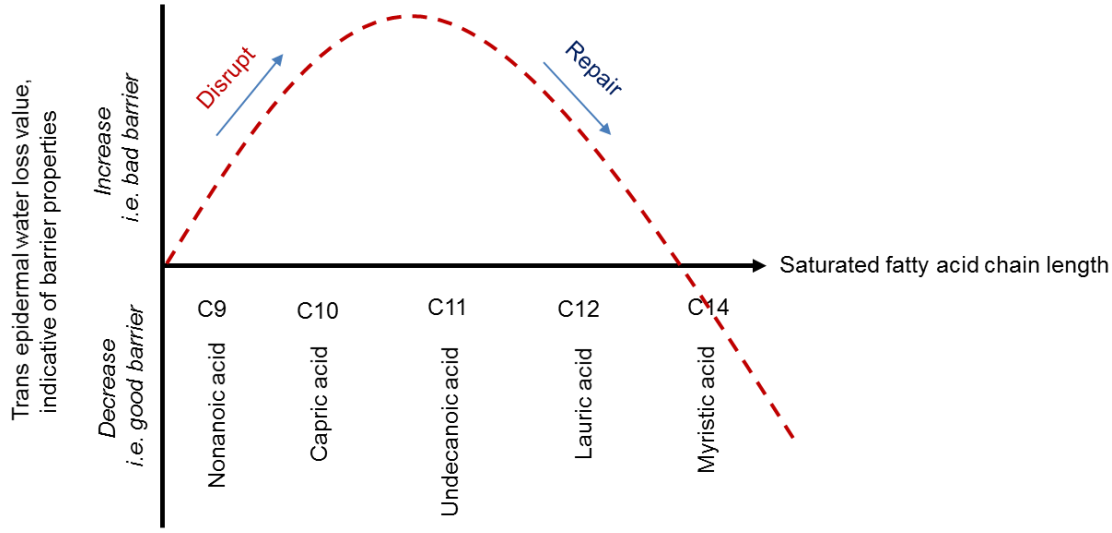

Figure 1.1-7 Schematic interpretation of results from Kandimalla et al. (1999) (63).

The most commonly used unsaturated fatty acid for skin permeation enhancement is oleic acid. Oleic acid is a long chain mono-unsaturated fatty acid and has been widely studied for its permeation enhancement in topical applications and effect of lipid

organisation (63, 65, 66). The main action of oleic acid is believed to be the fluidisation of the lipid layers within the matrix membrane which causes phase separation of these lipids (65).

1.5 Formulation Design strategies

This section outlines the formulation strategies used to enhance the skin penetration and stability of actives and how they can be applied to flavonoids.

There are many examples of formulation design strategies to stabilise flavonoids and enhance skin permeation. Micro/nano-emulsions (67), tailored emollient system (68) and encapsulation *via* liposomes (69). However, the latter have been found to be difficult to achieve capsule breakdown to release the contents once with the epidermal and dermal layers (70). Novel delivery methods include using cosmeto-textiles; intelligent fibres which deliver actives onto the skin (71)

1.5.1 Supersaturation

Supersaturation is a strategy to enhance the permeation of an active across the stratum corneum barrier by exceeding the saturated concentration of a active in the formulation (72). As the concentration of the active exceeds the saturation concentration, these systems are thermodynamically unstable and can result in the crystallisation of the active molecule (72).

An advantage of using the supersaturated method for permeation enhancement is that it is low cost and, as there is no addition of permeation enhancers, does not change the lipid morphology of the stratum corneum (73).

1.5.2 Formulating for Efficacy (FFE)

Wiechers *et al*. (2004) coined the concept “Formulating for Efficacy” where they theorised the delivery of an active from a tailored formulation based on the log $P_{O/W}$ of

the active (68). The “relative polarity index” (RPI) is a tool used on a logarithmic scale to visualise the relationship of log $P_{O/W}$; the solubility ratio of a molecule within octanol and water (discussed further on in detail in section **1.9.2**), representing the active solubility within stratum corneum and the emollients used in the formulation. From this a polarity gap between the active and the stratum corneum can be visualised and used to theoretically select an emollient system to aid delivery to the skin by increasing the thermodynamic activity of the active in the formulation. An active is solubilised into a primary emollient which has a similar log $P_{O/W}$ to that of the active and then a secondary emollient is introduced which will reduced the solubility of the active in the primary emollient. When this formula is applied to the skin, thermodynamics move the active from the formula to partition onto the skin. This is a relatively simple method for delivery, and includes ingredients (emollients) that would be used in a formula to provide skin conditioning benefits.

1.5.3 Emulsions

Emulsions are the most popular formulation for skin care products as they impart good sensory properties and can solubilise both hydrophilic and lipophilic substances. Emulsions are composed of two immiscible phases; a non-polar oil and polar aqueous phase. The most common emulsion type is oil-in-water (O/W) where the oil phase is 5-20 % dispersed in an aqueous phase.

Oil-in-water emulsions allow rapid evaporation on the skin as the continuous phase is water. The dispersed non-occlusive oil phase will slowly coalesce to form a continuous layer on the skin. In water-in-oil systems the oil is the continuous phase and comes in to direct contact with the skin. This gives an immediate occlusive effect and slow release of emulsified water to the skin and these w/o systems give time-release moisturisation (74).

Micro-emulsions are thermodynamically stable. They consist of an aqueous phase, and oily phase, a surfactant and a co-surfactant. Common surfactants used for micro-emulsions are Tween 80 and lecithin and usually small chain fatty alcohols are used as co-surfactants (75).

An advantage of micro-emulsions is the enhanced skin delivery of oil-phase ingredients because of reduced droplet size, however this high surfactant level can cause skin irritation (74). Alcoholic emulsions are a combination of an oil phase and an alcohol, which can be diluted with water. However, problems arise when trying to stabilise the oil in the alcohol and alkyl polyglycol phosphate can be used to deliver an effective performance (74). Sucrose fatty acid esters are non-ionic, biodegradable surfactants and have been used in studies to form micro-emulsions for the skin delivery of polyphenols (76).

A W/O micro-emulsion formulation consisting of water, propylene glycol, Span 80 and Tween 80 has been demonstrated to enhance the delivery of quercetin (77). Other

studies have formulated O/W micro-emulsions with a combination a 150 mM NaCl solution, ethanol, isopropyl myristate and Tween 80 for the skin delivery of quercetin, genistein and chlorogenic acid (75). Hydrophilic chlorogenic acid delivery was enhanced in an O/W microemulsion, compared to aqueous solution and W/O micro-emulsions. This is most likely because of increased solubility (78). Whereas Kitagawa *et al.* also found the opposite for quercetin which is hydrophobic, that W/O micro-emulsions considerably improved the intradermal delivery of quercetin (79).

Otto and du Plessis (2015) composed a detailed review on the subject of transdermal and dermal delivery of topical emulsions (5). In their concluding remarks they comment that although emulsions have been found to be good vehicles for the delivery of actives, it was however largely dependent on the type of emulsion system used, including the droplet size of the internal phase and the effect of emollient on skin penetration. The addition of other ingredients *e.g.* emulsifiers, can affect the system and can make it difficult to determine the mode of penetration.

Wiechers et al (2012) observed the permeation of radiolabelled actives from different formulation types from “in-use” conditions: hydro-alcoholic gel, O/W emulsion, W/O emulsion, a microemulsion and just an oil (3). The microemulsion used in their experiment was the only formulation to “significantly” enhance the permeation of polar and mildly lipophilic actives (compared to the other formulations which showed the permeation flux of all compounds to go in the predicted order of $\log P_{O/W}$ and increasing molecular weight). However their microemulsion contained propylene glycol (PG), a known permeation enhancer, whereas the other formulation did not contain PG

A study by Lalor et al. 1995 investigated the permeation effects of the hydrophilic surfactant Tween 60 on the enhanced permeation of methyl-p-aminobenzoate. This molecule has a molecular weight of 151.16 g/mol, a predicted LogP value of 1.362 and a predicted pKa value of 2.47. They found that the emulsifier and its distribution between the oil and the water phase played an important role in the solubility of the

active, and thus the thermodynamic activity, which is the driving force for the partitioning of the active from the formulation. The emulsifier used for an O/W emulsion will have a high HLB value, and therefore is classified as hydrophilic, preferred to be in the continuous phase and will be predominantly available in the external (water) phase. This emulsifier will form micelles around the actives in the water phase allowing solubilisation. However, by solubilising, it reduces the thermodynamic activity within the emulsion, which can hinder skin permeation (discussed in more detail in section **1.8**)

1.6 Pickering Emulsions

Pickering emulsions are emulsions that are stabilised with solid particles at the oil water interface, providing steric hindrance and static repulsion (80). As Pickering emulsions do not contain emulsifiers to stabilise the emulsion, skin irritancy is reduced and therefore they offer a novel approach for topical release formulations of actives into the skin (80, 81).

Duffus *et al.* (2016) explain that to make Pickering emulsions there needs to be particle collision with a newly created interfacial areas between the oil and the water during the droplet formation in the emulsion process (82). Next, the particles need to have proper adhesion to the interfacial layer and this is highly dependent on the electrostatic interactions and the size properties of the chosen particle. The last step involves the water displacement from the particle surface by the oil, which is determined by the contact angle, Θ_{ow}, of the particle to the water interface, which determines the hydrophilic / hydrophobic character of the particle. Particles that are hydrophilic will reside predominantly in the water phase and produce O/W emulsions, and hydrophobic particles will reside predominantly in the oil phase and thus form W/O emulsions. The contact angle of the particle to the water determines this effect where if $\Theta_{ow} < 90°$ then an O/W emulsion is formed and if $\Theta_{ow} > 90°$ then a W/O emulsion is

formed (82). Particles at the interface of Pickering emulsions have a high energy barrier to overcome for desorption. Free energy of spontaneous desorption can be calculated by r^2 (1-cosθ) where r is radius of the particle and θ is the contact angle of the particle at the interface (49). Particles that have a contact angle between 0˚ and 180˚ have a very high free energy of spontaneous desorption, *i.e.* the particles are very hard to be removed from the interface from the interface (49).

Studies of Pickering emulsions in the topical delivery of drugs have primarily investigated active loading into the dispersed phase of the PE, using silica, titanium dioxide (83) or cyclodextrins (84) to form the PE particle stabilisation. It has been postulated based on Scanning Electron Microscopy (SEM) results that the PE formed with cyclodextrin form a rigid and solid inflexible film around dispersed oil droplets due to crystal formation. This has also been observed for silica particle stabilised PE (80). This pertains to the delayed collapse and release of the oil droplets and the drug contents inside (84) and therefore PE can have a controlled released effect.

Flavonoids have been investigated to form Pickering emulsions for food applications (49, 85). They found that flavonoids with a log$P_{O/W}$ falling in the range of <-0.6 < 0 made the strongest Pickering emulsions and depended on the sugar moieties present in the flavonoid structure (49).

1.6.1 Formulation Design Conclusions

There are many examples of formulation design strategies that could be potentially applied to flavonoids and enhance skin permeation, for example micro/nano-emulsions (67), tailored emollient system (68) and encapsulation *via* liposomes (69). However, the latter have been found to have problems due to difficult lipid capsule breakdown and release of the active molecules once in the epidermal and dermal layers (70). Novel delivery methods include using cosmeto-textiles which are intelligent fibres which deliver actives onto the skin (71)

A good theoretical approach to formulation development is to build the formula around the key active ingredient and use multi-functional ingredients where possible. In practice, it can be more time consuming, but ultimately a more logical formulated product is created. The sustainability of the final product is increased as the number of ingredients in the formulation is reduced.

An ideal formulation strategy for this is utilising flavonoids in Pickering emulsions to form a stable and multifunctional system.

1.8 Skin permeation

Introduction

A topical formula is considered as two different platforms when viewed in a medicated or a personal care product. In a topical medicated product the primary purpose of the formula is to deliver the specific active drug through the skin to a specific target or to the blood supply, whereas a cosmetic formula conforms foremost to consumer aesthetic acceptability. The definition of a cosmetic outlined by the Cosmetics Regulations:

> *"A "cosmetic product" shall mean any substance or mixture intended to be placed in contact with the various external parts of the human body (epidermis, hair system, nails, lips and external genital organs) or with the teeth and the mucous membranes of the oral cavity with a view exclusively or mainly to cleaning them, perfuming them, changing their appearance and/or correcting body odours and/or protecting them or keeping them in good condition." (86)*

The Medicines and Healthcare products Regulatory Agency (MHRA) are a government organisation that decide whether a product is a medicine or borderline product. The MHRA provide guidelines on borderline products, which encompasses cosmetics (87). The MHRAs current definition of a borderline medicine product is as follows:

> *"Any substance or combination of substances presented as having properties of preventing or treating disease in human beings. Any substance or combination of substances that may be used by or administered to human beings with a view to restoring, correcting or modifying a physiological function by exerting a pharmacological, immunological or metabolic action, or making a medical diagnosis"*

Current personal care skincare products that are intended to have a therapeutic effect on the skin *e.g.* anti-ageing or prevention form free radical attack can encompass both definitions from the CTPA and MHRA and are coined as cosmeceuticals. These cosmeceutical products impart some physiological skin changes with specific actives.

Therefore, current questions that arise in the cosmetic industry is, when does a cosmetic become topical drug/medicine, and should the definition of a cosmetic product be altered to reflect the 21st century cosmetic formulation developments? To add complexity, in medicine, any compound administered through or to the skin is a drug. In cosmetics, any compound administered to the skin is an active.

For a cosmeceutical product that is intended to provide specific benefits to skin, the formula's inherent property must also be effective skin delivery of the active compound, as well as consideration to consumer acceptability. The formula to which an active is incorporated can have a great effect on the penetration behaviour of that compound into and through the skin (5, 88, 89). In addition to this, the formula itself can disrupt the *stratum corneum* which can modify the penetrating behaviour of compounds (88). How much the formula effects the penetration of active compounds is still a discussed topic and requires further investigation (6).

Skin permeation has been viewed as a passive process (90) in which the thermodynamic activity of permeant molecule is the driving force to move the molecule from an area of high concentration (topical formula) to diffuse to an area of low concentration (into and through the skin). Research into the skin permeation and penetration of drugs from topical formulations in pharmaceutical and medicinal research is applicable to the formulation design and penetration behaviour of "actives" that are incorporated into cosmetic formulations.

1.8.1 Skin permeation

The fundamental understanding of skin permeation of drugs has been well studied and documented; with the most influential years in this field being the 1940s to the 1970s (91). It has been suggested that the development of synthetic cortisteroids was the influence for formulation development for transdermal delivery in the 1960s and 1970s. As discussed in section1.2, the primary purpose of the skin is to act as a barrier

between the internal body and the outside world, as is the rate limiting step for skin permeation. It is apparent throughout the literature that to achieve successful skin permeation of an active/drug compound, the following key factors need to be thoroughly understood, theoretically and experimentally:

(i) the inherent physiochemical properties of the active and its stability within an application vehicle (formulation);

(ii) the ability for the active to partition from the vehicle onto the SC;

(iii) the ability of the active to then diffuse through the SC and epidermal layers to the target site; and

(iv) the path length of diffusion of the active within the skin.

All these parameters take into consideration the anatomical site and temperature of the skin (3, 7, 39, 92).

1.9 Physiochemical properties of the drug/active

1.9.1 Molecular weight and lipophilicity

Drug or active compounds are chosen primarily based on their physicochemical properties; small enough and with an ideal lipophilicity to permeate the skin. Often the rules that are applied to cosmetic actives are the same rules that are used in the pharmaceutical industry. (4). “Lipinski’s rule of Five” (93) where a molecule is more likely to permeate a membrane barrier if it has a molecular weight < 500 g mol^{-1}, has a partition coefficient between octanol and water ($\log P_{O/W}$) < 5, the number of groups in the molecule that can donate hydrogen atoms to hydrogen bonds is less than 5 and the number of groups that can accept hydrogen atoms to form hydrogen bonds is less than 10 (94). This is further refined for percutaneous penetration by Lin *et al.*, who suggest that a molecule with a $\log P_{O/W}$ higher than 3 hampers the skin penetration (95) which correlates with other researchers in the field who have found the best $\log P_{O/W}$

value to be between 1 and 3 (7, 91). As the lipophilicity and molecular weight have been regarded as the most influential physiochemical properties of a compound for skin penetration, these parameters been widely used in predicting the permeation of actives for cosmetic, food and drug application. (39, 49, 89, 95-97).

1.9.2 Determining the octanol-water partition coefficient

The partition coefficient of an active between a polar and non-polar solvent can indicate its behaviour with regards to skin permeation, the key for an effective product. An active compound needs to be delivered to the epidermis and the dermis of the skin otherwise it cannot perform its intended use. 1-Octanol is most commonly used as the non-polar phase in partition coefficient experiments because it has a long hydrophobic alkyl chain therefore is a good representative of a lipid membrane environment (97). The lipophilicity of a compound is expressed in terms of log*P*, the value of which is the logarithm of the ratio of the concentration a compound in octanol/water. The higher the value the more the compound favours partitioning into the octanol phase (hydrophobic) and the lower the value the more the compound favours partitioning into the water phase (hydrophilic). There are several methods to determine the log*P* of compounds including computational methods (98) and by chromatography (99), however results vary between methods and as yet there is not a universal method, which proves problematic in collating literature data (97)

1.9.3 Compound Ionisation state

Ionisation states of the compound are highly important parameter to consider for skin penetration. Molecules in the non-ionic form (more lipophilic) are more permeable into the skin than the ionic form (50). The pKa of flavonoids, example quercetin and rutin are both 6.17 (51).

1.10 Skin Permeation Pathways

There are several pathways in which a compound can penetrate through the skin and it is still a debated topic (6). The major direct penetration route through the skin is deemed as the diffusion through the intercellular spaces (6), however other authors argue that the hair follicles and sebaceous glands provide the most direct route through the skin (100) (101). Molecules diffusing through the skin *via* the intercellular route do so by diffusing around the cells in the SC within the lipid matrix (69). As the matrix is composed of lipid material one can assume that this penetration route is favoured by lipophilic molecules.

1.11 *In vitro* Permeation Studies

1.11.1 Measuring Diffusion of permeants

Several methods have been used to investigate the diffusion patterns of a permeant within the SC, such as fluorescence recovery after photo bleaching (FRAP), raster image correlation spectroscopy (RICS) and tape stripping. However, the former two are deemed to have limitations on determining spatial diffusion within SC lipids as the floursencent probe molecules themselves could alter the diffusion behaviour and these two techniques do not give information on the molecular structure of the lipids (102).

1.11.2 Franz Diffusion Cells

Franz diffusion cells have been widely used in the pharmaceutical and cosmetic industry to evaluate the percutaneous permeation of flavonoids *in vitro* (39, 95, 96). Franz diffusion cells (**Figure 1-8**) are specially designed to allow the qualification and quantification of compounds diffusing through a membrane *in vitro* into a receptor fluid which can be analysed by any means that the researcher chooses. Different membranes can also be chosen for penetration assays including human skin, animal skin, polymer membranes and human skin equivalents (103). Studies have demonstrated the percutaneous penetration *in vitro* through a porcine membrane (67, 96, 104) of cosmetic ingredients. Porcine membrane has been used because it has similar physiology to human skin (105) and is also cheaper and more readily accessible, compared to other membrane samples. Other methods for investigating the penetration of actives through the skin are tape stripping (101), Raman spectroscopy (106), or time-of-flight secondary ion mass spectrometry (TOF-SIMS) (107). Tape stripping however has been deemed to be an unreliable method for quantifying skin penetration as it has low reproducibility (69).

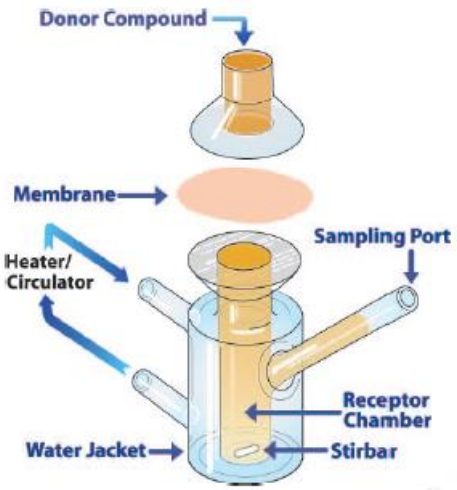

Figure 1-8. Franz diffusion cell used for skin permeation assays (103).

1.11.3 Membrane

Skin membrane choice for permeation assays is determined by the experiment design. However, choice should follow Guidelines based on The Organisation for Economic Co-operation and Development (OECD) on approved membranes; excised human skin, animal models such as pig or mouse, and synthetic models such as cellulose membranes can be used (108). If excised skin is used it can follow pre-treatment procedures such as separating the *stratum corneum* or epidermis from the epidermis / dermis by the water bath-heat extraction method (58) or prior to permeation assays left to equilibrate with receptor mediums (76).

1.11.4 *Stratum corneum* integrity

It is important to check the integrity of the SC in diffusion studies as false results could be obtained if the SC is damaged. The guidelines for testing SC integrity recommend three methods that can be used; (i) measuring the trans epidermal water loss (TEWL) for a normal skin range, (ii) measuring the electrical resistance to an alternating current, max 2 volts for a normal skin range or (iii) measuring the penetration characteristics of reference material (*e.g*. titrated water) (109).

1.11.5 Receptor Medium

The OCED guidelines state that a receptor medium should be selected that will facilitate sink conditions and the solubilisation of all permeating compounds through the skin. The fluid should be of physiological pH, pH 7.4, and typical examples they suggest are a 1:1 water:ethanol mix or a 6 % polyethylene glycol 20 oleyl ether solution in water (109). The receptor fluid must not be a rate-determining step in skin permeation studies.

Receptor fluids that have been used in polyphenol skin permeation studies are phosphate buffer saline (PBS), (76, 78, 79), PBS with 1 % bovine albumin + 10 mM sodium ascorbate to stabilise phenolic compounds (79) and studies have also used 50

% ethanol: water only (58) or with the addition of 5 gL^{-1} polyethylene glycol sorbitan monolaurate, a non-ionic surfactant known as Tween 20 (39). In static diffusion cells the receptor medium must be continually stirred to provide sink conditions and uniform distribution of permeating compounds throughout the medium, allowing for accurate sampling.

1.11.6 Mathematical Models for Skin Permeation

There are several mathematical models for determining the permeability of a compound through the skin, both empirical and mechanistic. Lian *et al.* (2008) and Mitragotri *et al.* (2011) provide comprehensive reviews and comparison of mathematical models for predicating the skin permeability of compounds through the skin (110, 111).

In a simple diffusion mathematical model, all that is needed is the partition coefficient of the active between the vehicle and the SC lipids $P_{v/sc}$, the diffusion coefficient, and the path length of diffusion (111). More complex mathematical modelling of skin permeation requires parameters that are complicated to obtain. The partition coefficient of the active between the vehicle and the skin lipids, $P_{v/sc}$ can be represented by the partition coefficient of the active between water an isotropic solvent *e.g.* octanol, as isotropic solvents reasonably represent the chemical environment in the SC lipids (111). There are two methods to determine the diffusion coefficient: lag time method and Higuchi model. The former method requires and infinite dose (constant reservoir) to be applied to allow for a constant concentration gradient across the membrane (90).

1.11.7 Theoretical determination of permeation

A thoroughly research theoretical permeation model of actives through skin membrane is the Potts & Guy model (110, 112). Potts and Guy 1992 (112) estimated the permeability coefficient (K_p, cm s^{-1}) of a large group of compounds through mammalian epidermis using a predictive model based on quantitative structure permeability relationships (QSPR), encompassing the partition $P_{O/W}$) coefficient and the molecular weight (Mw) of each compound (**Equation 1)**

$$\log Kp = 0.71 \log P_{O/W} - 0.0061 \text{ Mw} - 6.3$$

Equation 1

Their study investigated the permeability of over 90 compounds with varying log$P_{O/W}$ (-3 to +6) and molecular weight (18 to > 750 g mol^{-1}) and found that the model cannot be used to determine the permeability for very lipophilic compounds. With these parameters in consideration the permeation rate of an active can be determined, which is universally used to conclude its percutaneous delivery success.

1.11.8 Steady-State Diffusion: Fick's First Law and permeability (experimental determination of permeation)

The amount of a material flowing through a unit cross section of a barrier in a unit time with a concentration gradient is referred to as flux, also known as Fick's law of diffusion (113). Originally developed for the diffusion of heat transfer (113), Fick's first law of diffusion can be applied to express the permeability rate of compounds across the skin when steady state permeation arise, and has been used throughout percutaneous permeability research (91). Fick's First law for diffusion in is expressed in (**Equation 2)**:

$$J = \frac{DK\left(C_{donor} - C_{receptor}\right)}{h}$$

Equation 2

where *J* is the flux, *D* is the diffusion coefficient of the active compound in the skin, *K* is the partition coefficient of active compound between the formulation and the skin, C_{donor} is the concentration of the active compound in the formulation and $C_{receptor}$ is the concentration of the active compound through the skin and *h* is the path length *i.e.* the thickness of the membrane used (6). The steady state flux is known when the mass transferring over a unit area does not change with time, *i.e.* there is no rate of change over time. When an infinite dose is applied (C_{donor} is kept constant), from the plot of the penetrating amount of permeant per unit area (µg cm^{-2}) against a unit area of *t* the gradient of the linear portion of the data points (see **Figure 1-9**) can be taken as the flux J_{ss}, given by **Equation 3** (90) where *D* is the diffusion coefficient within the SC. After the flux has been determined from the gradient of the steady state region, the permeability *Kp* can be calculated using **Equation 4** where C_0 is the applied concentration in the donor compartment in µg cm^{-2} (39)

$$J_{ss} = -D\frac{d_m}{d_t}$$

Equation 3

$$Kp = \frac{J_{ss}}{C_0}$$

Equation 4

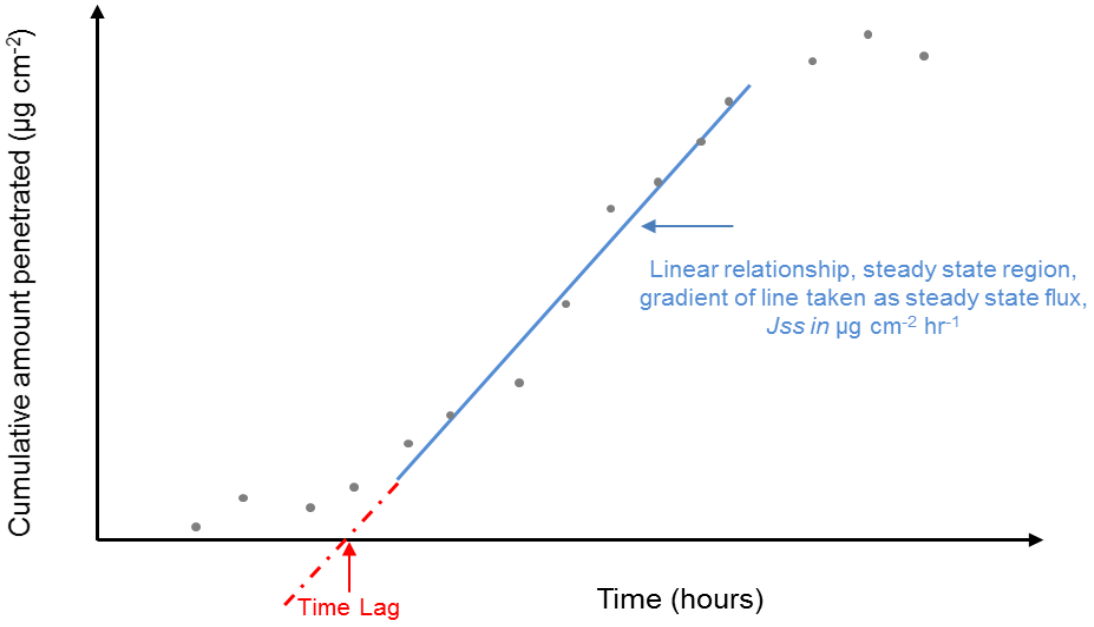

Figure 1-9. Steady state flux depicted as the gradient of the linear portion (steady state region) of cumulative amount penetrated of permeant against time. From the extrapolation of the linear region to the x-axis, the lag time is determined (from infinite dose).

1.11.9 Diffusion within the membrane

Diffusion is the random movement of molecules from an area of high to low concentration until equilibrium is reached. Thermodynamics is the driving force. The diffusivity coefficient can be altered if there is a change in concentration of the permeant, temperature and pressure within the membrane, solvent properties of the surrounding permeant as well as the chemical nature of the permeant (113). The concentration gradient is a driving force for actives to diffuse through the skin.

Furthermore diffusion (*D*) of the permeant within the skin membrane can be calculated by the time lag (**Equation 5**):

$$D = \frac{h^2}{6t_L}$$

Equation 5

Where *D* is the diffusion coefficient ($cm^2\ hr^{-1}$) of the permeant within the skin calculated using time lag (t_L) where *h* represents the skin membrane thickness (cm). When an infinite dose is applied in experimentation, the most used model for determining the permeation analysis is the lag time method after steady state of the permeant across the membrane has been reached (90). The lag time is defined as the time it takes for the permeant's concentration gradient to become stabilised across the membrane (114). When the amount of active permeating per unit area of membrane (µg cm^{-2}) is plotted against time the steady state region is found by the linear relationship between the data points (linear fit regression line) Figure 1-9. The time lag can be then calculated by the extrapolation of the linear fit to the x-axis (90, 111, 113).

There are a few limitations of the time lag method. It is assumed that the diffusion coefficient of the permeant through a membrane does not change in its diffusing path length. However, as viable skin samples differ in structure and chemical composition at different depths, the diffusion coefficient could change therefore this value can be misleading. In addition, the diffusional path length is difficult to measure and it can be difficult to determine when steady state arises (90). It is deemed that the determination of *D* and K_p may be inaccurate if the steady state has not been reached. The duration of the experiment may have to run for prolonged hours (> 30 hours) to reach steady state, and for viable biological membranes can prove impossible. (90).

1.12 Permeation Analysis

The work by Wiechers *et al*. (2012) provides a cornerstone in skin permeation research (3). This study displayed the experimental techniques and example formulations to investigate the permeation behaviour of different actives with varying molecular weights and lipophilicity. Studies that investigate the permeation behaviour of actives from topically applied formulas, and to determine the steady state flux commonly use infinite doses – an excess of formulation and therefore active that will not limit the amount or rate of permeant across the skin. However, the draw backs of this will be that the constant contact and the occlusive nature of the formulation on the skin which over time will change the barrier properties of the SC *e.g*. becoming super hydrated. The opposite of this would be to use a finite dose; an amount that would be representable of real life conditions of the end user using the formulation. This amount had been quoted by Wiechers *et al*. (2012) as 2 mg cm^{-3}. In permeation assays this would be "real life" conditions, and will allow for solvent evaporation and the "recovery" of the SC after the formulation has been applied and "sunk in" or post-solvent evaporation. Therefore when the permeation amount and rate is determined, it can be more representative of the behaviour of the active when used by the end consumer. The disadvantages of using finite doses is that when and if the solvent evaporates and leaves a supersaturated or crystallised layer of the active on the SC surface, the permeation of the active may not reach steady state kinetics (steady state kinetics will help determine what effects the formulation is having on the skin permeation; related to *K* (partition coefficient) and *D* (diffusion coefficient)). This is because the steady state flux may not be determined because of the depletion in applied concentration of the active in the donor compartment. These advantages and disadvantages of infinite and finite dosing are summarised in **Table II**. Careful consideration also needs to be applied when the solvent used to deliver the active in the formula, *e.g*. ethanol, as the rapid evaporation can lead to crystallisation of the active on the SC surface. The

permeation behaviour would show as a rapid amount of active permeating followed a decrease in permeation, as shown by Wiechers et al. (2012) (3). Due to the rapid evaporation of ethanol this depletes the amount of ethanol in the formulation, and as it is a permeation enhancer, if it is depleted it cannot facilitate the permeation enhancement of the actives. One question they raised in their discussion is knowing what happens to the formulation structure and integrity when the main solvent (the external phase) evaporates, leaving the residue. This has been further raised and postulated that once the external phase evaporates the internal phase droplets will coalesce to form a layer on the SC surface (115).

Table II Advantages and disadvantages of infinite and finite dosing in permeation assays using Franz diffusion cells. Summarised by Wiechers *et al.* 2012 (3)

Finite Dose	**Infinite Dose**
Advantages	***Advantages***
Represents the end consumer use	Determine the steady state flux
Does not alter SC barrier function long term; SC can "recover"	Active permeation behaviour and thermodynamic activity, observation of change of formulation on permeation kinetics.
Allows for solvent evaporation and residual formulation behaviour determination	
Behaviour of active on the SC surface; location and SC depth profile with tape stripping	
Disadvantages	***Disadvantages***
The steady state flux may not be determined	Non-representative of "real life" conditions
If Jss not determined, effects of formula on the permeation of active (related to K and D) cannot be determined	May alter the SC barrier properties with constant formula contact/occlusive effect causing super hydration of SC that would not occur in "real life"

Chapter 2 Experimental

2.1 Equipment List

School of Design, University of Leeds

Brookfield viscometer LV-DVE with small sample adapter

Carbon fibre composite digital callipers (Tooltec)

Centrifuge: Grant-bio Microspin 12

Dionex Ultimate 3000 (High Performance Liquid Chromatography)

IKA Hotplate RCT

IKA Temperature probe ETS-D6

IKA RO 10 magnetic stirrer

Franz Diffusion cells (Permagear)

Gilson pipettes: 50-200 µL, 200 – 1000 µL and 500-5000 µL

Perkin Elmer Spectrum BX (Fourier transform infrared)

pH meter: Orion Per**pH**ec**T** LogR meter 310

Sartorius CP 225 D weighing scales

Tewameter TM 300 (Courage & Khazaka)

VeriVide lightbox

School of Food and Nutrition, University of Leeds

Jet homogeniser (Food sciences department, University of Leeds)

Mavern Mastersizer 2000

Ultra-Turrax T25 high shear mixer

Faculty of Biological Sciences, University of Leeds

Zeiss LSM880 Upright confocal with Airyscan (Confocal Scanning Laser Microscope)

2.2 Chemical List

Ingredient	Supplier	Purity	Product Code
Almond oil	Sigma Aldrich		
2-bromophenol	Sigma Aldrich	98 %	130915-10G
Coconut oil	Sigma Aldrich		C1758-100G
Ethanol	University of Leeds		
Formic acid	Sigma Aldrich	HPLC Graade	33015-M
HPLC grade water	University of Leeds		
Isoquercetin	Sigma Aldrich	>90 %	17793-50MG-F
Methanol	Sigma Aldrich	HPLC Grade ≥99.9%	34860
Octanol	Sigma Aldrich	Analytical standard	95446
Oleic Acid	Sigma Aldrich	≥99% GC	O1008
Paraffin oil	Sigma Aldrich	Analytical grade	18512
Phosphate buffer tablets, pH 7.4	Sigma Aldrich		P3288
Quercetin	Sigma Aldrich	≥95%	Q4951
Rutin	Sigma Aldrich	≥94%	R5143

2.3 Pickering Emulsion

2.3.1 Pickering Emulsion process

Pickering emulsions were made using a jet homogeniser made and patented by Prof. Brent Murray in the Food colloids Group of the School of Food Sciences and Nutrition department at the University of Leeds. The two phases for the emulsions were comprised of water+flavonoid and oil. The oils chosen were paraffin, almond and coconut oils., the latter two used as these are common oils used in personal care. Almond and coconut oil both have different states at room temperature, almond is liquid whereas coconut is solid and sublimes into liquid at skin temperature. The flavonoid suspensions were rutin, isoquercetin and quercetin, each at a concentration of 1 mM in aqueous.

Flavonoid solutions were prepared as follows the day previous to the jet homogenisation with oil. Into a 50 mL Eppendorf tube, mass of flavonoid was weighed out and 40 mL of HPLC grade water was added to the tubes measured out by volumetric glass wear (**Table III**). Suspensions were stored in a cool dark place for 18 hours. Due to the limited water solubility of the flavonoids, prior to emulsion making, an Ultra-Turrax T25 was used at 24, 000 rpm on the water+flavonoid suspensions to disperse the flavonoid as much as possible. Suspensions were dispersed for 2 minutes at room temperature.

Table III Mass of flavonoid to obtain a 1 mM aqueous solution for Pickering emulsion

Flavonoid	Mass weighed (mg)	Concentration in 40 mL (mM)
Rutin	24.42	1
Isoquercetin	25.86	1
Quercetin	12.09	1

The methodology for making the emulsions was the same for every formulation, apart from when using coconut oil. Coconut oil has a melting point 23-27 ºC and was semi-solid at room temperature (22-25 ºC) therefore the oil required melting prior to homogenisation and was done so to approximately 35 ºC. To prevent rapid solidification of the oil when combined with the aqueous phase, both formulation phases and the jet homogeniser chamber were also pre-heated using heated water at 45 ºC. As the chambers and pistons were metal the heat was retained during homogenisation.

The volumes on the chambers used for jet homogeniser were as follows: external/water phase 28 mL, internal/oil chamber 7 mL. The total volume in theory produced is 35 mL, however the actual volume of emulsion made is less due to loss of water and oil fractions in the neck of the chamber (prior to pressure applied) and not all the liquid is expelled from the chambers.

The clean homogeniser chambers were charged with water+flavonoid phase (80 %) and the oil phase (20 % volume), the pistons then gently placed by hand into the top of the chambers until secure. The homogeniser, pictured in **Figure 2-1**, was placed into the piston chamber and a pressure of 300 bar was used to plunge the pistons down to

extrude the emulsion into a glass beaker. Particle distribution measurement, pH, viscosity and photographs were done immediately after the emulsion formulation, and the skin permeation and confocal microscope images taken within 48 hours. The emulsions were placed in sample vials for analysis and stored at 4 ºC in between analysis. All analysis of the emulsions were done at room temperature.

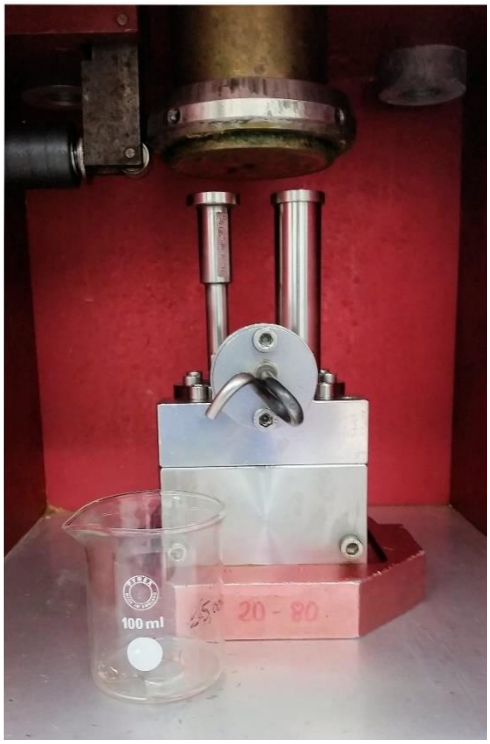

Figure 2-1 Jet Homogeniser and Piston Chamber

2.3.2 Pickering emulsion controls

Control Pickering emulsion were made with water+flavonoid and oil mixed in the same proportions as in the jet homogeniser (28 ml aqueous phase and 7 ml oil phase) in a beaker with a magnetic stirrer at 800 rpm for 1 hour.

Once the controls were removed from stirring, they quickly separated into two distinct layers. Prior to skin permeation experiments the controls were gently mixed with the magnetic stirrer to try and obtain a temporary homogeneous solution for pipette removal and adding to the donor compartment. Overnight the coconut oil had solidified. It was gently heated to just above melting temperature to obtain the liquid oil state before gentle mixing.

2.3.3 Confocal Scanning Laser Microscope

The Confocal Scanning Laser Microscope (CSLM) used was a Zeiss LSM880 Upright confocal with Airyscan equipped with the following lasers: Diode 405 nm, Argon 458, 488, 514 nm, DPSS 561 nm and HeNe 633 nm. For observing Pickering emulsions, a welled microscope slide had to be used so the emulsion could pool within the well and the coverslip place over the liquid without displacement of the liquid. Approximately 20 µL of each Pickering emulsion was transferred onto the slide using a Gilson pipette and the coverslip laid across. Oil immersed objective lenses were used: Plan-Apochromat 40x/1.4 Oil DIC and Plan-Apochromat 63x/1.4 Oil DIC.

2.3.4 Particle size Distribution

Particle size distribution was done with a Malvern Mastersizer 2000 and measurements were done by the help of Dr. Didem Sanver at the Food Sciences and Nutrition department at the University of Leeds.

2.3.5 Viscosity measurements

The viscosities of the emulsions were measured using a Brookfield viscometer LV-DVE with a small sample adapter set. Spindle number s18 and speed 60 rpm was used for low viscosity measurements, with a sample size of 6.7 mL of each Pickering emulsion. This was done via Gilson pipette, taking care to extrude the emulsion down the sides of the chamber to avoid forming air bubble which would affect the viscosity measurement. Measurements were taken at room temperature (22 – 24 °C)

2.3.6 pH measurements

Measurements were taken with pH meter: Orion PerpHecT LogR meter 310 at room temperature.

2.4 Permeation Assay

2.4.1 Franz Diffusion Cell Assembly

Skin permeation studies were performed using six Franz Diffusion cells purchased from PermaGear, Inc. Hellertown, PA, USA. Franz cells were made from clear glass with a 5 cm^3 receptor chamber and a 9 mm diameter orifice for membrane placement, giving a surface area of 0.64 cm^2. **Figure 1-8** in section **1.8** displays the Franz diffusion cell.

The jacketed cells were connected to each other *via* rubber tubing; the first and last Franz cells were connected to a water bath maintained at 37 ºC by using an IKA temperature probe connected to the hot plate. A water pump provided constant water flow through the tubing system. Franz cells were placed on a multi-magnetic stirrer plate and held in place with clamps. Small magnetic stirrers were placed into the receptor chambers prior to skin membrane placement to ensure even distribution of flavonoids permeating through the skin in the receptor chamber and to promote sink conditions.

The distribution within the receptor chamber was checked by adding a red acid water soluble dye and observing the colour distribution within the cell and the sampling port. It was confirmed that there was fast adequate dispersion throughout the cell with the magnetic stirrer at speed 1200 rpm. However, it was observed that the colour distribution in the sampling port was uneven, even after 30 minutes; the concentration of colour being greater at the lower portion of the sampling port connected to the receptor chamber, compared to the top of the port. Therefore the technique of using a syringe to pull up and down the liquid in the sampling port to obtain even distribution was employed to ensure there was no error in sampling.

The receptor fluid was chosen to ensure solubilisation of all flavonoids permeating through the skin and sink conditions. It is important that sink conditions are met to

ensure a concentration gradient across the skin membrane. The receptor fluid is described in 2.4.3.

2.4.2 Porcine Skin Membrane Preparation

Food grade porcine skin was obtained from a slaughter house and came from the ears. On the day of obtaining the skin it was prepared for experimentation at room temperature (20-24 °C). The subcutaneous fat was carefully removed from the dermis using a surgical scalpel and discarded. The epidermis was removed from the dermis using the heat separation method (109). This involved submerging the skin tissue in 60 ºC for 1 minute then the epidermis was carefully removed by peeling off from the underlying dermis with forceps. The skin was visually inspected and was not used if there were any blemishes or marks present on the surface including irregular pigmentation, veins or scars. The skin was washed with cold distilled water to remove surface dirt and was patted dry. The skin was then cut into 1.5 cm x1.5 cm squares using surgical scalpel and placed in plastic bags and stored at -20 ºC until required.

Skin samples were removed from the freezer 24 hours before permeation studies and were thawed in the plastic bag at 4 ºC. This prevented the skin samples from drying out in the thawing process after freezing.

It was noted that the skin samples became drier after freezing, compared to what the tissue would have been fresh. The skin samples were re-hydrated using distilled water for 15 minutes prior to permeation assays. The rehydration lead to a better seal of the tissue between the donor compartment and the receptor fluid, avoiding leaks and loss of sample.

2.4.3 Receptor Medium

Receptor medium was chosen to solubilise the flavonoid compounds permeating through the skin and maintain skink conditions.

This solvent system of 50 *v*/v % ethanol and 50 *v*/v % pH 7.4 phosphate buffer (EtOH:PBS) was chosen because flavonoids are readily soluble in the solvent mixture (see solubility section 2.5) and the pH represented physiological pH (108). They were both prepared with a known concentration of the internal standard 2-bromophenol. This was chosen as an internal standard as it contains a benzene ring for detection at 254 nm in RP-HPLC and does not form complexes with flavonoids. Phosphate buffer saline at pH 7.4 was made by using tablets from Sigma Aldrich.

The 50 % v/v EtOH:PBS receptor medium was made by measuring out equal volumes of ethanol and phosphate buffer saline in volumetric flasks and combining in a separate container and allowing to equilibrate. The internal standard 2-bromophenol was weighed out into a volumetric flask and topped up with the 50 % *v*/v EtOH:PBS mixture to yield a final concentration of 1.7 mM.

2.4.3.1 Maximum Solubility of Flavonoids in Receptor Medium

Maximum solubility of the flavonoids rutin, isoquercetin and quercetin in the receptor medium of 50 % *v*/v EtOH:phosphate buffer saline (pH 7.4 was done to determine whether the solubility in this solvent was a limiting factor for the permeation studies. This was done by adding excess flavonoid to the receptor medium in Eppendorf tubes. Samples were shaken and incubated at 37 ºC on 250 rpm rotation for 24 hours. Tubes were then centrifuged for 5 minutes at 14.5k rpm. The supernatant was then carefully removed with a syringe then diluted with corresponding receptor medium and filtered using 0.45 µm PTFE filter prior to RP-HPLC analyses. Receptor medium contained the internal standard, 2-bromophenol, at 1.7 mM. Dilutions of the supernatant were made as supernatants were too concentrated for accurate HPLC analysis. Concentration of the flavonoids were calculated using the peak area of the flavonoid from the HPLC trace using the response factor, *F*, with the internal standard. All maximum solubilities were greater than 1 mM in aqueous (concentration in applied emulsions) therefore the receptor medium was deemed not a limiting actor for sink conditions (**Table IV**).

Table IV Maximum solubility of rutin and quercetin in receptor medium 50 % *v*/v EtOH:PBS.

Flavonoid	**Maximum solubility concentration (mM)**
Rutin	3.23 ± 0.42
Isoquercetin	3.37 ± 0.26
Quercetin	3.60 ± 0.12

l

2.4.4 Procedure

The thickness of the skin samples was measured with a pair of carbon fibre composite digital callipers (Tooltec) and only samples with a thickness of 1 ± 0.1 mm were selected for use in the assay. Samples which were not in this thickness range or which showed signs of damage were rejected. Skin samples were placed over the orifice of the receptor chamber stratum corneum facing upwards (underside of epidermis touching the receptor fluid). The donor chamber was carefully aligned and clipped into place over the skin membrane with a Teflon washer in-between. Using a needle and syringe the internal phase was added to the cell *via* the sampling port and trapped air bubbles under the skin were released by tilting the Franz cell so the bubble could escape *via* the sample port. Doing this several times ensures that there was no air gap between the skin and the internal phase. The epidermal membrane was left for 1 hour to equilibrate with the internal phase (receptor chamber heated to 37 ºC with a circulating water bath). After this cells were again tilted to release any trapped air bubbles that may have formed before the start of the permeation study.

2.4.5 Trans-Epidermal Water Loss (TEWL) Measurement

In skin permeation assays it is necessary to evaluate the barrier properties of the skin membrane sample prior to testing to establish uniformity and normality of the membrane. The OECD guidelines on skin permeation assays outlines several methods to evaluate skin barriers by electrical capacitance, titrated water or measuring the trans-epidermal water loss (TEWL).The integrity of the skin barrier – the stratum corneum – was measured using a Tewameter TM 300 (Courage & Khazaka) and values obtained were used to determine if the porcine skin, under experimental conditions, was representable of “normal skin”. Measurements on the porcine skin were taken before the skin permeation assay (after 1 hour equilibrium). If the trans-epidermal water loss measured was within the range of “normal skin condition” then it was deemed satisfactory to use for the permeation experiments. If TEWL values were high and above the “normal range” i.e. values above 25 g m^{-2} hr^{-1}, indicating a loss of barrier function, then the skin sample was not used and replaced. Courage & Khazaka have provided guidelines for the TEWL values obtained by the Tewameter TM 300 and the interpreted corresponding skin condition, displayed in **Table V**. These guidelines were used to determine the skin condition.

Table V Trans Epidermal Water Loss (TEWL) values recorded by the Tewameter TM 300 and interpretation of data in accordance with skin condition. Guidelines set by manufacturer Courage & Khazaka (116)

TEWL- values g/h/m^2	Interpretation guide
0-10	Very healthy condition
10-15	Healthy condition
15-25	Normal condition
25-30	Strained skin
Above 30	Critical condition

After the 24-hour experimental period of permeation, TEWL measurements were taken again to observe if there had been a change in the barrier function after the applied formula had been absorbed.

2.4.6 Donor Compartment: Dosing

To obtain release kinetic data of the flavonoids from Pickering emulsions, an infinite dose had to be applied to the skin.

Samples of 200 µL of each Pickering emulsion sample and control were pipetted on to the exposed skin and cells were rotated gently to ensure even coverage of the skin. In **Table VI** the mass of flavonoid applied, C_0, in Pickering emulsions and controls is shown, calculated using a 0.64 cm^2 surface area. This information is needed to calculate the % of flavonoid permeating the membrane after 24 hours, expressed as % applied dose. Immediately after the emulsions had been applied to the skin, samples were taken from the internal phase which signified time 0 (T_0) representing the start of the experiment. Aliquots were taken every hour up to 7 hours and then at 24 hours. Each sample volume was noted and immediately replaced with an equal volume of fresh receptor fluid. Aliquots were filtered using a 0.45 µm PTFE filter into vials ready for Reverse Phase – High Performance Liquid chromatography analysis (outlined in section 2.4.7). These permeation assays were done in an environmentally controlled room; with 22 °C and 75 % humidity.

Table VI Mass of flavonoid applied to the donor phase

Flavonoid	Molecular mass	Applied volume to donor phase, µL	Applied mass, µg from 1mM	C0 in donor phase in µg cm^{-2}
Rutin	610.52	200	120	187.5
Isoquercetin	464.38	200	92.88	145.12
Quercetin	302.24	200	60.45	94.45

2.4.7 Qualification and quantification in the receptor chamber

To identify and quantify the flavonoids permeating the epidermal membrane, reverse phase – high performance liquid chromatography (RP-HPLC) was used.

2.4.7.1 Reverse Phase-High Performance Liquid Chromatography (RP-HPLC)

A Dionex Ultimate 3000 equipped with a diode array detector (DAD) was used for reverse-phase high performance liquid chromatography (RP-HPLC) to identify and quantify the presence of flavonoid compounds in formulations and samples taken from skin permeation assays. Chromeleon™ Version 6.80 software was used to analyse chromatograms. The HPLC machine was equipped with a Waters Novapak C-18 column, 150 x 3.9 mm, particle size: 5 µm with a Waters Novapak C-18 guard column. The injector volume was 20 µL. No auto-sampler was equipped to the RH-HPLC machine therefore manual injection of each sample was done.

The programme used for analysis was as follows: solvent A water with 0.1 % formic acid and solvent B acetonitrile with 0.1 % formic acid. The programme was based on a gradient system between the two solvents and is as follows: Time 0 min. 5 % B, 0-2 min. 50 % B; 2-4 min. 50 % B; 4 – 6 min. 60 % B; 6-8 min. 60% B; 8-10 min. 100 % B; 10-11 min. 100 % B and 10-14 min. 5 % B Temperature was maintained at 25 ºC and DAD set at 254 nm for the detection of the aromatic rings of the flavonoids and the internal standard.

2.4.7.2 Retention Times of Reference Flavonoids

Rutin and the mono-glycoside, isoquercetin, and the aglycone, quercetin were investigated. For possible identification of flavonoids in unknown aliquots from permeation assays, the retention times of these flavonoids were determined by running reference samples through RP-HPLC analysis. **Table VII** displays the properties of the reference flavonoids

Table VII Retention times of three flavonoid reference samples, using HPLC programme.

Flavonoid	Retention Time (minutes)
Rutin	3.3
Isoquercetin	3.7
Quercetin	4.05

2.4.7.3 Internal Standard for RP-HPLC analysis

An internal standard (IS) was used in the receptor solvents of the Franz cells to determine the concentration of the flavonoid compounds that had permeated the skin membrane. The IS also provides a way to monitor the accuracy of the HPLC programme and machine. By using an IS the response factor, *F*, can be calculated between the reference flavonoid sample and the IS by using **Equation 6.**

$$\frac{A_{IS}}{A_{Ref}} = F \frac{C_{IS}}{C_{Ref}}$$

Equation 6

Where A_{IS} is the peak area of the internal standard, A_{Ref} is the area of the reference sample, C_{IS} is the concentration of the internal standard and C_{Ref} is the concentration of the reference samples. The IS chosen for quantification of the flavonoids permeating the skin was 2-bromophenol. It was chosen as it can be detected at 254 nm due to aromatic ring and retention time at 4.7 minutes does not mask the flavonoids (**Table VII**).

2.4.8 Calibration curves and response factor, *F*, of flavonoids reference samples with internal standard 2-bromophenol

Calibration curves of reference flavonoid samples were done in receptor solvents along with the internal standard (IS). Reasons for doing this are twofold: (I) to determine if a line of regression exists within the data over a concentration gradient and (II) determine the response factor, *F*, with the flavonoid and the IS. The reason for determining the response factor between the internal standard is to calculate the unknown concentration of flavonoid compound in permeation experiments. Response factor values are displayed in **Table VIII**.

This method of determining the unknown concentration of flavonoid is preferred as the concentration will be relative to the concentration of the internal standard.

Calibration curves were done in the receptor solvent used in the permeation experiments, 50 % *v*/v ethanol:phosphate buffer saline at pH 7.4 (EtOH:PBS). A stock solution of each flavonoid was made in the receptor solvent and consecutive dilutions made with the solvents. **Figure 2-2** displays the calibration curves for rutin, isoquercetin and quercetin respectively. From these graphs it was determined that there is a regression line fit between concentration and peak area as each calibration gave a R^2 value of 0.999. The graphs in **Figure 2-2** show that the internal standard remains constant which indicates a good internal standard for determining the response factor and reproducibility of the HPLC machine injection port.

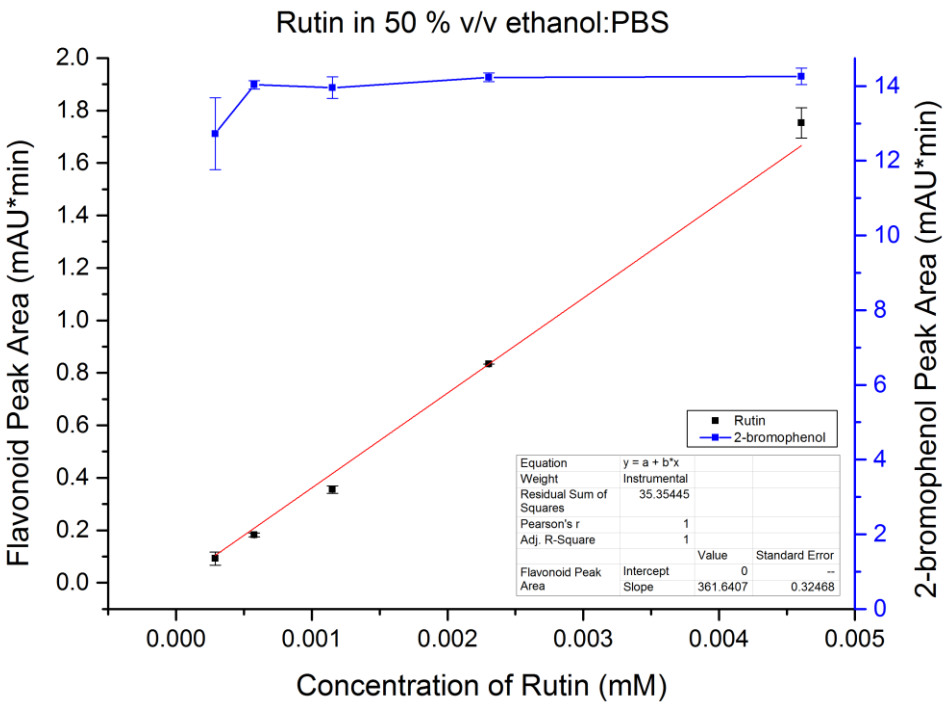
Rutin in 50 % v/v ethanol:PBS
Flavonoid Peak Area (mAU*min)
2-bromophenol Peak Area (mAU*min)
Concentration of Rutin (mM)
Rutin
2-bromophenol
Equation y = a + b*x
Weight Instrumental
Residual Sum of Squares 35.35445
Pearson's r 1
Adj. R-Square 1
Value Standard Error
Flavonoid Peak Area Intercept 0 --
Slope 361.6407 0.32468

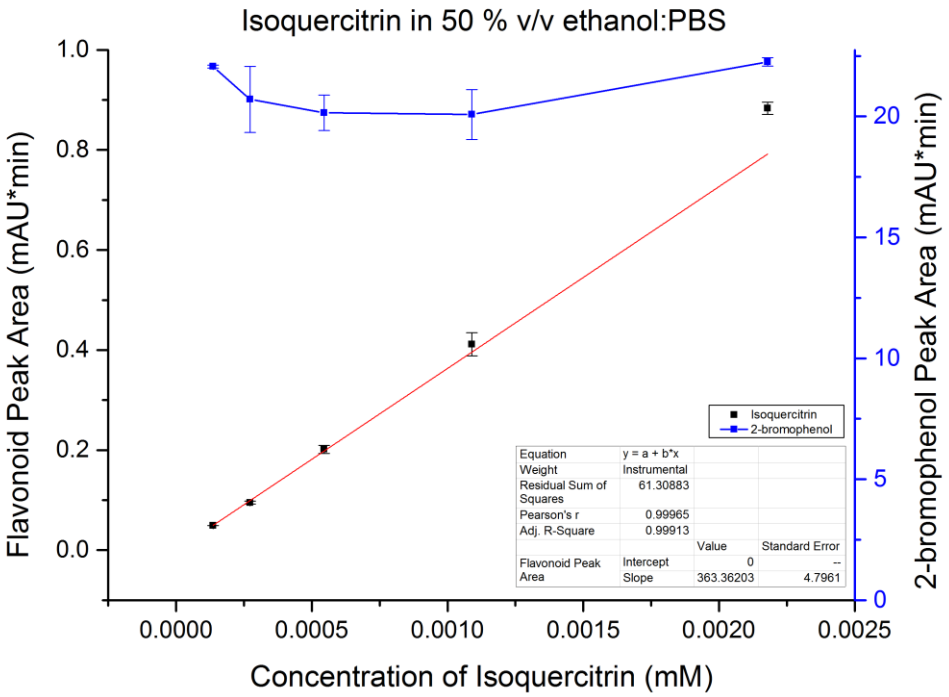
Isoquercitrin in 50 % v/v ethanol:PBS
Flavonoid Peak Area (mAU*min)
2-bromophenol Peak Area (mAU*min)
Concentration of Isoquercitrin (mM)
Isoquercitrin
2-bromophenol
Equation y = a + b*x
Weight Instrumental
Residual Sum of Squares 61.30883
Pearson's r 0.99965
Adj. R-Square 0.99913
Value Standard Error
Flavonoid Peak Area Intercept 0 --
Slope 363.36203 4.7961

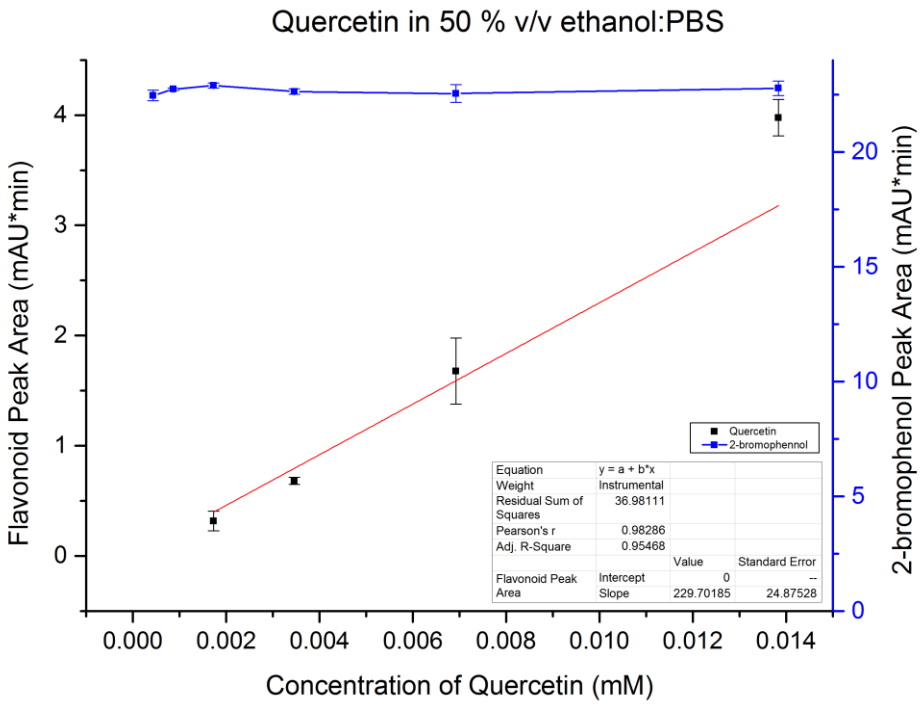

Figure 2-2 Calibration curves of (a) rutin, (b) isoquercetin and (c) quercetin in receptor medium 50 %v/v EtOH:PBS and with the internal standard 2-bromophenol at 1.7 mM

Table VIII Response factor determined between flavonoid and internal standard 2 - bromophenol using calibration curves in Figure 2-2

Flavonoid	Response Factor with Internal standard
Rutin	41.48
Isoquercetin	38.90
Quercetin	22.03

2.4.9 Amount of flavonoid permeating

In this study the amount of flavonoid permeated per unit area of skin in µg cm^{-2}, was calculated by dividing the amount of flavonoid detected in the receptor phase in µg by the surface area of the skin sample exposed in the Franz diffusion cell, 0.64 cm^2.

The cumulative amount permeating was then expressed as a % of applied dose in **Equation 7** where *Qt* is the cumulative amount of flavonoid in µg cm^{-2} at time *t* and C_0 the original dose applied in µg cm^{-2}.

$$\%\ applied\ dose = \left(\frac{Q_t}{C_0}\right) \times 100$$

Equation 7

2.5 Mathematical Modelling on the flavonoids permeating through porcine epidermis over 24 hours

Mathematical models were used to determine the permeation parameters and to describe the release kinetics of flavonoids through the epidermal skin membrane. If a linear relationship exists between any of the models, it is taken as an indication of the validity of that model for the data. The following models were applied to each flavonoid permeating the skin over the aliquot sampling time frame. Software Microsoft excel was used to process the models.

2.5.1 Steady state diffusion

2.5.1.1 Zero-order kinetics / Fick's first law and determination of time lag.

From a plot of the amount of flavonoid penetrating per unit area against time, a linear regression indicates a constant rate of permeation, zero-order kinetics (113). The increase is independent of the starting concentration and the rate of increase is constant. When there is a constant release rate of active permeating the membrane, the flux of the active is said to be in steady state. The gradient of the slope is taken as the rate or flux in steady state, J_{ss}, and can be integrated into Fick's first law of diffusion (**Equation 8**) (39).

$$J_{ss} = KD\frac{\Delta C}{h} = K_p\, C_0$$

Equation 8

where, *K* is the partition coefficient of the solute between the vehicle and the membrane, *D* is the diffusivity of the solute within the membrane, Δ*C* is the concentration gradient over the membrane and *h* is the path length. The permeability coefficient, *Kp* in cm min^{-1}, is combination of the parameters of lipophilicity and diffusivity of a solute.

2.5.1.2 Diffusion coefficient using time lag method

Time lag was determined for each by extrapolating the linear portion of the permeation profile to intercept the x-axis. When the time lag is found, the diffusion coefficient, D_s of the flavonoid within the skin can be found using Equation 9 (90, 113).

$$Ds = \frac{h^2}{(6t_L)}$$

Equation 9

Where *h* is the thickness of the epidermal membrane in cm and t_L is the time lag in minutes.

2.5.1.3 Permeability coefficient

Once the steady state flux, J_{ss} has been determined from the derivative of cumulative amount penetrated per unit area against time the permeability coefficient, *Kp* in cm min^{-1} , can be calculated from **Equation 10**

$$Kp = \frac{Jss}{C_0}$$

Equation 10

where C_0 is the original concentration in the donor compartment applied to the skin. When an infinite dose is applied, the concentration of the active in the receptor phase is much less that the concentration of the active in the donor side, therefore the concentration in the donor compartment approximates the original concentration applied, C_0 (39).

2.5.2 Non-Steady State Models

First order kinetics is when an exponential decay of the active permeating the membrane with a concentration rate change (113).This relationship is found by plotting the logarithm of the amount permeating in µg cm^{-2} over time. Fick's second law of diffusion, which describes non-steady state diffusion can be applied to determine the

permeability and diffusion coefficients. This requires the Laplace transformation which was unavailable during this research and was not used. Therefore this data can only be used to state whether the system is in a non-steady state.

2.5.3 Release Kinetics:

2.5.3.1 Higuchi Model

Release kinetics and diffusivity determined by the Higuchi principle are found by plotting the square root of time against the cumulative amount of permeant normalised by the original concentration applied in the donor phase (39). The correlation coefficient is investigated and the slope of linearity taken as Higuchi's coefficient, K_H. Rearrangement of **Equation 11** provides the diffusion coefficient (D_v) of the permeant within the vehicle (**Equation 12**).

$$K_H = 2\sqrt{\frac{D_v}{\pi}}$$

Equation 11

$$Dv = \left(\frac{K_H}{2}\right)^2 \cdot \pi$$

Equation 12

2.5.3.2 Korsmeyer-Peppas Model (The Power law)

The Korsemye-Peppas Model, which characterises the release component from cylindrical matrices, is found by plotting the fraction of flavonoid released from the membrane over the logarithm of time. The slope of the linear portion, *K*, is used in

Equation 13 to determine the n component. Values of n component are cross checked in **Table IX** to determine the release behaviour.

$$\frac{M_t}{M_\infty} = Kt^n$$

Equation 13

Where M_t/M_∞ is the fraction of flavonoid released at time Mt from the applied concentration M_∞, *K* is the release rate constant and n is the release component (117).

Table IX Korsmeyer-Peppas release component value and definitions

Release exponent (n)	Drug Transport Mechanism	Rate as a function of time
0.5	Fickian diffusion	$t^{-0.5}$
0.5<n<1	Non fickian diffusion	t^{n-1}
1	Case II transport	Zero order release
Higher than 1	Super case II transport	t^{n-1}

2.6 Octanol-Water Partition Coefficient (LogP)

To determine the octanol-water partition coefficient, Log$P_{O/W}$, the logarithm of the ratio of flavonoids peak area between the octanol phase and the PBS phase was calculated, expressed in **Equation 14**:

$$LogP = log\left(\frac{[octanol]}{[water]}\right)$$

Equation 14:

The octanol water partition coefficient of the three flavonoids investigated was determined based on the work carried out by Rothwell et al. (2005). (97).

Solutions of flavonoids with known concentrations were prepared in methanol before 250 µL of each were pipetted into 1.5 mL Eppendorf tubes, a total of three replicates per flavonoid solution. The methanol was left to evaporate off at 37 ºC to leave flavonoid residue in the tubes. To each tube 750 µL of octanol was added and tubes gently shaken, before 750 µL of phosphate buffer saline (pH 7.4) was added to each tube. Tubes were shaken vigorously by hand for 1 minute and visually inspected. In all cases there were no visual particulates that were undissolved. The octanol and PBS layers were separated by centrifugation for 3 minutes at 12.5k rpm with a IKA microcentrifuge. As octanol is less dense that water, the majority of the octanol layer at the top of the tube was carefully removed via syringe before filtering for HPLC analysis. The remaining octanol at the PBS interface was carefully removed and discarded, followed by the filtration of the PBS layer before HPLC analysis. The HPLC programme used for analysis is outlined in section 2.4.7.1.

2.7 Attenuated Transform Reflectance Fourier Transform Infrared (ATR FT-IR) Spectroscopy

The ATR FT-IR machine used in this study was Perkin Elmer Spectrum BX coupled with the software Spectrum v5.3.1. Spectra were measured over the wavelength 4000 – 600 cm^{-1} with 32 scans and a resolution of 4 cm^{-1} and interval of 2 cm^{-1}.

Infrared spectral measurements are sensitive to background noise. Prior to all sample measurements a background scan was measured and automatically subtracted from the sample spectra. This was done to remove background noise and interference peaks from the surrounding air which would give false peaks in the spectra of samples.

Between each sample measured, the ATR crystal was wiped with acetone to prevent cross contamination and a background scan run before a new sample measured.

2.7.1 Measurement of Flavonoids

Powders of rutin, isoquercetin and quercetin were individually compacted down onto the ATR crystal and the clamp screwed down with automatic uniform pressure (force unmeasured) to complete closure to secure a tight compressed powder on the crystal. Measurements were then taken.

Measurement of porcine stratum corneum samples

All skin samples were placed with stratum corneum face down on the ATR crystal and the clamp screwed down to complete closure to secure a tight seal before measurements were then taken.

2.7.1.1 Untreated skin sample

Untreated porcine epidermis using 200 µL distilled water in the donor compartment was set up as a blank control, and to be the baseline spectra for comparison of further permeation assays. The Franz cell set up was identical to the procedure outlined in section 2.4, as to keep conditions for the skin samples same as the permeation assays of the Pickering emulsions (same receptor fluid, temperature and time of experimentation). The stratum corneum lipids of each sample were evaluated with FT-IR after 24 hours.

2.7.1.2 Effect of oleic acid on lipid morphology

Positive control experiments were done on skin samples in the Franz diffusion set up to investigate the technique for using FT-IR analysis and determine the change skin lipid morphology after topical application of a donor formula. A known permeation enhancer, oleic acid, was selected as it has been demonstrated to change the lipid morphology of the stratum corneum (65). Two solutions of oleic acid were made; 5 %w/w (0.25 mL in 4.75 ml water) and 10 %w/w, (0.5 mL in 4.5 mL water) using Gilson P200 and P1000 pipettes. For the experiment, 200 µL

aliquot of the solutions were taken with a Gilson P200 and transferred to the skin in the Franz diffusion cell. The stratum corneum lipids of each sample were evaluated with FT-IR after 24 hours.

2.7.1.3 Oil type on lipid morphology

To observe effect of the oils used in the study on the skin without flavonoids present, aqueous solutions of 20 % w/w paraffin, almond and coconut oils were made and applied to skin samples. This was done by mixing 1 mL of each oil with 4 mL distilled water using a Glison P1000 pipette. Coconut oil required to be heated to approximately 40 ºC before transferring to water phase, which was also warmed to approximately 40 ºC so to prevent solidification when mixing. As there was no emulsifier present in the solution to stabilise the oil and water phase, the solutions were kept under constant stirring conditions using a magnetic stirrer in glass beakers to maintain oil dispersion. Under mixing, 200 µL aliquot of the oil solutions were swiftly taken with a Gilson P200 and transferred to the skin in the Franz diffusion cell. The stratum corneum lipids of each sample were evaluated with FT-IR after 24 hours.

2.7.1.4 Skin Permeation Assays

Immediately after 24 hours of the permeation assay, skin samples were removed from the Franz diffusion cells and transferred to the FT-IR analysis directly. This was done as soon as possible to avoid further ageing and environmental change of the skin sample, which can change the lipid morphology.

2.7.2 Post-analysis of the spectral data

2.7.2.1 Normalisation

For skin samples, all spectra were normalised at the amide I band, 1629-1633 cm^{1}.

2.7.2.2 Spectral Analysis – Curve fitting

Curve fitting of the FT-IR spectra was done to measure the peak shift and width (29) *via* the software Origin Pro.The purpose of curve fitting is to measure not only the frequency in which bond strength of the molecule of interest absorbs at, but also the vibrational interaction of that molecule with the surrounding environment (29). The line shape of the curve is a sum of the individual molecules in the surrounding environment absorbing or scattering the energy (29).

The correct curve fitting model depends on the state in which the test sample is measured. A bell curve *Gaussian* function is used for solid materials due to the environment of the molecule not being in motion and the surrounding molecules experience a statistical distribution in the environment; in a gaseous state the molecules have a high level of rotations and collisions therefore a *Lorentzian* curve function is used and for liquids a combined *Gaussian-Lorentzian* function is used as the curve profile will take on attributes of both *Gaussian* and *Lorentzian* (29).

Curve fitting functions for chain conformation in the stratum corneum primarily use the *Gaussian* function as the packed lipids are in “solid” form within the matrix, however *Gaussian-Lorentizian* and *Lorentzian* function have been used on ceramide mixtures (1, 118-121).

Baseline correction was done prior to curve fitting. For the CH_2 symmetric stretching at ~2850cm^{-1}, baseline correction was 2825 – 2880 cm^{-1} and for the CH_2 scissoring modes at ~1468 cm^{-1} , baseline correction was 1450 - 1480 cm^{-1}.

In this research the *Gaussian* curve fitting function was used to determine peak location and bandwidth of the CH_2 symmetric stretching at ~2850 cm^{-1}, of the CH_2 scissoring modes at ~1468 cm-1 with 2nd derivative analysis to find hidden peaks.

Statistical Analysis

2.8 Statistical Analysis

On all data average and standard deviations (n = 3) were calculated, followed by one direction ANOVA on all comparative data then by Student's one tailed paired T-test using Microsoft excel software. The *P* value of statistical significance was taken as 0.05.

2.9 Discussion of experimental / errors

2.9.1 Franz diffusion cell dose and viscosity of formula applied

In Franz diffusion cells, the permeation of the active from a formulation is dependent on the viscosity of that formulation and the dose applied (122). High viscosity infinite dose application can impede the skin permeation of actives because of limitations of thermodynamic activity of the active. The active in such formulations cannot efficiently migrate through the bulk of the formula to the skin surface and partition into the SC layers, *i.e.* it's thermodynamic activity is reduced, compared to low viscosity formulas. In addition, the formula immediately in contact with the skin can become depleted in the active, and bioavailability of the remaining active within formula is dependent on the rate of external phase / solvent evaporation. Therefore overall there is not a constant concentration gradient across the membrane. When a small amount of high viscosity formula is applied to the skin, in finite dose conditions, the rate of skin permeation is increased, attributed to the increased skin hydration from thick formulations (122).

In literature there are discrepancies to a specified volume that represents a infinite dose, (OECD guidelines to finite dose), mathematical models used to describe the permeation of active through the membrane and receptor fluids to provide sink conditions. Dose dependant permeation of actives can occur when there is a surplus or pooled formulation applied to the skin in the donor compartment, which is not representable in "in use conditions" (122). Selzer *et al*. 2013 provide a comprehensive review on skin permeation assays, and the difference of permeation data obtained when using an infinite or finite dose technique (123).

2.9.2 Skin membrane choice

To be as close as possible to “real-life” situation porcine skin was used. The reasons for this as stated previously is because porcine skin offers as a viable skin membrane that is the closest biologically to human skin. In this study human cadaver skin could not be obtained.

There comes a degree of unpredictability in using porcine membrane. The biological composition and integrity cannot be fully controlled; only the source, preparation, storage and experimental use can be controlled. Repeating the exact experimental procedures reduces the amount of error. This unpredictability produce skin permeation results that lack sensitivity with large errors over the mean sample data. All skin permeation data in this study collection and statistical models gave the same magnitude of error per formulation sample (Figure 5-1Figure 5-2Figure 5-3Figure 5-14). A reduction in error between experimental repeats can be achieved by either increasing the number of experiments run, *n*, or using an artificial membrane in replacement of porcine skin. An artificial membrane, *e.g.* cellulose membrane will have uniform pore sizes, membrane volume and chemical integrity which would reduce variability, however, as an artificial membrane, is not representable of biological skin permeation. In addition, artificial membranes used for skin permeation assays cannot be evaluated *post-hoc* for the skin lipid morphology.

2.9.3 Alternative membranes

The skin membrane used in this research was porcine ear skin which has been used in skin permeation studies as an appropriate ex vivo animal model.

Other animal skin models such as rat, mouse and guinea-pig have been used, however porcine ear skin is closer to human skin; with a comparable *stratum*

corneum thickness of 21 – 26 µm and hair follicle density of 20/cm^2 (human 14-32/cm^2) (124, 125). The structure of the skin appendages from porcine ear skin are very similar also to that of human skin with sebaceous glands connected to the hair follicle and sweat glands in the dermis being connected to the skin surface via ducts (124).

Barrier properties of porcine ear skin and human skin have been found to be similar (125). In human skin equimolar ratios of cholesterol, free fatty acids and ceramides are present, however in porcine skin it is quoted as being different (125). The arrangement of lipids are also reported to be different where human skin lipids are arranged in a tightly packed orthombic lattice and porcine lipids are arranged in a hexagonal phase (125).

2.9.4 Choice of receptor fluid for Franz cell

Flavonoids are not readily soluble in water or phosphate buffer therefore a solubilser in the receptor medium has to be introduced to obtain sink conditions. A common additive to the receptor medium is an emulsifier (Tween 80 or bovine albumin to reversibly solubilise lipophilic permeants (123). However, bovine albumin binds and forms complexes with polyphenols (126). Preliminary experiments in this research used bovine albumin with phosphate buffer for a receptor fluid to investigate the solubilisation of flavonoids. Flavonoids were not detectable by RP-HPLC with the defined programme and was theorised that a complex with the bovine albumin was occurring. Therefore a water-ethanol mixture was preferred as a receptor solvent for sink conditions. Ethanol mixed with phosphate buffer has been used at 25, 40 and 50 %v/v ethanol as the receptor fluid for skin permeation assays (3, 39, 127). It should be noted that ethanol in the receptor medium within the Franz cell could dehydrate the epidermal membrane and cause shrinkage of the skin (123). Even

though this has been done in these skin permeation assays, the continuity across all skin samples allows for valid comparison.

2.9.5 Determining steady state region

It has been discussed in literature that the steady state region of penetration is difficult to determine (90). Some authors have taken the steady state region as from the initial release time frame (127) while another study by Weichers et al. 2012 took the steady state region from the later release time frame of 6 – 24 hours (3).

Accurate deduction of whether the flavonoids reached complete steady state across the membrane within 24 hours could not be achieved. From experimental design and laboratory access, time frame of 7 – 24hours could not be measured, which may affect the results of accurately determining steady state flux and time lag.

Time lag could not be determined for rutin in Pickering Emulsions for all three oils as detection was not until 6 or 7 hours, producing only 2-3 data plots. Time lag could also not be detected for quercetin Pickering emulsions as this was not detected in permeation studies.

The permeation profiles of the flavonoids showed different stages of permeation; steady state followed by a slower permeation between 7-24 hours. When the system of permeation through a membrane is not in steady state, Fick's 2nd law of diffusion can be applied. Fick's second law describes the rate of change over time of a permeant across the membrane. It is determined using specialist software, out the scope and availability of this research. The most common algorithm to solve Fick's 2nd law is the Laplace transformation (111).

Chapter 3 Pickering Emulsions for the stability of Flavonoids

3.1 Introduction

Flavonoids are used as actives in cosmetics primarily for their potent antioxidant activity, which contributes to protection of the skin from reactive oxygen species and thus skin damage. However, due to their poor water solubility it is often difficult to incorporate flavonoids into a stable formulation and obtain efficient skin permeation (39, 55, 127). Flavonoids with amphiphilic structures due to the presence of sugar moieties pose as interesting, multifunctional ingredients if utilised as an emulsifier to help stabilise an oil-water formulation. **Figure 3-1**Figure 1-1 displays the chemical structure of flavonoids that exhibit this amphiphilic property; a di-glycoside flavonoid, rutin (**1**) and a mono-glycoside flavonoid isoquercetin (**2**). The flavonoid rutin has a rutinose moiety at the 3-OH position, which provides emulsifier like properties and therefore can form Pickering emulsions (49, 85). Forming Pickering emulsions with flavonoids could be a useful technique to change the skin delivery of the flavonoids, as well as to stabilise the flavonoids in the formulation. The benefits to forming Pickering emulsions with flavonoids are: i) increasing flavonoid stability in formulation; ii) using actives with multifunctional benefits to provide stability as well as therapeutic benefits to the skin.

Rutin and isoquercetin chemical structures can be classed as surface active; the conjugated benzene rings contributing to the non-polar portion of the molecule and the sugar moieties pertaining to the polar region of the molecule. As previously mentioned, this parameter of the molecule lends these flavonoids to be used as stabilisers for emulsions. Research into rutin and its aglycon, quercetin (**Figure 3-1**), to form Pickering emulsions for food applications has been investigated (49, 85), however, the application of flavonoids for emulsion stabilisation has a huge potential for personal care application as flavonoids also provide an active benefit to the skin.

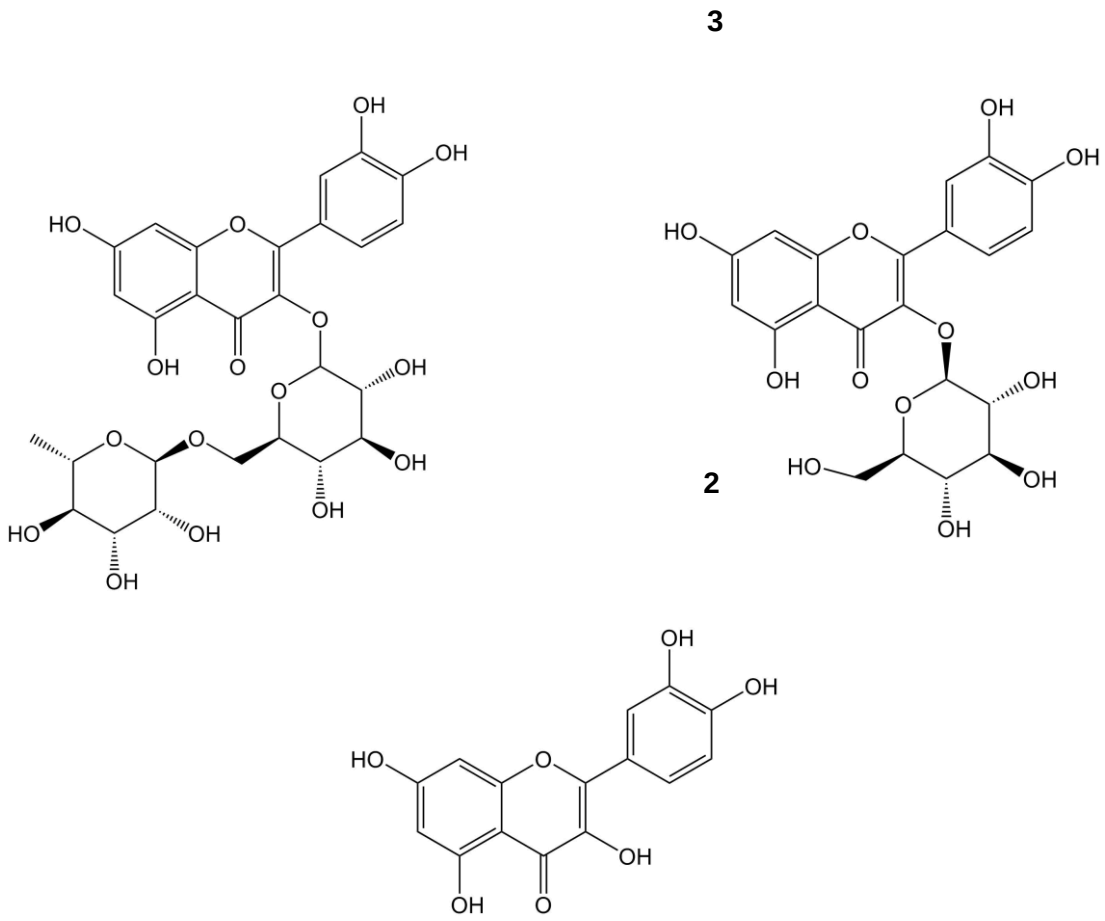

Figure 3-1 Chemical structure of three flavonoids: 1) Rutin, 2) Isoquercetin and 3) Quercetin

Unlike other studies that have investigated the formation and then penetration enhancement of actives through the skin encapsulated within the solid coated particles (80) the active in the Pickering emulsions in this study are the stabilising agent and outside coating of the oil droplet, rather than the flavonoids being encapsulated within the oil droplet. This could lead the way to multi-component formulas as a technique to deliver multiple actives; soluble in the oil phase and the coating of the oil droplets. Increases the use of multi-functional ingredients, reduces emulsifiers in the formulation that can cause skin irritancy.

3.2 Pickering Emulsions

Using a jet homogeniser, aqueous and oil phases are combined under high pressure to form an emulsion. With the inclusion of a flavonoid, a Pickering emulsion (particle stabilised) emulsion can be formed; rutin particles aggregate at the oil-water (O/W) providing emulsion stabilisation by stearic hinderance at the interface preventing of oil droplets coalescing. A hydrocarbon oil such as *n*-tetradecane, paraffin oil or mineral oil forms strong PEs due to the inert properties of the oil (49), and the flavonoid is only wetted by (not soluble) in these oils. There is an increasing trend of natural persona care formulations using vegetable derived oils such as sunflower, almond, soybean and coconut oils. These oils however may prove not to make good Pickering emulsions with rutin and other flavonoids because these oils contain fatty acids and triglycerides which can impart surface active properties due to their structure, and therefore displace the flavonoids at the O/W interface.

In previous studies by Luo *et al.* (2011), both rutin and quercetin had been investigated for their Pickering emulsion formation capabilities with *n*-tetradecane; they found that rutin formed good stable Pickering emulsions with *n*-tetradecane, whereas quercetin did not (49). They investigated a range of flavonoids with differing aglycon structures and sugar moieties. They found that flavonoids with very high or very low log$P_{O/W}$ values were not good emulsifiers for forming PE. The presence of sugar moieties in the flavonoids have a significant effect on the PE formation: the sugar groups provide increased water solubility to the molecule, increasing the surface activity of the flavonoid and thus adsorption to the O/W interface. The study by Luo *et al.* (2011) did not investigate the PE potential of the mono-glycoside of quercetin, isoquercetin.

3.3 Aims and Objectives

This study herein looked at three flavonoids with the same aglycon but differing in sugar moieties at the 3-OH position: rutin (rutinose moiety, di-glycoside), isoquercetin (glucose moiety, mono-glycoside) and quercetin (aglycon, no sugar moieties)**Error! Reference source not found.** shown previously in **Figure 3-1** on p **98**. The emulsions were formed with three oil types commonly used in cosmetics; paraffin oil, almond oil and coconut oil. To the best of knowledge, this is the first study to look at the formulation or rutin, isoquercetin and quercetin as emulsifiers to form Pickering emulsions with three different types of oil that would be used in a personal care formulation: paraffin oil, almond oil and coconut oil because they are different in fatty acid composition and different physical states at room temperature (refer to section **1.4.4** on p**35** of chapter 1), the change in *stratum corneum* lipid morphology after application and the skin permeation and release kinetics from porcine epidermis.

Research questions in this chapter are:

- Can Pickering emulsions be formed with three different flavonoid types with differing structures: rutin (di-glycoside), isoquercetin (mono-glycoside), quercetin (aglycon) with three different oil types used in personal care formulations: paraffin oil, almond oil and coconut oil at a 20 % oil fraction.
- Using confocal scanning microscopy, where are the flavonoids aggregating in the emulsion.
- What is the particle size distribution of these emulsions.
- Are these flavonoids chemically or physically stabilised in the emulsion/are the emulsions stable enough to be used in personal care.

Control emulsions were composed of the same oil:water ratio of 20:80 % *w*/w with a concentration of flavonoid in the aqueous phase, 1 mM. The experimental procedure for the controls was changed by omitting the jet homogeniser (high pressure sheer mixing) step. This step is key to forming Pickering emulsions (49). An alternative approach could have been using a different emulsifier to form oil droplets, but this would have been a modification factor to the formulation and potentially to the skin barrier properties. The control had to represent the same ingredients with no droplets.

3.4 Results

The following section displays image results of the formation of Pickering emulsion with flavonoids rutin, isoquercetin and quercetin with the oils paraffin, almond and coconut.

3.4.1 Pictures of emulsions formed with rutin

The Pickering emulsions formed with paraffin, almond and coconut oils with rutin as the emulsion stabiliser are visually represented in **Figure 3-2.** All oils formed a uniform, opaque emulsion, differing in colour because of the oil used: paraffin oil formed the whitest emulsion, whereas almond was cream-yellow in colour due to the natural yellow colour of the starting oil. All the emulsions had a small distinct layer of the original oil at the top of the vial. This is because within the jet homogeniser there is a small volume of oil that will not be homogenised as it is passed through and expelled from the system. Analysis of expelled liquid would confirm this. The emulsion made with coconut oil possessed a “bitty” appearance as the coconut oil cooled from +35 ºC and solidified at room temperature (22-25 ºC). Visually, the best emulsion was formed in the order: paraffin oil > almond > coconut oil. After 6 months stored at room temperature the Pickering emulsions still visually remained, however a larger oil layer was prominent at the top of the vials. This demonstrates the stability of the Pickering emulsions is weakening over time, as expected.

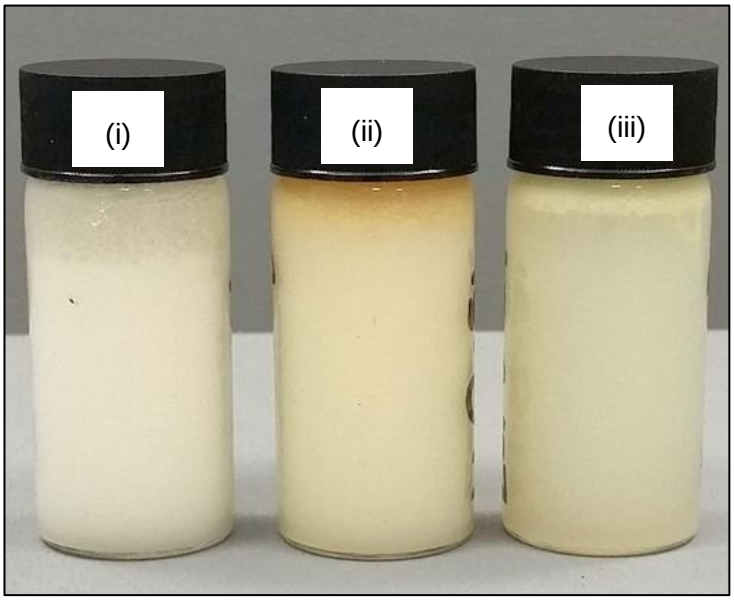

(a)

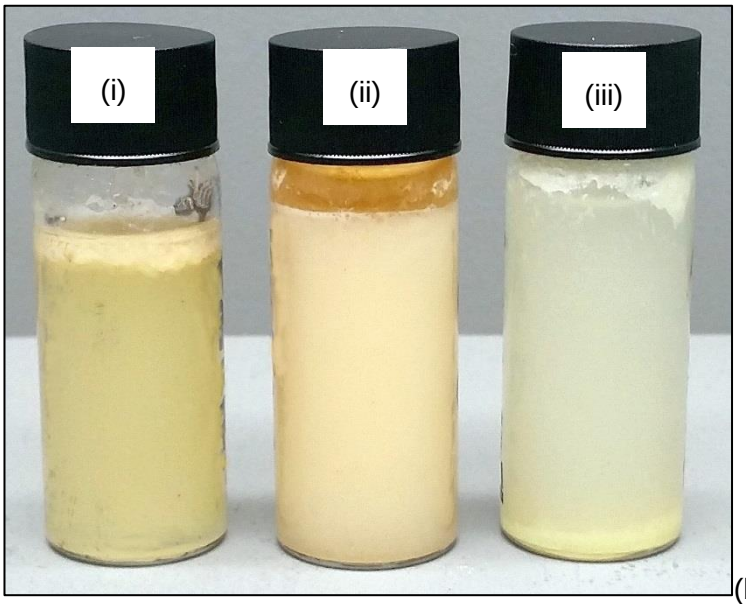

(b)

Figure 3-2 Pickering emulsions formed with rutin 1mM and 20 vol % of (i) paraffin oil, (ii) almond oil and (ii) coconut oil. Pictures taken after formation with jet homogeniser. 1.3(a) after homogenisation and 1.3(b) 6 months after homogenisation at room temperature (22 ºC).

3.4.2 Pictures of control mixtures formed with rutin

Control “non-emulsions” in **Figure 3-3** clearly show two distinct layers of oil and aqueous layers with a sedimentation of rutin at the bottom of the vial. However the aqueous layer with almond oil showed slight opaqueness and a reduced oil layer at the top compared to almond and coconut oils. After 6 months at room temperature there was no visual change in the control emulsions, apart from almond oil (ii) which showed a darkening orange colour. This could be due to autoxidation of the fatty acids within almond oil.

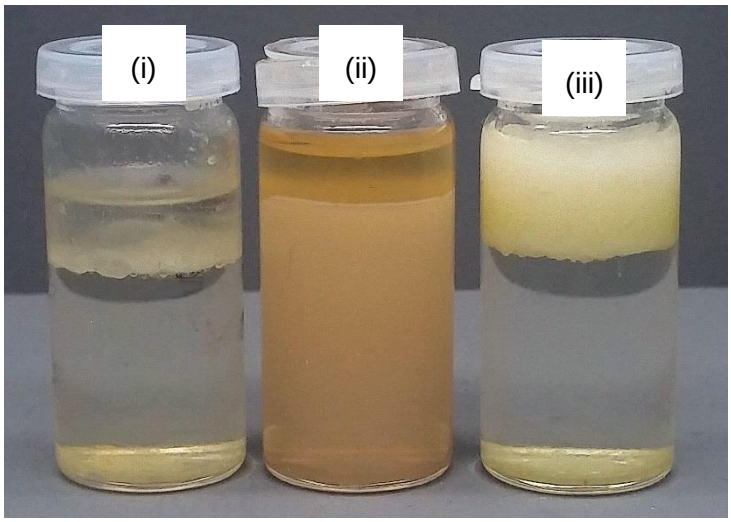

Figure 3-3. Control “non- emulsions” formed with rutin 1mM and 20 vol % of (i) paraffin oil, (ii) almond oil and (ii) coconut oil.

3.4.3 Pictures of emulsions formed with isoquercetin

The Pickering emulsions with paraffin, almond and coconut oils with isoquercetin as the emulsion stabiliser are visually represented **Figure 3-4** (p **106**) after homogenisation. All the oils initially formed emulsions, paraffin oil forming the most opaque and uniform looking emulsion. As with PE with rutin and the oils **Figure 3-2** there was a layer of un-homogenised oil at the top of the vials. However, the emulsions formed with isoquercetin also displayed a layer of large oil droplets at the top of the vials which is an indication of a reduced level of stabilisation of the oil. From observation, the order of stabilised emulsions formed for isoquercetin was in the order: paraffin oil > almond oil > coconut oil. After 6 months the Pickering emulsions with isoquercetin show complete emulsion break down (**Figure 3-4 (b)**). Larger oil layers at the top are distinct of phase separation of the oil and aqueous phase. There was also seen a layer of flavonoid sedimentation at the bottom of the vials. The volumes of the almond and coconut oil vials are low as availability of isoquercetin raw material was low.

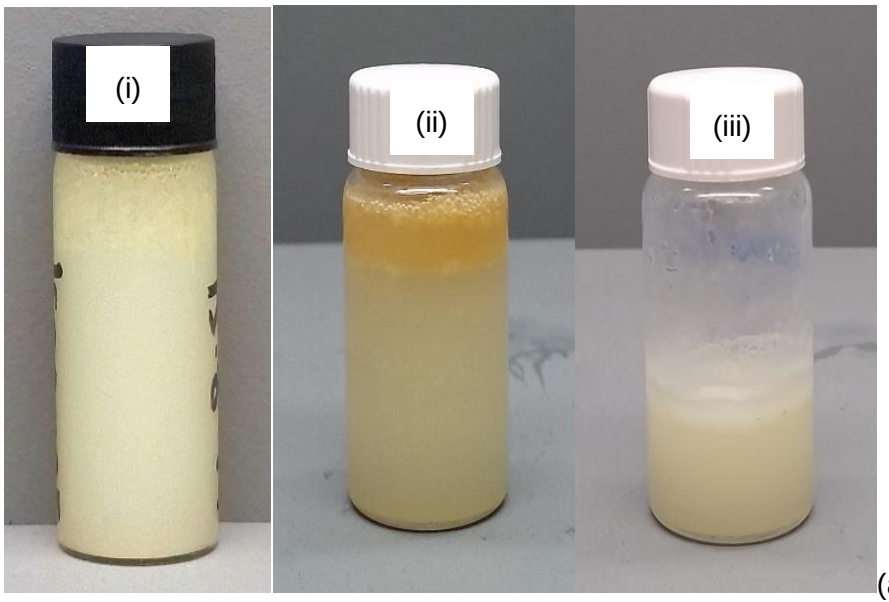

(a)

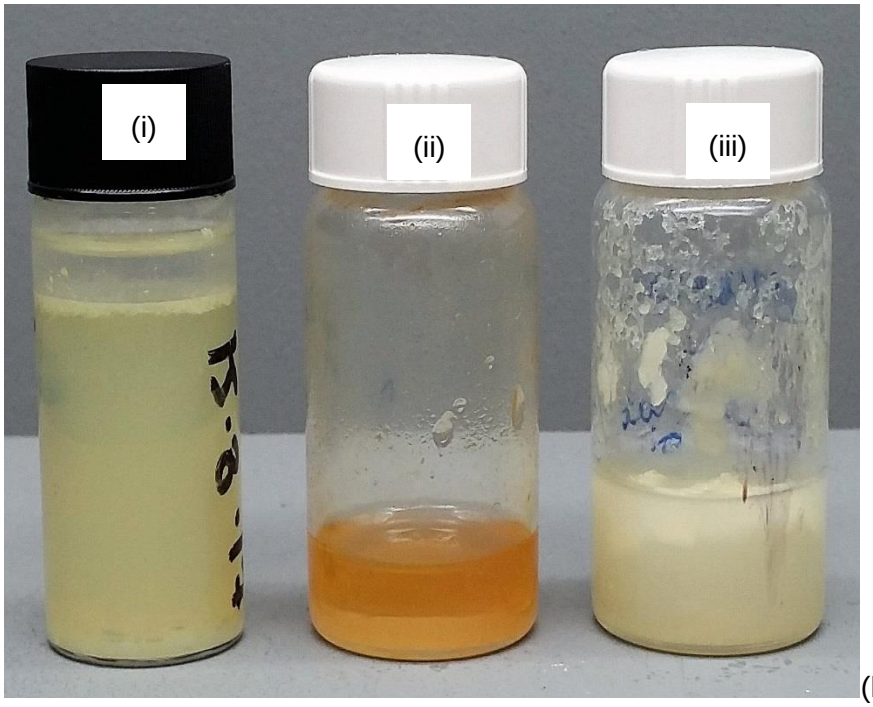

(b)

Figure 3-4 Pickering emulsions formed with isoquercetin 1mM and 20 vol % of (i) liquid paraffin oil, (ii) almond oil and (iii) coconut oil. Pictures taken after formation with jet homogeniser: (a) after homogenisation; and (b) 6 months after homogenisation at room temperature (22 ºC).

3.4.4 Pictures of control mixtures (non-emulsions) formed with isoquercetin

Control “non-emulsions” for isoquercetin in **Figure 3-5** showed distinct layers of oil and aqueous phases with an isoquercetin sedimentation at the bottom of the vial. No emulsion was formed. After 6 months there was no change visually.

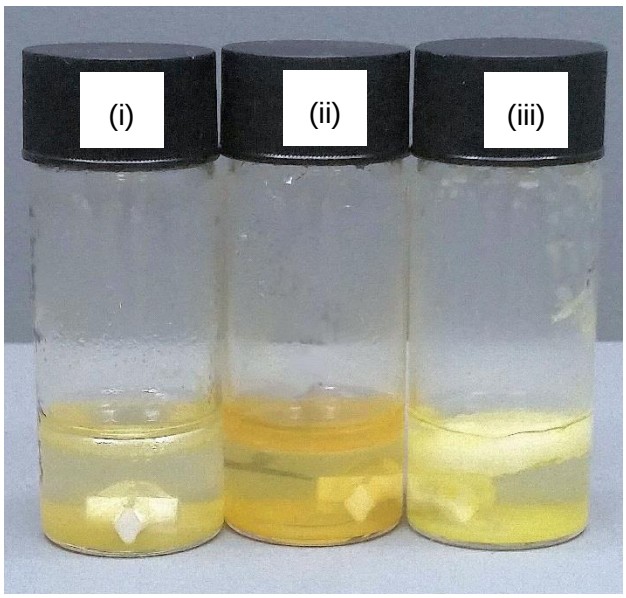

Figure 3-5 Control “non- emulsions” formed with isoquercetin 1 mM and 20 vol % of (i) paraffin oil, (ii) almond oil and (ii) coconut oil.

3.4.5 Pictures of Pickering emulsions formed with quercetin

The Pickering emulsions with paraffin, almond and coconut oils with quercetin as the emulsion stabiliser are visually represented **Figure 3-6**.From observations the oil and aqueous phases showed signs of separation rapidly after homogenisation stage, evident by the large oil layers at the top of the vial. It was seen more predominantly in the PE made with almond oil than paraffin oil.

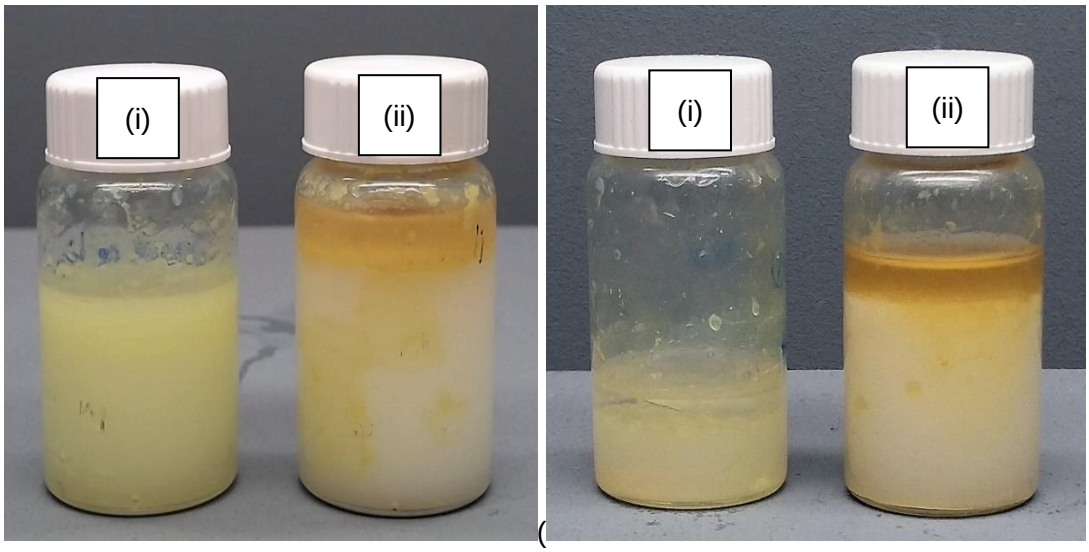

(a) (b)

Figure 3-6. Pickering emulsions formed with quercetin 1mM and 20 vol % of (i) liquid paraffin oil, (ii) almond oil. and (b) 6 months after homogenisation at room temperature (22 ºC). An emulsion with quercetin and coconut oil formed no emulsion

Despite this there was still some apparent emulsion formation. The attempted PE emulsion with quercetin and coconut oil did not form, it was immediately apparent that the two phases separated. The order of quercetin PE formation from strongest to weakest from visual observation was paraffin oil > almond oil > coconut oil. After 6 months there was little change in the appearance, however the oil layer slightly more distinct. The aqueous phase was still opaque.

3.4.6 .Pictures of control mixtures (non-emulsions) formed with quercetin

Control “non-emulsions” for quercetin showed two distinct layers of oil and aqueous. It is difficult to decipher from the image in **Figure 3-7**, but the opaqueness in the aqueous phase comes from the suspension of quercetin. There is also a sedimentation of quercetin and the bottom of the vial.

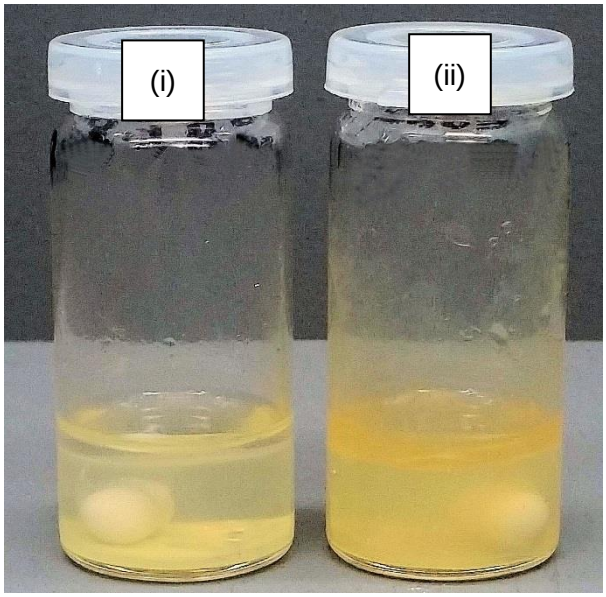

Figure 3-7. Control “non- emulsions” formed with quercetin 1 mM and 20 vol % of d (i) paraffin oil and (ii) almond oil.

3.4.7 Viscosity and pH of emulsions formed with flavonoids

Viscosities of the Pickering emulsions are relatively low (**Table X**), and it is seen that the mixture of rutin and paraffin oil has the highest viscosity.).

Table X. Viscosity measurements of emulsions (cP).

Flavonoid	Paraffin Oil	Almond Oil	Coconut Oil	Conditions of measurement (speed, spindle)
Rutin	2.03	1.65	1.86	60 rpm, SC-4 18
Isoquercetin	1.71	1.64	1.73	60 rpm, SC-4 18
Quercetin	1.97	1.74	n.a.	60 rpm, SC-4 18

Table XI. pH values of Pickering emulsions.

Flavonoid	Paraffin Oil	Almond Oil	Coconut Oil
Rutin	6.70	6.37	7.04
Isoquercetin	6.83	6.46	6.90
Quercetin	6.80	6.59	n.a.

3.4.8 Confocal images of Pickering emulsions

Due to the auto-fluorescence of flavonoids, confocal scanning laser microscopy (CSLM) is a useful technique to locate the flavonoids in the Pickering emulsions, and as previous work has demonstrated (49). As seen in **Figure 3-8**, rutin forms poly-dispersed emulsion with paraffin, almond and coconut oil. The majority of particles are spherical oil droplets with rutin visually located at the O/W interface evidenced by the green fluorescence (difficult to observe in print). A closer magnification of rutin paraffin oil in (d) and (e) shows an Aggregation of the rutin particles have occurred forming crystals, noticed by the “clump-like” images and some oil droplets are held within these rutin aggregates.

Similar results to rutin were observed for isoquercetin with the three oil types (**Figure 3-9**); a poly dispersed emulsion was formed although the droplet sizes appear to be much larger than droplets with rutin. As the oil droplets are larger, this would lead to instability over time. Their appears to be aggregation and crystal formation of isoquercetin, entrapping oil droplets as seen in **Figure 3-9** images (d) and (e).Images of Pickering emulsions of quercetin with paraffin and almond oil are in **Figure 3-10**. With paraffin oil, the droplets are clustered in quercetin crystals, whereas almond oil forms droplets that appear to begin coalescing, leading to instability.

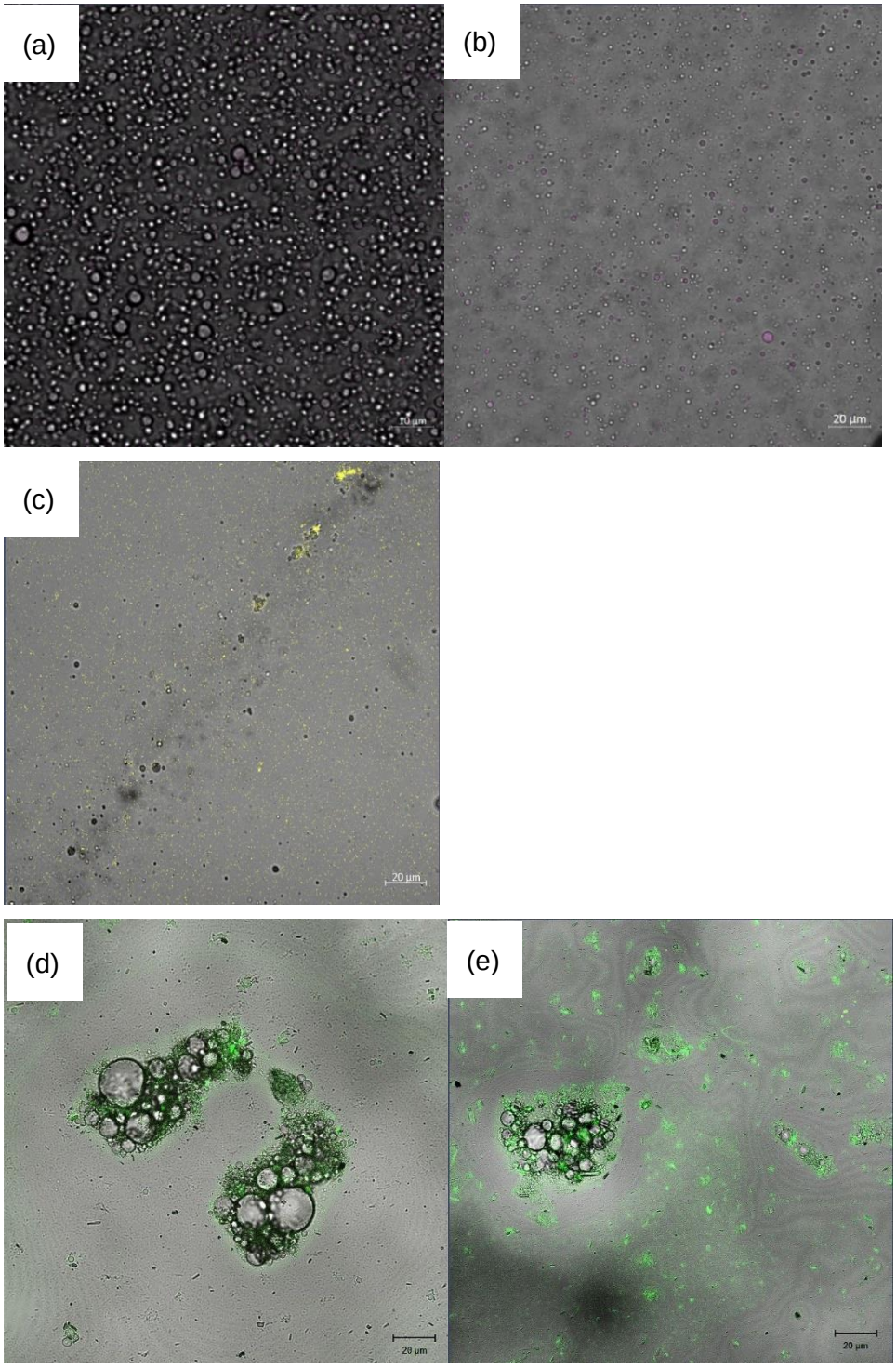

Figure 3-8. Confocal Laser Scanning Microscopy images of Pickering Emulsion with Rutin and 20 vol % of (a) paraffin oil (b) almond oil and (c) coconut oil. Rutin and paraffin oil crystal aggregation seen in (d) and (e).

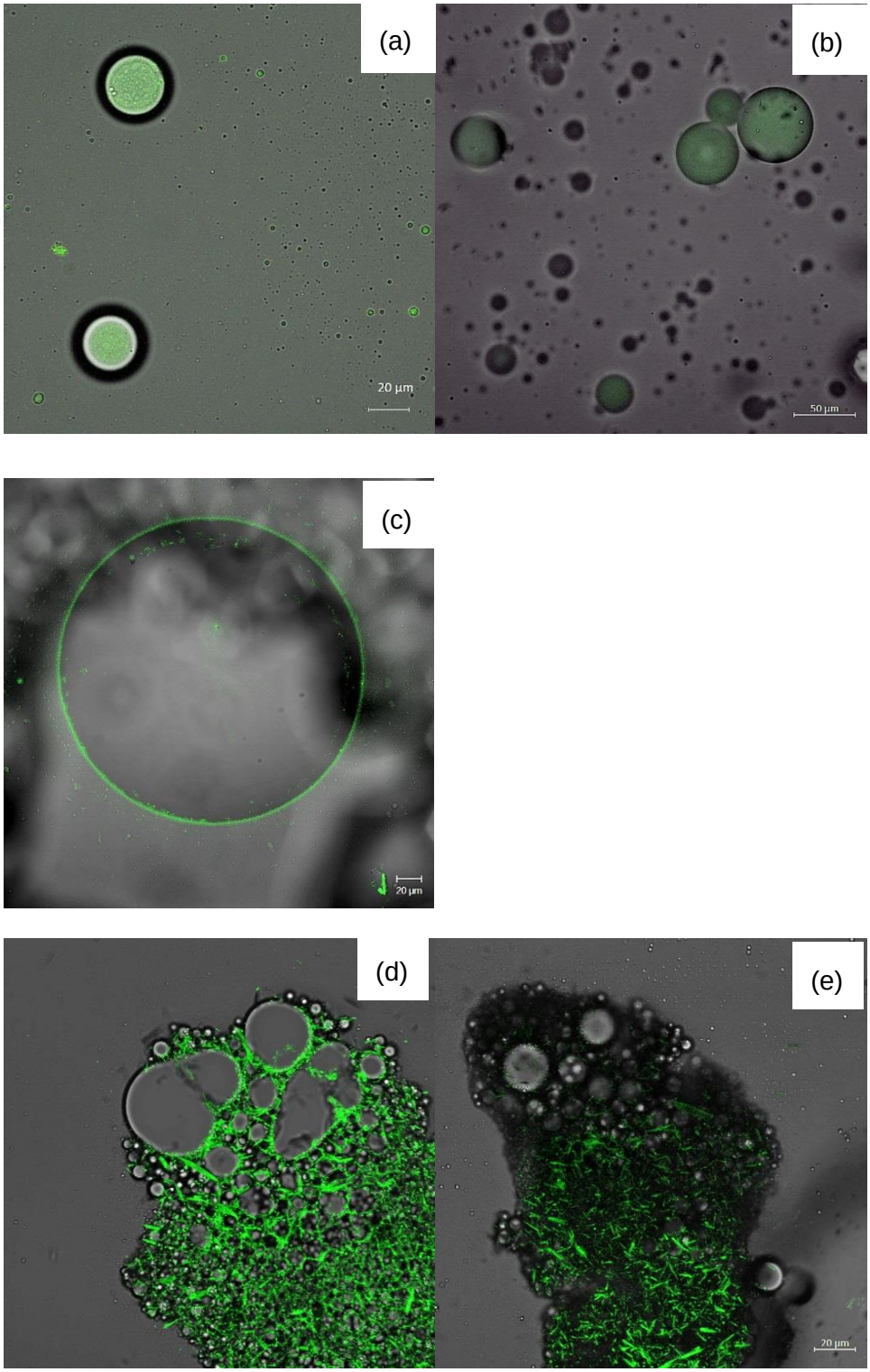

Figure 3-9 Confocal Laser Scanning Microscopy images of Pickering Emulsion with isoquercetin and 20 vol % of (a) paraffin oil (b) almond oil and (c) coconut oil. Isoquercetin and paraffin oil crystal aggregation seen in (d) and (e).

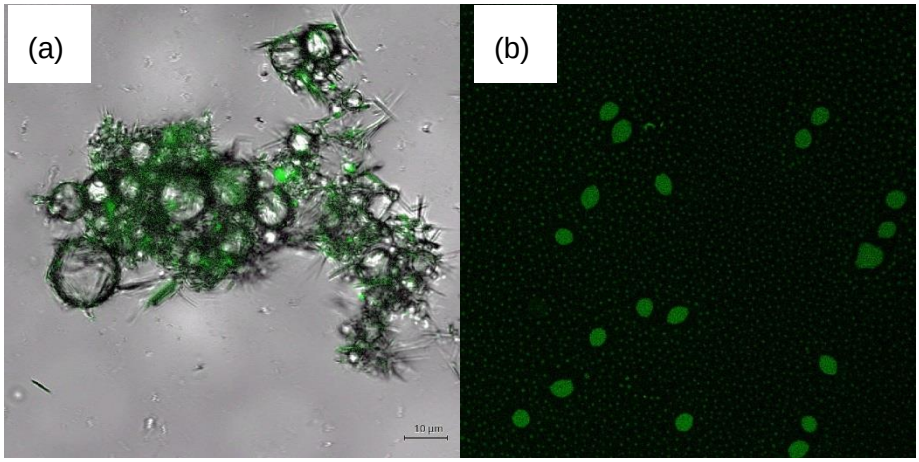

Figure 3-10. Confocal Laser Scanning Microscopy images Pickering Emulsion with isoquercetin and 20 vol % of (a) paraffin oil (b) almond oil.

3.4.9 Particle size distribution

Particle size distribution was attempted on the Pickering emulsions using with a Malvern Mastersizer diluted in distilled water and results tabulated in **Table XII**. Unfortunately, although attempted, results for the particle size distribution could not be determined from Pickering emulsions formed with isoquercetin and almond and coconut oil, or for quercetin and paraffin and almond oils. This could be because of emulsion collapse when added to the deionised water.

All Pickering emulsions formed with the flavonoids and oils were poly-disperse with ranges displayed in **Table XII (p 116)**. Pickering emulsions formed with rutin and paraffin and almond oil formed the smallest particle sizes with an average particle size of 295 and 186 µm respectively. Rutin and coconut oil formed a particle size much larger of 405 µm. The particle size distribution or rutin varied providing a poly-dispersed emulsion with a large volume density of small particle sizes in the range 0.15-4.0 µm then 30-650 µm. A smaller droplet in an emulsion pertains to higher emulsion stability, therefore the overall strength of Pickering emulsions based on droplet size:

Rutin Paraffin ≥ Rutin Almond > Rutin Coconut > Isoquercetin Paraffin > Isoquercetin Almond / Isoquercetin Coconut / Quercetin Paraffin / Quercetin Almond.

Table XII. Particle size distribution of droplets in Pickering emulsions formed with flavonoids and different oil types (N/A = not available). Average of 3 repetitions made immediately after homogenisation.

Flavonoid	Pickering Emulsion	Particle range (μm)	Average Particle size, (μm)
Rutin	Paraffin Oil	0.15-4.0; 30-650	295 ± 59
	Almond Oil	0.2-500	186 ± 42
	Coconut Oil	6.0-800	405 ± 27
Isoquercetin	Paraffin Oil	N/A	618 ± 115
	Almond Oil	N/A	N/A
	Coconut Oil	N/A	N/A
N	Paraffin Oil	N/A	N/A
	Almond Oil	N/A	N/A

3.4.10 Octanol-Water Partition Coefficient

Table XIII Experimentally determined Octanol-Water Partition Coefficient, $LogP_{o/w}$ of Flavonoids.

Flavonoid	Octanol – water partition coefficient, $LogP_{o/w}$
Rutin	-0.36 ± 0.05
Isoquercetin	0.53 ± 0.16
Quercetin	2.02 ± 0.09

3.5 Discussion

Pickering emulsions are particle stabilised droplets. The particle aggregation at the interface prevent droplet shrinkage, flocculation and coalescence via steric mechanism, and the strength of the stability depends on how easy it is to remove the particles from the interface (128). Flavonoid particles can be utilised to from Pickering emulsions due to their amphiphilic structure. When oil and water are mixed, a temporary dispersion of the two phases is formed before the two phases separate. To maintain separation, the flavonoid particles coating the oil droplets create stearic hinderance by adsorbing at the O/W interface, preventing coalescence of the oil droplets and creaming.

Particle Size

As the particles are adsorbed at the O/W interface, flavonoids forming Pickering emulsions can also improve the flavonoid solubilisation and stabilisation within a formulation for a cosmetic product. Improving the solubility of an active in a formulation is an important property of that active that is intended to partition from a topical formula and penetrate into the skin (3, 7, 39, 92).

In this research, the droplet size in Pickering emulsions formed varied in size (**Table XII** on p**116** and displayed in **Figure 3-11)**. Taking the average particle size, the smallest particle size was measured from rutin and almond oil PE, which was smaller than rutin and paraffin oil PE and 4 times smaller than particle size of rutin and coconut oil PE. Unfortunately, the only particle size distribution data obtained from isoquercetin was for the paraffin oil PE. The particle size of isoquercetin and paraffin oil were twice the size that of rutin and paraffin oil.

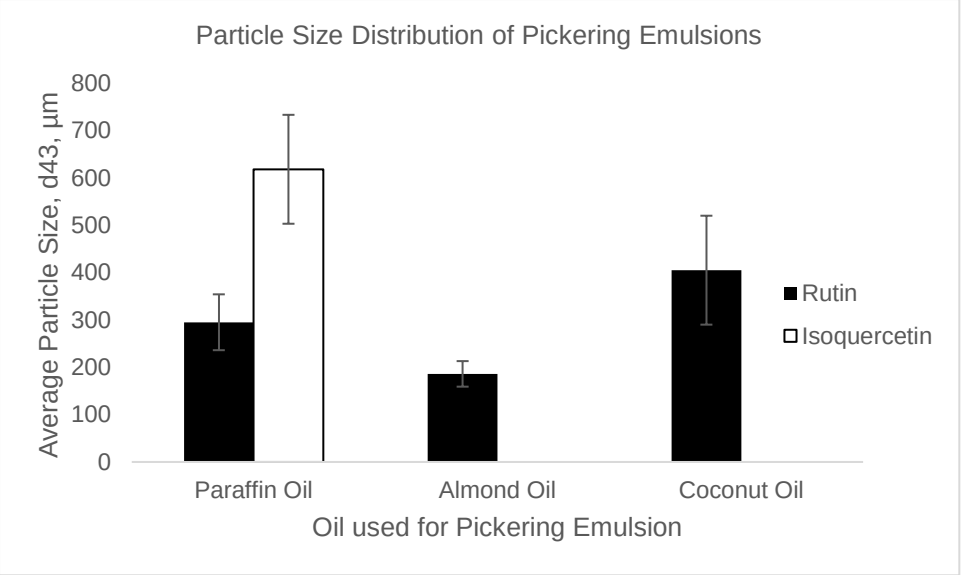

Figure 3-11 Particle size distribution of Pickering emulsions with flavonoids and different oil types. Data taken from Table XII.

Observing particle size distribution, all Pickering emulsions with rutin showed a poly-dispersion, with rutin and paraffin oil forming the smallest droplet sizes. Compared to surfactant stabilised emulsions, the droplet size in Pickering emulsions is usually larger (49) because the droplet cannot be smaller than the stabilising particle size. Emulsion stability can be improved by obtaining small oil droplet dispersions, however requires a large amount of energy to stabilise. A smaller droplet size leads to higher Laplace pressure with a large oil-water interface area and requires high amounts of energy to stabilise. Laplace pressure leads to Otswald ripening *i.e.* oil droplets form small to large oil droplets, and therefore particle size provides an indication of comparative stability.

. An experimental error with using a Mastersizer for quantification of particle size is that the equipment cannot distinguish the difference between emulsion droplet and particle crystals (49), therefore some of the data for particle size may be a distribution of emulsion droplet and flavonoid particle aggregates. Particle sizes were also done immediately after homogenisation, and could not be repeated on

storage samples due to equipment availability. It is essential for clear conclusions to be made that the measurements are repeated after 6 months to compared particle sizes.

Viscosity

Between samples there was no significant differences between viscosity, although rutin and paraffin oil did provide the highest value. As the particle size distribution showed that Rutin formed a poly dispersion with the smallest droplet size (**Table XII** on p**116**) and visually form CSLM images (section **3.4.8**), it suggests that the higher viscosity is attributed to the small particle size of rutin and paraffin oil PE. This PE also visusally showed the best emulsion stability, which may be attributed to the small particle size. Increasing the viscosity of the external aqueous phase with polymers can improve emulsion stability which will slow down coalescence and Ostwald ripening of the oil phase. However choice of polymer for aqueous thickening should be carefully selected in conjunction with flavonoids, as flavonoids are incompatible with anionic polymers (55). However, it was important in these first studies not to over complicate the system and make the formula too viscous with the addition of polymers. In further permeation assay analysis, when a highly viscous formula is applied on the donor side it would pose challenges in release kinetics data. This is because in a high viscous formula, a depletion of the concentration of the flavonoids from the bottom of the formula on the skin surface would occur, whereas the rest of the flavonoid would remain in the bulk formula “non-moving”; a high viscous formula reduces the thermodynamics of the permeant of interest (3).

Visual Stability

Collating data from visual inspection of the emulsions samples after 6 months (**Figure 3-2** to **Figure 3-6**), the Pickering emulsions which visually showed the most stable emulsions (lowest degree of visual phase separation) were in flavonoid order rutin > isoquercetin ≥ quercetin, and in oil order paraffin > almond ≥ coconut oil.

The order of flavonoids follow the order of increasing polarity. The determined octanol-water partition coefficient of the flavonoids are Rutin, -0.36, Isoquercetin, 0.56 and Quercetin 2.02 (**Table XIII p116**). This increasing polarity correlation is suggestive that the $LogP_{o/w}$ of the flavonoids in this research does influence the stability of the Pickering emulsions over time in storage. However other studies have shown that $LogP_{o/w}$ alone does not determine the viability of a flavonoid to form stable PEs (49).

Flavonoids outside the range of $\log P_{O/W}$ –0.6 < 0 are considered inadequate for forming Pickering emulsions as species that are strongly hydrophilic or lipophilic partition into the water or oil soluble phase more preferentially therefore do not stabilise the emulsion (49). Of these, rutin has the ideal lipophilicity to form the emulsion, however Pickering emulsions were seen to be formed initially with isoquercetin and quercetin and remain as emulsions 6 months later. Stability and partial wetting of isoquercetin and quercetin could be occurring in the early stages of PE formation, and over time the flavonoids migrate into the preferential phase (lipophilic portion). Another possibility is that quercetin and isoquercetin are forming large crystal aggregates as seen in the confocal images in section **3.4.8**. These large aggregates could form partial flocculation of the oil droplets. In aqueous and oil phases, quercetin could form aggregates as the solubility is very poor in both mediums (79). The wetted particles adhering to the interface will have a contact angle to the O/W interface. If the contact angle of the particle is too close to 0º or

180º then the emulsion will collapse as the free energy of spontaneous desorption will be low (49). Rutin particles have a contact angle with water which less than 90°(85) and therefore has a high de-absorption energy.

The order of oil stability is interesting. Paraffin oil is a hydrocarbon oil which is more polar compared to almond and coconut oils, and contains no naturally occurring emulsifying molecules such as fatty acids and triglycerides which can displace flavonoids adsorption at the O/W interface. This could be the main reason for a visual change in stability between flavonoid and oil type is observed after 6 months. In addition, almond oil and coconut oil are examples of vegetable oils with different melting points and physical states at room temperature (25 ºC); almond oil remains liquid whereas coconut oil is semi-solid and will melt upon skin temperature, 32-35 ºC. This would change the stability properties of the emulsion in storage as coconut oil solidifies below its melting point (25-27 ºC). A state change from liquid-solid will increase the density of coconut oil, increasing the force required to prevent phase separation, leading to obvious creaming.

The " control" emulsions, where the jet homogenisation step was omitted, showed no emulsion formation (**Figure 3-3**, **Figure 3-5** and **Figure 3-7**). Flavonoid particles showed sedimentation and the oil creaming. It is therefore conclusive that high energy input is essential to form Pickering emulsions and for particles to adhere at the O/W interface.

Location of Flavonoids in the Emulsions

The concertation of the flavonoids used in these Pickering emulsion was 1 mM aqueous as previous studies (49), therefore allow a valid comparison to research. In addition, as isoquercetin has not been studied to form Pickering emulsions, using a concentration of 1 mM also provides comparative date to literature. From CSLM images it can be seen that there is a layer of the flavonoid crystals around the oil

droplets, highlighted by self-fluorescence of the flavonoid particles. However, some flavonoids were observed as large aggregated crystals (**Figure 3-8** to **Figure 3-10).** **I**t is therefore unknown whether flavonoids, including rutin, form a uniform layer or a crystal aggregation around the oil droplets in the Pickering Emulsions. This may be due to self-assembly of the flavonoid particles, or the particles not being fully being dispersed in the system. At a concentration of 1 mM, the flavonoids are in excess (85) and not all flavonoid particles are located at the O/W interface; particles are seen to be in the external aqueous phase as a suspension (from visual inspection and from CSLM images).

pH

The pH between the PE systems does not differ significantly (**Table XI on p110**). The pH of the emulsions were slightly above the pK_a of the flavonoids (rutin pK_a 6.17, isoquercetin 6.17 quercetin 6.31 (51). Which means that the flavonoids are partially ionised form in the emulsions.. This will increase water solubility of the flavonoids and can change the emulsion stability (49).

Quercetin formed Pickering emulsions, although the hypothesis is that as it is more polar than rutin and isoquercetin, and does not posses sugar moieties that can provide stearic stabilisation, quercetin would not form stable PE. In addition, other studies found quercetin to form none or poor PEs (49).The pH of the system is above the p*Ka* of quercetin, therefore it is partially ionised, increasing water solubility. The spontaneous energy of de-adsorption of a particle from the O/W interface is high (49) therefore the stabilisation could be occurring as a combined result of the polarity of quercetin (2.02) which provide oil solubilisation, and the ionisation of the molecule that improves water solubility.

Conclusive remarks

Pickering emulsions were successfully made with flavonoids rutin, isoquercetin and quercetin together with paraffin, almond and coconut oils as seen by CSLM images and by visual observation. The greatest visual stability of flavonoids was in the order rutin > isoquercetin > quercetin, and in oil order this was paraffin > almond > coconut oil. Although quercetin and coconut oil PE did not form. In this research the degree of stability is a combination of flavonoid polarity, and oil type.

Particle size distribution data did not provide any meaningful conclusive data as particle size measurements could only be obtained for rutin PE samples, of which only slightly provide correlated stability data with observed data, and viscosity. However, more repetitive experiments on particle size are required.

As the pH of all the emulsion systems are slightly above the p*K*a of the flavonoids, they are in a partial ionised state which does increase their water solubility. This may effect the flavonoids adhereance to the O/W interface, thus emulsion stability.

The next chapters look at the flavonoid-lipid interaction within the *stratum corneum* of porcine epidermis and skin permeation assays with release kinetics. It will provide knowledge of both improved stability and skin permeation effects when incorporated into a Pickering emulsion.

Chapter 4 FT-IR analysis of the skin lipids

4.1 Introduction

The principle of topically applied actives is for them to penetrate into the skin through the *Stratum corneum* (SC), otherwise their function for benefits in deeper skin layers is lost. The rate limiting barrier of the SC is the “brick and mortar” structure from the corneocytes and the extracellular matrix (ECM), of which composes of tightly packed lipids; ceramides with varying molecular configuration, as well as cholesterol and free fatty acids.

Aliphatic chains of lipids in the ECM of the stratum corneum are arranged in all-*trans* conformation, which results in a dense crystal lattice structure. (1). This arrangement of the lipids is known as orthorhombic (OR) phase (1) and is indicative of an intact, impermeable barrier, attributed to a healthy skin condition. Changes in the lateral packing indicate a change in the permeability of the lipid matrix. Hexagonal (HEX) and liquid crystal (LIQ) disordered packing conformation indicate increased fluidity of the matrix (1). In HEX phases, the acyl chains become less densely packed and rotate in the crystal plane and in LIQ phases there is no organisation to the aliphatic chains, leading to disordered phase and highest permeability (1). As the lipid matrix prevents water loss from the body (19), an impaired barrier leads to higher water evaporation indicated by an increase in trans epidermal water loss (TEWL).

A higher permeability of the skin barrier also allows entry of particles from the external environment that can cause adverse skin irritation. Liquid crystal formation of the lipid packing would therefore be undesirable after topical application of a cosmetic. However, an impermeable barrier (OR phase) is also undesirable as penetration of active substances would be perturbed. Therefore a “balance” is

desired in the permeability of the SC barrier; OR-HEX phases of the ECM lipids favoured.

The lateral conformational order of the lipid chain packing can be evaluated by Attenuated Transform Reflectance Fourier Transform Infrared (ATR-FTIR) spectroscopy, a non-invasive technique that does not destroy the skin sample integrity. A change from orthorhombic to hexagonal to liquid crystal (OR-HEX-LIQ) lateral packing order is determined in ATR-FTIR transmittance spectra by:

(i) a shift to higher wavelength and broadening of the 2850 cm^{-1} peak (CH_2 symmetric stretching) which is an indication of the rotational motion of the alkyl chains in phase transition (1) and

(ii) the convergence of the two split scissoring modes at ~1468 cm^{-1} into one peak is an indication of OR-HEX-LIQ phase transition (1).

4.1.1 Aims and Objectives

The aims and objectives of this chapter are:

1. Can ATR-FTIR be used to decipher the stratum corneum lipid morphology?
2. Can changes in the lipid morphology be identified when a known skin penetration enhancer, oleic acid, is used compared to untreated skin?
3. What changes have occurred in the stratum corneum lateral packing conformation after skin permeation assays with Pickering emulsions, between different flavonoid and oil types?
4. Does the change of the lipid packing correlate with the release kinetics of the flavonoid from permeation data?

Using this technique will contribute to the understanding of what changes are occurring to the *Stratum corneum* after topical application of formulation.

Gaussian curve fitting function was used to determine peak location and bandwidth of the CH_2 symmetric stretching at ~2850 cm^{-1}, and of the CH_2 scissoring modes at ~1468 cm^{-1} with 2^{nd} derivative analysis to find hidden peaks. All results are based on FT-IR analysis of the *stratum corneum* of skin samples post permeation assay (n =3). Raw data shown in attached Appendix.

Section **4.2** displays the Fourier Transform Infrared transmittance spectra of the flavonoids rutin, isoquercetin and quercetin, and untreated porcine epidermis used in this experiment. They are displayed for the purpose of showing that the flavonoids used in this research cannot be identified on the epidermis surface and in addition validating that FT-IR analysis can be used for identifying SC lipid morphology according to literature. Following in section **4.3** contains the results for changes in lipid morphology after topical treatment and permeation assays using FT-IR spectra.

4.2 Fourier Transform Infrared Transmittance Spectras

4.2.1 Flavonoids

The Fourier Transform Infrared (FT-IR) transmittance spectra for the flavonoids used in this research are displayed in **Figure 4-1** where they have been superimposed. Rutin, isoquercetin and quercetin have identical vibrational spectra. There is a broad peak ~3250 cm^{-1} which is assigned to the hydroxyl O-H bond stretching (129), highlighted in **Figure 4-1**.

As the flavonoids differ only in structure by the presence and number of sugar groups, there is no comparative distinguishable peaks in vibrational spectra, which is why the spectra of each flavonoid overlap. The peak in the rutin spectra ~2300 cm^{-1} is due to the C-O bond stretching of CO_2 from air whilst measuring. This can be removed by ensuing measuring clamp is securely fastened.

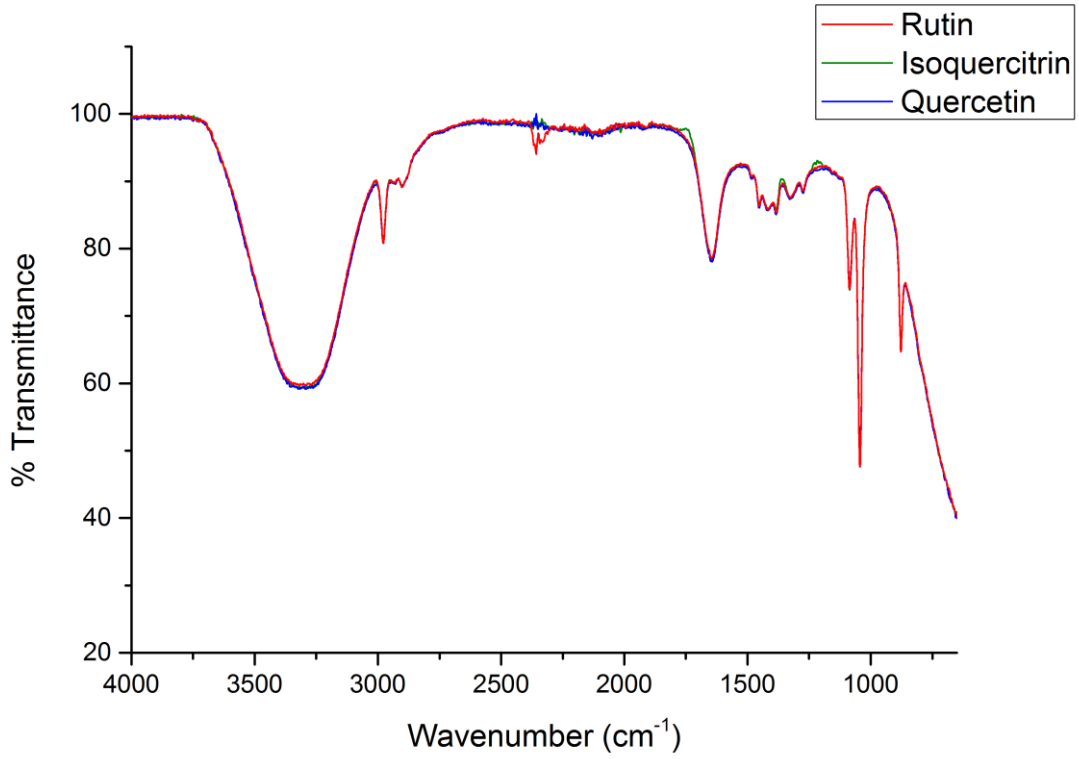

Figure 4-1 Fourier Transform Infrared Spectra of Rutin, Isoquercetin and Quercetin

4.2.2 *Stratum corneum* of porcine epidermis used in experiment (untreated)

Porcine epidermis is an acceptable membrane to use for *in vitro Stratum corneum* lipid morphology analysis. There are similarities in the lipid composition and morphology between human epidermis and porcine epidermis, both containing high ceramide, cholesterol and fatty acid content (130, 131). In using ATR-FTIR analysis, comparable peaks are present in *Stratum corneum* IR spectra of human, porcine and lipid models, namely the CH_2 symmetric stretching at ~2850 cm^{-1} and CH_2 scissoring at ~1460 cm^{-1} (12, 22, 31). The FT-IR transmittance spectra of untreated (control) porcine stratum corneum used in this research (**Figure 4-2**).The regions of interest in the FT-IR spectra for determining the lipid chain conformation in the SC in ordered orthorhombic (OR) phase or disordered hexagonal (HEX) and liquid crystal (LIQ) phases are summarised in **Table XIV**.

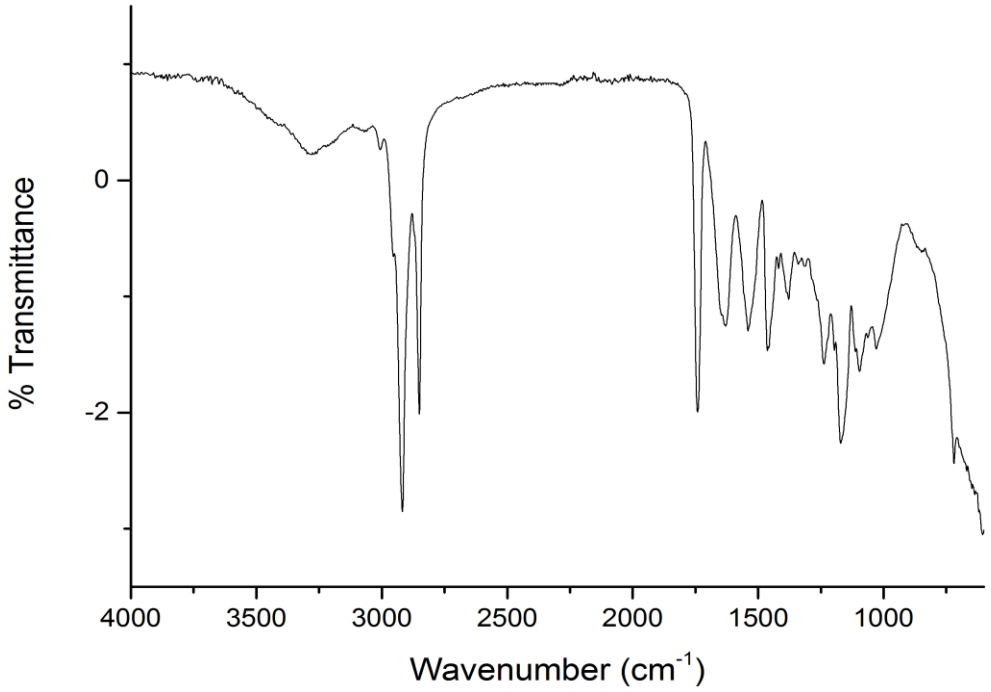

Figure 4-2 Fourier Transform Infrared Spectra of Porcine Epidermis. Assignments in Table XIV

Table XIV Assignment of peaks in porcine epidermis spectra to determine lateral packing conformation of the lipids in the Stratum corneum (1, 12)

Wavenumber cm^{-1}	Group Assignment	Lipid Packing Arrangement
2920	Asymmetric CH_3 stretching	Shift to higher wavelength and broadening of the peak indication of disorder phase transition
2850	Symmetric CH_2 stretching of the acyl chains	Shift to higher wavelength and broadening of the peak indication of disorder phase transition
1740	Ester C=O stretching – triglycerides/phospholipids	Sensitive marker of hydrogen bond formation.
~1630	Amide I band (80% C=O) (Normalised)	Sensitive to hydrogen bond formation and used for normalisation
1540	Amide II (60% NH bending)	Sensitive marker of hydrogen bond formation.
1463-1468	Symmetric CH_2 scissoring	Splitting into two separate bands indicative of orthorhombic phase. Convergence of two scissoring peaks indicative of disordered phase transition.
728/721/720	CH_2 rocking	Phase transitions OR/HEX/LIQ

4.2.3 Flavonoids and *Stratum corneum* lipid spectra superimposed

The FT-IR analysis in this experiment was used for the determination of the aliphatic chain packing order of the lipids in the extracellular matrix within the *Stratum corneum*. However, FT-IR spectra of the skin samples after permeation assays were further analysed to identify any peak markers specific to flavonoids. Flavonoid spectra was first superimposed over the untreated porcine epidermis spectra to observe any overlapping or distinguished peaks **Figure 4-3** and in **Figure 4-4** which display zoomed in regions of the spectra at 4000 – 1450 cm^{-1} and 1450 – 650 cm^{-1}. These spectra clearly indicate that ATR-FTIR could not be used for identifying flavonoids on the skin surface in post-permeation assays as all three flavonoids show overlapping peaks with the SC spectra. Therefore ATR-FTIR could only be used for identifying SC lipids and change in morphology.

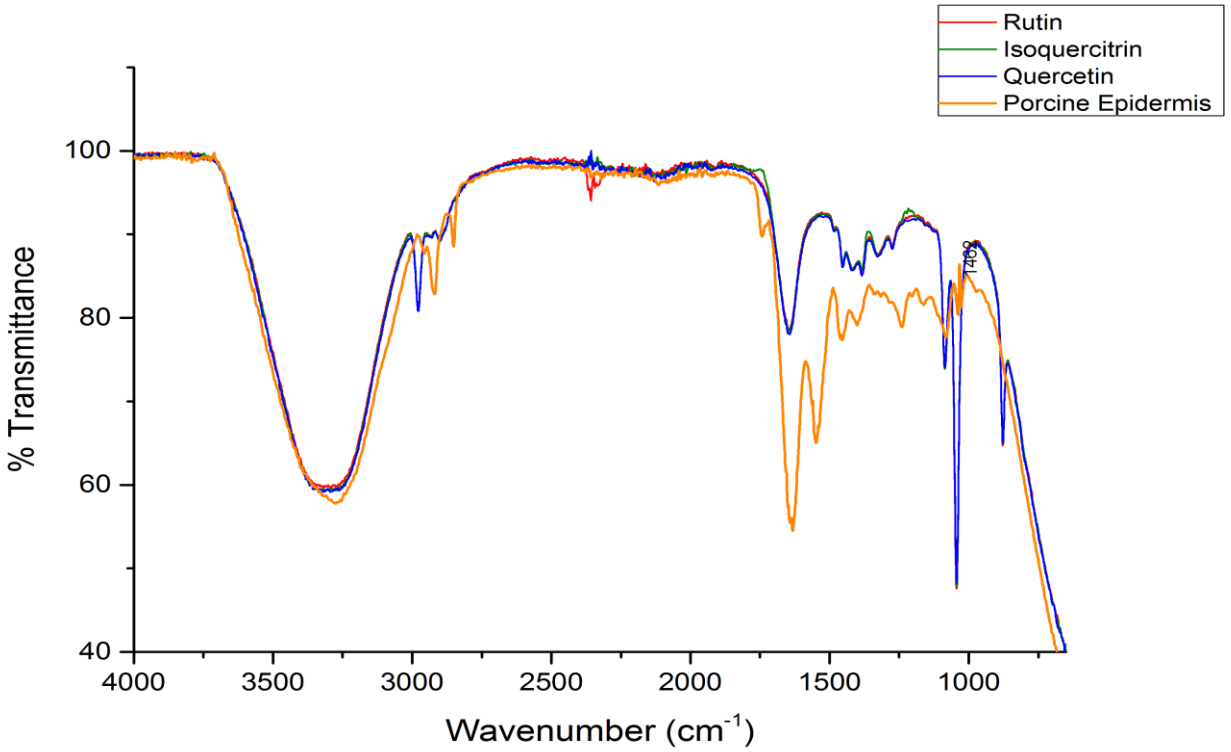

Figure 4-3 Fourier transform infrared transmittance spectra of rutin (red), isoquercetin (green) and quercetin (blue) superimposed with porcine stratum corneum lipids (orange) transmittance spectra.

(a)

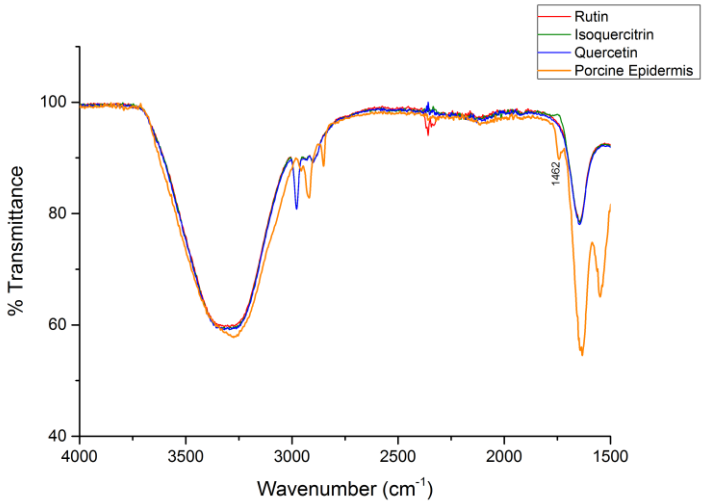

(b)

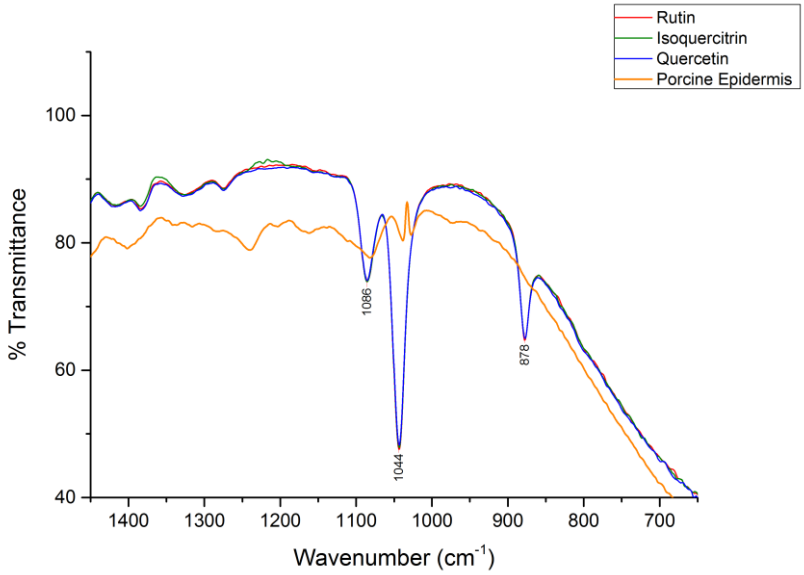

Figure 4-4 Fourier transform infrared transmittance spectra of rutin, isoquercetin and quercetin superimposed with porcine epidermis control, at spectral regions (a) 4000 – 1450 cm^{-1} and (b) 1450 – 650 cm^{-1}

4.3 Changes in lipid morphology in porcine *Stratum corneum* after topical treatment and permeation assays

4.3.1 Change in SC lipid packing with oleic acid: positive control:

Oleic acid (OA) is a long chain mono-unsaturated fatty acid, and in the *cis* configuration is a known permeation enhancer that changes the lipid domains and morphology in the SC (64). OA is thought to fluidize the lipids and cause phase separation (65).

An aqueous dispersion of OA was used to observe effect on the lateral packing morphology of the skin lipids compared to skin not exposed to OA. This was done to validate the analytical method for lipid chain packing in conjunction with literature. Oleic acid is not soluble in water, however is soluble in ethanol. Water was used only to be representable to the other solutions used in this study. Using ethanol would have cause further disruption to the lipid chain packing and not been representable of oleic acid action (64).

Table XV Curve fitting results using *Gaussian* function on the FT-IR transmittance spectra of (a) Lipid chain CH_2 scissoring and (b) Lipid chain CH_2 symmetric stretching within Porcine *Stratum corneum* (SC) after topical treatment with oleic acid.

(a)

	CH_2 Scissoring mode				
	R_2 value	Reduced Chi-Squared	**Peak 1** cm^{-1}	**Peak 2** cm^{-1}	**Distance between split peaks** cm^{-1}
Untreated SC	0.99	2.02E-04	1463.1	1469.95	6.85
SC with oleic acid 5%	0.99	3.57E-05	1465.28	1470.25	5
SC with oleic acid 10%	0.99	2.34E-05	1464.19	1469.47	5.3

(b)

	CH_2 Symmetric stretching mode				
	R_2 value	Reduced Chi-Squared	**Peak** cm^{-1}	**Peak shift from untreated SC** cm^{-1}	**Peak width (FWHM)**
Untreated SC	0.99	7.24E-04	2851.6	n/a	17.24
SC with oleic acid 5%	0.98	2.98E-05	2853.50	1.87	17.89
SC with oleic acid 10%	0.97	1.44E-05	2853.93	2.33	19.27

FWHM – Full width at half maxima

From the results in **Table XV** it can be deduced that the oleic acid is having an effect on the lipid chain conformation order of the porcine *Stratum corneum*.

The lipid chain CH_2 scissoring mode in **Table XV (a)** showed a slight change in peak position; the distance between split peak position of oleic acid samples narrowing slightly, compared to the untreated SC which is indicative of the peak convergence. Peak 1 position of CH_2 scissoring mode for oleic acid samples shifted to a higher wavelength compared to the untreated SC. These changes indicate a phase change

from orthorhombic to hexagonal (OR-HEX). Liquid crystal phase transition occurs when there is a complete convergence of the two-split peaks in the CH_2 scissoring mode, which was not seen in these results.

A much more sensitive marker is the lipid chain CH_2 symmetric stretching at 2850 cm^{-1} , **Table XV (b)**. Oleic acid sample showed a bathchromic shift in wavenumber of the CH_2 symmetric stretching bandwidth to ~2854cm^{-1} and an apparent broadening of the peak indicated by an increase of peak width compared to the untreated sample. This indicates phase transition from OR to HEX, and therefore a change in the barrier properties of the SC.

As this preliminary experiment demonstrates, a difference of the lipid conformation has been observed between untreated skin samples and skin samples treated with a known skin permeation enhancer. Therefore this experimentation is a useful technique to use in identifying lipid chain confirmation post-permeation assays with Pickering emulsions and flavonoids. In addition, curve fitting procedure with the *Gaussian* function was appropriate as the R_2 values were > 0.97 (**Table XV**)

Other skin permeation enhancers could have been used such as ethanol, which changes the lipid morphology by removing and depleting the SC lipids (64). Oleic acid was used as it is a well-studied permeation enhancer and it is also present in the almond oil (refer to section **1.4.4** on p**35** in literature review), which serves a discussion point later on in the chapter.

4.3.2 Vegetable and mineral oil

Table XVI Curve fitting results using *Gaussian* function on the FT-IR transmittance spectra of (a) Lipid chain CH_2 scissoring and (b) Lipid chain CH_2 symmetric stretching within Porcine *Stratum corneum* (SC) after topical treatment with 20 % oil in aqueous.

(a)

	CH_2 Scissoring mode				
	R_2 value	Reduced Chi-Squared	**Peak 1** cm^{-1}	Peak 2 cm^{-1}	**Distance between peaks** cm^{-1}
Untreated SC	0.99	2.02E-04	1463.1	1469.95	6.85
SC with Paraffin Oil	0.99	8.22E-05	1467.93	1470.36	2.43
SC with Almond Oil	0.98	2.18E-05	1467.03	1470.28	3.25
SC with Coconut Oil	0.99	2.27E-05	1467.2	1469.88	2.68

(b)

	CH_2 Symmetric stretching mode				
	R_2 value	Reduced Chi-Squared	**Peak** cm^{-1}	**Peak shift from untreated** cm^{-1}	Peak width (FWHM)
Untreated SC	0.99	7.24E-04	2851.6	n/a	17.24
SC with Paraffin Oil	0.96	7.37E-05	2852.2	0.6	21.3
SC with Almond Oil	0.98	2.18E-05	2852.7	1.1	2.7
SC with Coconut Oil	0.98	1.11E-04	2582.8	1.2	17.6

FWHM – Full width at half maxima

Skin samples treated with an oil-water dispersion showed a change in lipid morphology compared to untreated skin samples (**Table XVI**). The lipid chaine CH_2 scissoring split results displayed in **Table XVI (a)** showed a narrower distance between split peaks and a shift of peak 1 to a higher wavenumber compared to

untreated SC, indicative of possible convergence of peaks to from orthorhombic to hexagonal lipid morphology.

In the lipid chain CH_2 symmetric stretching results, **Table XVI (b)** , peaks for SC treated with oil dispersions shifted to higher wavelength, compared to untreated SC. This indicative of phase transition from OR-HEX of the SC lipids when treated with oil solutions. Furthermore, the vegetable oils displayed a greater bathchromic shift of the CH_2 symmetric stretching compared to paraffin oil; almond and coconut oils shifted by 1.1 and 1.2 cm^{-1} respectively, paraffin oil shifted by 0.6 cm^{-1}. The vegetable oil contain naturally occurring fatty acids that can change the lipid morphology of the SC more so than paraffin oil (for fatty acid composition of almond and coconut oil see literature review section **1.4.4 on p35**). The effect of oil type on lipid morphology is discussed in further detail in section **4.4.1.** The calculated peak widths showed some discrepancies; both paraffin and coconut oil widths were slightly broadened, however the peak for almond oil sample was very small.

4.3.3 The effect of *Stratum corneum* lipid morphology after treatment with Flavonoid Pickering emulsions with different oil types.

Results for the lipid chain CH_2 scissoring modes and CH_2 symmetric stretching mode are in **Table XVII** and **Table XVIII** respectively. The *Gaussian* function was a good fit for the CH_2 scissoring modes as the R_2 values for this fit were > 0.97 and >0.95 for the CH_2 symmetric stretching.

Table XVII Curve fitting results using *Gaussian* function on the CH_2 scissoring of porcine *Stratum corneum* (SC) lipids after treatment with Pickering emulsions and controls

	Oil Type	R_2 value	Reduced Chi-Squared	**Peak 1** cm^{-1}	**Peak 2** cm^{-1}	**Distance between peaks** cm^{-1}
Untreated SC		0.99	2.02E-04	1463.1	1469.95	6.85
	Pickering Emulsions					
Rutin	PO	0.99	3.23E-06	1462.1	1468.4	6.3
	AO	0.99	3.67E-05	1462.3	1468.3	6.0
	CO	0.99	1.49E-06	1466.6	1469.6	3.0
Isoquercetin	PO	0.97	0.002	1462.6	1469.7	7.1
	AO	0.99	1.97E-04	1462.4	1467.7	5.3
	CO	0.97	8.05E-05	1463.1	1468.9	5.8
Quercetin	PO	0.97	0.001		1466.6	
	AO	0.97	0.005		1466.6	
	Control Emulsions					
Rutin	PO	0.99	1.19E-05	1462.1	1468.4	6.3
	AO	0.99	4.07E-04	1462.6	1467.8	5.2
	CO	0.98	3.67E-04	1462.8	1469.6	6.8
Isoquercetin	PO	0.98	2.38E-04	1461.9	1468.2	6.3
	AO	0.98	2.64E-04	1462.6	1469.2	6.6
	CO	0.98	3.49E-04	1464.1	1470.4	6.3

Quercetin	PO	0.99	4.96E-05	1462.3	1468.3	6.0
	AO	0.99	3.48E-04	1464.8	1469.8	5.0

PO = paraffin oil, AO = almond oil, CO = coconut oil

The CH_2 scissoring split peaks were closer together for the vegetable oil Pickering emulsions with rutin and isoquercetin compared to untreated SC and corresponding paraffin oil PEs, indicated by a decrease in distance between peaks value. This indicates presence of an orthorhombic-hexagonal phase transition in the lipid packing conformation as a result from vegetable oil in the formula samples. Rutin PE with coconut oil showed the greatest narrowing between peaks of 3.0 cm^{-1}, compared to the untreated SC (6.85 cm^{-1}) and paraffin oil, (6.3 cm-1). Quercetin in a Pickering emulsion with both paraffin and almond oil skin samples displayed only one peak at 1466 cm^{-1} indicating a liquid crystal phase of the SC lipids and a disrupted barrier.

Control emulsions did not show distinct changes in distance between the peaks, although split peaks for all samples were closer together compared to the untreated SC.

Table XVIII Curve fitting results using *Gaussian* function on the CH_2 symmetric stretching of porcine *Stratum corneum* (SC) lipids after treatment with Pickering emulsions and controls

	Oil Type	R_2 value	Reduced Chi-Squared	**Peak** cm^{-1}	**Peak shift from control** cm^{-1}	**Peak Width (FWHM)**
Untreated SC		0.99	7.24E-04	2851.6	n/a	17.24
	Pickering Emulsion					
Rutin	PO	0.98	5.25E-05	2852.2	0.57	4.68
	AO	0.98	8.61E-05	2852.7	1.06	6.09
	CO	0.98	0.00133	2852.7	1.1	18.38
Isoquercetin	PO	0.99	2.15E-04	2852.2	0.64	16.19
	AO	0.98	2.85E-04	2853.4	1.78	17.76
	CO	0.97	0.002	2852.1	0.46	16.86
Quercetin	PO	0.92	0.001	2852.2	0.50	17.51
	AO	0.98	0.003	2852.6	1.03	17.19
	Control Emulsions					
Rutin	PO	0.99	7.19E-05	2852.7	1.05	15.29
	AO	0.99	1.09E-04	2853.1	1.46	15.77
	CO	0.99	1.66E-05	2852.7	1.08	15.53
Isoquercetin	PO	0.98	2.29E-05	2852.9	1.26	6.44
	AO	0.99	2.19E-05	2853.1	1.48	16.25

	CO	0.99	2.56E-05	2852.3	0.66	14.22
Quercetin	PO	0.99	1.44E-04	2852.2	0.57	16.81
	AO	0.99	4.22E-04	2852.0	0.37	15.24

PO = paraffin oil, AO = almond oil, CO = coconut oil. FWHM – Full width at half maxima

The shift in peak position of the CH_2 symmetric stretching at ~2851 cm^{-1} has occurred for all skin samples after skin permeation studies, displayed in **Table XVIII**. Compared to untreated skin at 2851.6 cm^{-1}, the smallest peak shift was from the control with quercetin and almond oil (0.37 bathochromic shift) and the highest shift was from Pickering emulsion with isoquercetin and almond oil (1.78 bathochromic shift).

The CH_2 symmetric stretching shift in peak position form the untreated skin sample in **Table XVIII** is graphically represented in **Figure 4-6, p146.**

4.4 Discussion - Altered barrier function of *Stratum corneum* as a result of changes in lipid morphology of the extracellular matrix

Several vibrational modes are indicative of phase transitions of the lipid packing conformation (**Table XIV**). The two markers prevalent in literature are the CH_2 symmetric stretching at ~2850 cm^{-1} and the CH_2 scissoring at ~1463 - ~1470 cm^{-1}. Changes in both these markers were seen in this research, indicating that after permeation assays the SC barrier function was changing which can influence the percutaneous permeation behaviour of the flavonoids.

The CH_2 scissoring bands for orthorhombic packing shown a split doublet peak at ~1463 and ~1473 cm^{-1} (1, 12, 132). The split peaks are a result of a short-range bending of the C-H chain in a planar movement (scissoring). These are interactions of the acyl chains, and indicates that a large number of lipids are present in a tightly packed, orthorhombic conformation (132). Convergence of the split peaks into a single peak and a shift in bandwidth indicate hexagonal phase (1468 cm^{-1}) and liquid crystal phase (1466cm^{-1}) (1, 12).

An illustration of the change in distance between split peaks of the CH_2 symmetric stretching modes between flavonoid and oil types, comparable to untreated SC are displayed in **Figure 4-5**.

(a)

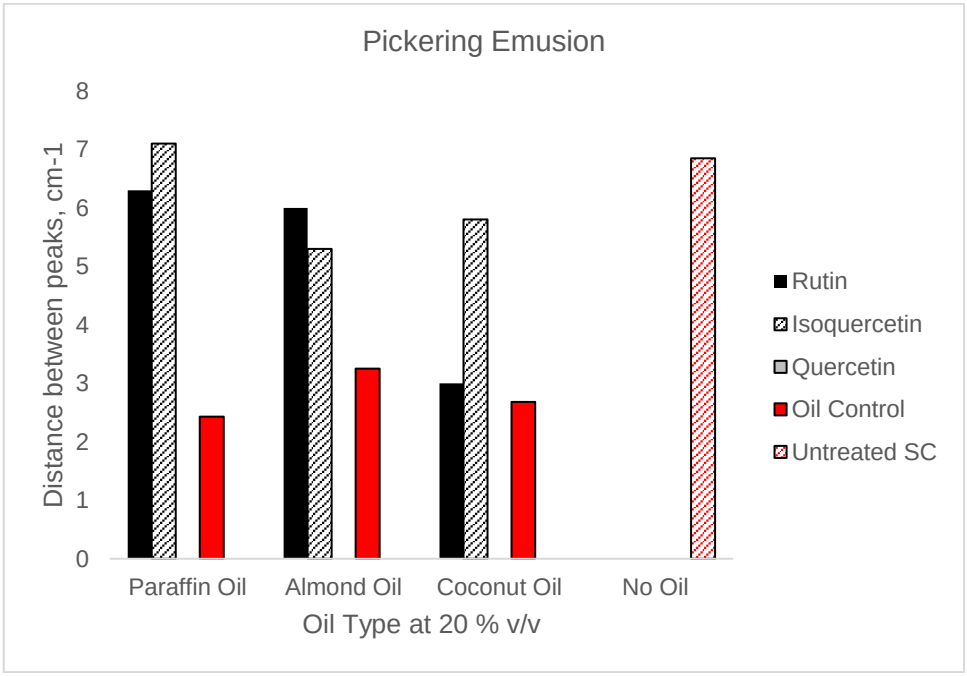

(b)

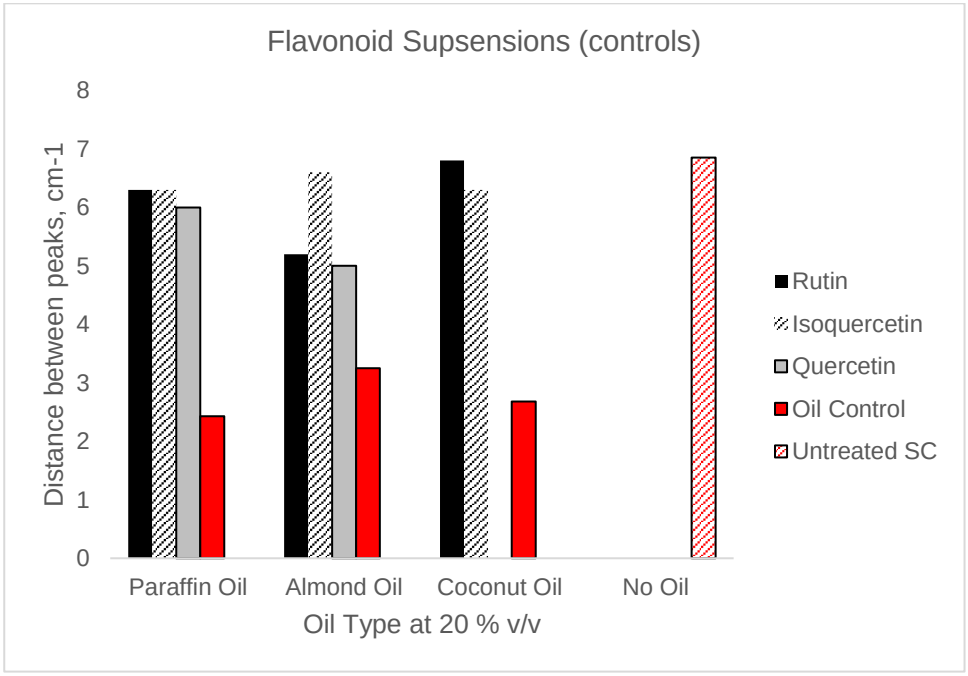

Figure 4-5 Distance between split peaks of the CH2 Scissoring mode, indicative of lipid conformation change in the *Stratum corneum* after FT-IR analysis. (a) After Pickering emulsion treatment and (b) after flavonoid suspensions (Pickering emulsion control). Data displayed from Table XVI on p136 and Table XVII on p138.

This graph shows that the oils alone have a greater effect on barrier properties, indicated by the CH_2 scissoring modes; a shorter distance between peaks, which implies orthorhombic – hexagonal lipid packing transition. The effects of oil solutions alone had more of an effect on lipid transformation than the Pickering emulsions with flavonoids + oil, as the latter had a greater distance between peaks, not significantly different from the untreated SC control. This indicates that flavonoids coating oil droplets may affect the barrier properties of the SC lipids by preventing oil contact with the SC. As there was no difference in peak distance for the flavonoid suspensions (PE controls), flavonoid particles within a solution with oil are still perturbing the oil from affecting the SC lipids. This could be due to flavonoid particle aggregation and crystallisation forming on the SC as the water evaporates from the surface.

However, an interesting observation is the SC samples with quercetin. For PE samples, there was a convergence of the CH_2 scissoring peaks indicative of a liquid crystal phase transition of the lipids which is a highly disrupted barrier. Whereas when in a suspension with the oil and no PE formation, the distance between CH_2 scissoring peaks is not affected and is similar to that of the untreated SC. A possible theory is that after high shear jet homogenisation, quercetin particles are forced into and preferentially solubilised into the oil phase droplets. As the water evaporates, quercetin particles will remain in the oil phase which allows for greater partition into the SC lipids, where quercetin can cause additional lipid phase disruption. Within the control suspensions, quercetin remains as a particle dispersion which crystallises on the SC surface as the water evaporates.

As previously mentioned, a key additional experiment that would help this theory is analysis of the oil phases after jet homogenisation, and the solubility of these flavonoids, particularly quercetin, in paraffin, almond and coconut oils.

Coconut oil and rutin PE had a similar effect on the lipids as the distance between split peaks was shorter than other PEs, comparable to the oil alone.

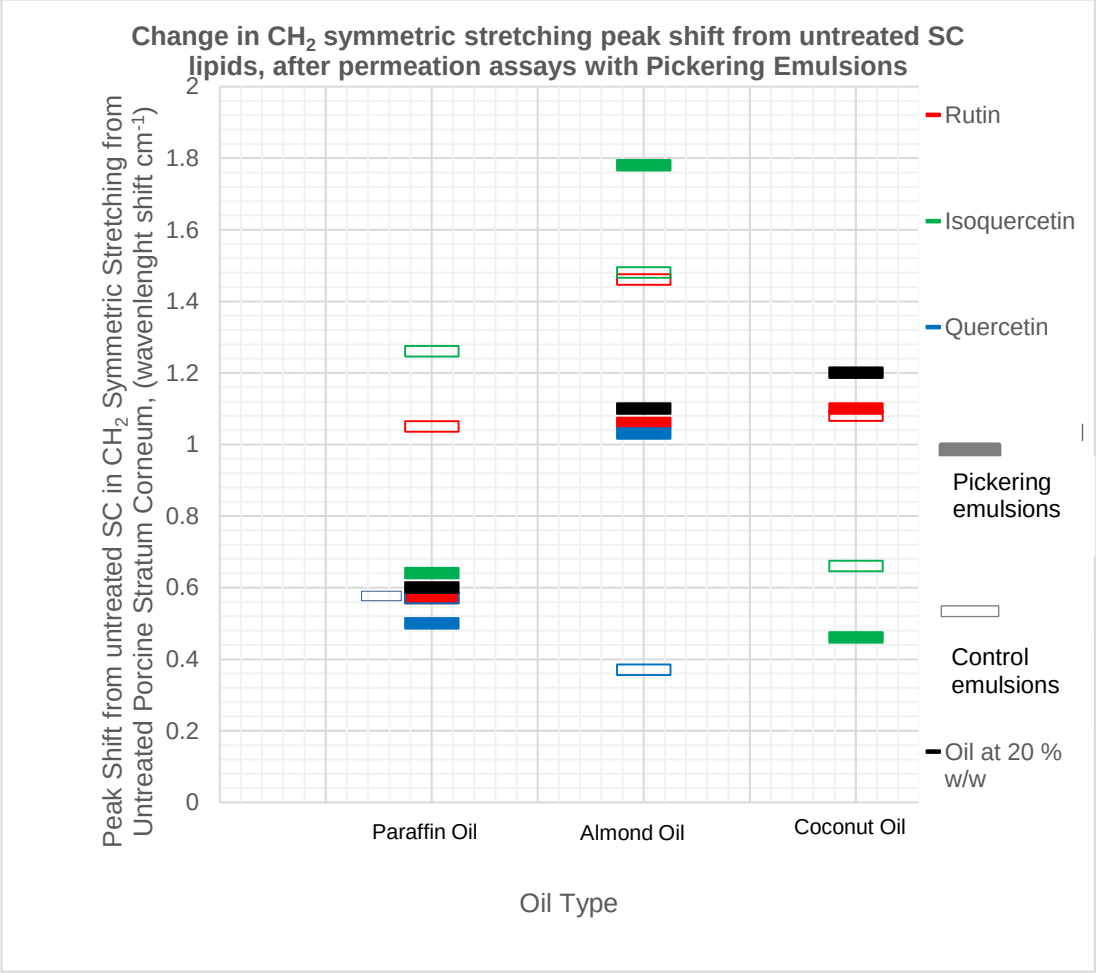

Figure 4-6 Bathochromic shift in peak position of the CH_2 symmetric stretching lipid chains in porcine *Stratum corneum* (SC) skin samples after skin permeation assays. Shift from untreated SC. Rutin (red), Isoquercetin (green), quercetin (blue), Pickering emulsion (solid colour) and corresponding controls outlined box. Oil controls (black) were 20 % paraffin, almond and coconut dispersions alone.

The symmetric stretching of the CH_2 mode ~2850 cm^{-1} is a dominant marker of the lipid conformation and is extremely sensitive to phase change and of any interactions with compounds and the lipid membrane (12). As space between the acyl chains become larger, C-H stretching bond absorbs higher energy, lending to a higher absorbed frequency and thus higher wavenumber position (129). An increase

in wavenumber, bathochromic shift, is therefore an indication of lipid transition from orthorhombic – hexagonal – liquid crystal packing.

The results of the shift in CH_2 symmetric stretching for pure oils (**Table XVI (b)**), Pickering emulsions and control emulsions (**Table XVIII)** are displayed in **Figure 4-6** which poses as a useful illustration to refer to within the discussion and findings

From **Figure 4-6**, comparing flavonoids, quercetin had the lesser effect on changing the lipid conformation (blue solid and open box) which is shown by a small bathochromic shift compared to untreated SC, indicating orthorhombic-hexagonal lipid phase and a slightly disrupted SC barrier. Quercetin in a PE with almond had the greatest disruption out of the quercetin samples.

Comparing flavonoids, isoquercetin (green solid and open box) and rutin (red solid and open box) have more effect on the lipid chain packing detected by the CH_2 symmetric stretching mode, especially when in a free suspension and not in a Pickering emulsion. However, when coconut oil is combined with rutin and isoquercetin in a Pickering emulsion or dispersion (control), the shift in CH_2 symmetric stretching is lowered.

Oils alone (black box) depict that all three oils do change the lipid packing, as seen in CH_2 scissoring mode. The vegetable oils almond and coconut oil alter the lipid packing of the SC more than paraffin oil, thus causing a disrupted barrier. When the oils are stabilised in a PE with flavonoids, the peak shift was similar or lower than that of the oil solution alone. However greatest disruption between oil types was seen when the oils were not in a Pickering emulsion with the flavonoids, and in an unstable suspension (controls).

A noteworthy consideration is that the CH_2 symmetric stretching results do not fully correlate with the CH_2 symmetric stretching results.

4.4.1 *Stratum corneum* lipids disrupted by oil type

The vegetable oils, compared to paraffin oil, showed a greater disruption of the lipid chains both in the oil controls Pickering Emulsions (PE) and control emulsions (**Figure 4-6**). The vegetable oils had the highest degree of disruption of the lipid chains; changes in lipid transition from orthorhombic to hexagonal lateral packing, seen by the FT-IR transmittance spectral changes in the lipid chain CH_2 scissoring and CH_2 symmetric stretching modes (**Table XVI p136, Table XVII p138 and Table XVIII p140**). This is an interesting observation when the fatty acid compositions of the oils is noted. Fatty acid composition of the almond and coconut oils were not conducted in this study, therefore literature provides fatty acid composition guidance of these oils which are displayed in **Table XIX**.

Table XIX Predominant fatty acid composition in (a) almond oil and (b) coconut oil. a(Pantzaris and Basiron 2002) (61) b(Roncero et al. 2016) (62)

(a)

Predominant fatty acids in almond oil	% mass	Chain length saturation
Oleic acid	57.5-78.[7a]	C18:1
Linoleic acid	12.0 – 33.9 [a]	C18:2
Palmitic acid	5.2 – 6.7 [a]	C16:0
Strearic acid	0.2 – 1.7 [a]	C18:0
Palmitoleic acid	0.3 – 0.6 [a]	C16:1

(b)

Predominant fatty acids in coconut oil	% mass	Chain length saturation
Lauric acid	45.1-50.3[b]	12:0
Myristic acid	16.8-20.6 [b]	14:0
Palmitic acid	7.7 – 10.2 [b]	16:0
Oleic acid	5.4 – 8.1 [b]	18:1
Capric acid	5.5 – 7.8 [b]	10:0

Fatty acids, notably oleic acid have been investigated in permeation enhancement studies (63, 133, 134). Fatty acids can disrupt the lipid packing of the lipid matrix within the stratum corneum (135) and the effect dependent on the chain length and saturation/degree of unsaturation (63). A study by Kandimalla et al. 1999 looked at the effect of fatty acids on the permeation of melatonin and the relationship between the fatty acid enhancement and trans epidermal water loss. Saturated fatty acids with chains < 12 disrupt the lipid barrier and long chain fatty acids with 14 or greater carbons are important for the improved barrier (orthorhombic lateral packing) of the

lipids (63, 132). Results from Kadimalla at al. 1999 were taken and interpreted into **Figure 4-7** to depict the changes in lipid barrier function after fatty acid application.

The fatty acids present in almond oil are predominantly in the form of triglycerides, the most abundant being the triglyceride of oleic acid (57 – 78 %) (61). As almond oil has a high content of oleic acid, a “disruptive” fatty acid, it is accountable for the results seen in this study which show there is a higher degree of discorded lipids in SC, compared to untreated SC and SC treated with paraffin (**Figure 4-6**).

Coconut oil has a high content C_{12} and C_{14} unsaturated fatty acids (lauric and myristic acid, respectively, **Table XIX (b)**), and therefore explains why coconut oil has a lower change in lipid transition compared to almond oil. However, in addition it also contains oleic acid (5 – 8 %) (62) that as previously mentioned can disrupt the SC lipids. Coconut oil may simultaneously disrupt and repair the lipid barrier in the SC, which accounts for its lower disruptive effect on the SC lipids compared to almond oil, yet higher lipid disruption than paraffin oil. The lauric acid and myrisitic acids are also responsible for coconut oils sharp melting point (61). Due to the high level of unsaturated fatty acids, coconut oil is also very stable to oxidation (61).

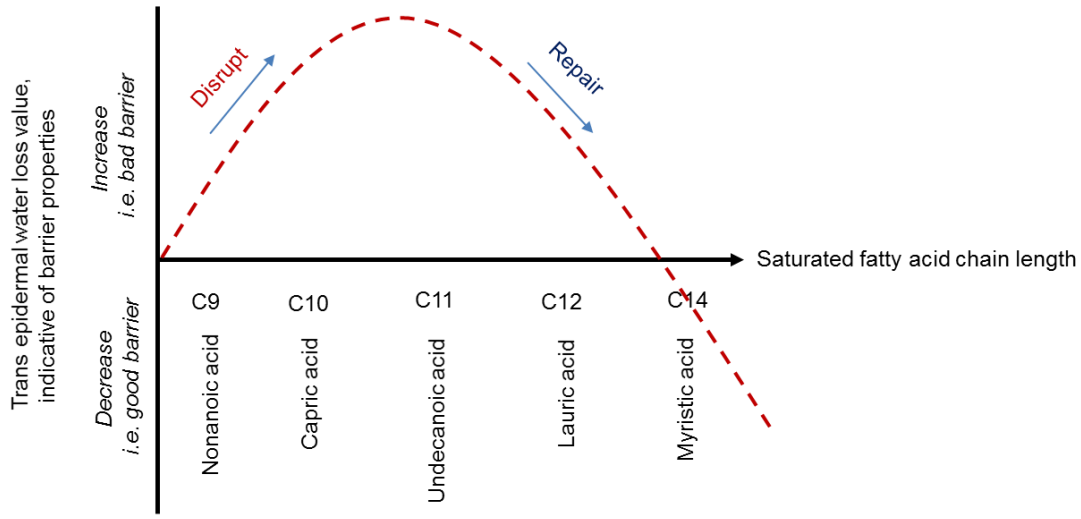

Figure 4-7 Interpretation of Kandimalla at al. 1999 results on *Stratum corneum* barrier properties after application of different saturated fatty acid chains, (63).

Other studies in literature have also investigated how far into the *Stratum corneum* mineral and vegetable oils can permeate, which is important in understanding the affect the oils in this study are having on the SC membrane. Both mineral and vegetable oils penetrate the upper layers of the SC 1 hour after application (136) however both oil types have been found not to permeate the skin further than the stratum corneum. These oils have been found to absorb onto the surface of the skin and are located surrounding the corneocytes in the lipid matrix in the first few layers of the SC (136-138).

In addition, vegetable oils have been found not to penetrate deeper than 11 µm into the stratum corneum in both human and porcine skin, and no SC swelling was observed (139). As the chain conformation and lateral packing of the lipids are at a maximum at a depth of 4-8 µm (20 – 40 %) into the SC, (140), the vegetable oils in this study would affect the extracellular matrix (ECM) lipids detected by FT-IR. This disruption would aid the permeation of flavonoids through the SC.

A study by Patzelt *et al.* (2012) on the skin absorption of mineral oils and vegetable oils found that of the vegetable oils, almond and soybean oil penetrate deepest into the *Stratum corneum* compared to mineral oils (137). Patzelt *et al.* (2012) offered no explanation for this, however their results could be explained again by composition of the vegetable oils since these oils contain naturally occurring fatty acids, particularly high amounts of oleic acid (61), a known permeation enhancer (64, 65). These results are however in contradiction from Stamatas *et al.* (2008) who found there to be no statistical difference in the stratum corneum uptake or swelling between paraffin oil and vegetable oils (jojoba and almond oil) using Raman spectroscopy for depth profiling (141). It has then been suggested in another study by Intarakumhaeng *et al.*2018 that the oleic acid present in soybean could be having an enhanced permeation effect on the skin delivery of soybean oil (136). Mineral oil hydrocarbons are retained in the lipophilic layers of the stratum corneum where they are removed by constant cell renewal (138). Paraffin oil contains no polar head groups to interact with polar regions of the ECM, and has properties that perturb it from membrane permeation; long hydrocarbon chains in the range of C_{15}-C_{50} MW range of 230-270 g mol^{-1}, and is highly hydrophobic/non-polar with a log$P_{O/W}$ range of 7.7-24.2 and (138). These attributes give reason to why paraffin oil has minimal lipid interaction and disruption.

4.4.2 Effect of Pickering emulsion on *Stratum corneum* lipids –controlled release of oil

Flavonoid particle aggregation around oil droplets in a Pickering emulsion are rigid and inflexible due to the high energy that needs to be overcome of spontaneous de-absorption (49). Particle coating at the O/W interface would thus prevent the oil from having an immediate effect upon the skin. However, the aggregation of the flavonoids particles around the oil droplets in this research were found not to form a uniform coating (seen in Confocal Scanning Laser Microscopy in Chapter **3**), making the flavonoid particle coating porous and possibly leading to the leaching of oil content. As previously mentioned in section **4.4.1 on p148** the degree of lipid disruption is dependent on the oil type used, therefore Pickering emulsions preventing Oil – SC exposure would control the delivery of the oil to the skin, thus controlling lipid disruption.

Studies of Pickering emulsions in the topical delivery of drugs and topical actives have primarily investigated active loading into the dispersed phase of the PE, using silica, titanium dioxide (83) or cyclodextrins (84) to form the PE particle stabilisation. It has been theorised from Scanning Electron Microscope (SEM) results that PE formed with cyclodextrin form a rigid and solid inflexible film around dispersed oil droplets due to crystal formation. This has also been observed for silica particle stabilised PE (80). This pertains to the delayed collapse and release of the oil droplets and the drug contents inside (84) and therefore PE can have a controlled released effect.

In this research, the flavonoid crystal aggregation at the O/W interface are having a controlled release effect of the oil on the SC .

4.4.3 Effect of flavonoid particles on *Stratum corneum* lipids and membrane interactions

Rutin and isoquercetin where seen to influence the chain packing in CH_2 symmetric stretching more compared to quercetin.

There are two types of bonding identified between the lipids in the SC; polar hydrogen bonding between polar head groups and non-polar Van der Waals between the acyl chains, which can be modified by the ratio of lipids present (22). In addition, polar regions within the ECM occur from bonded water molecules, which make up a third of the water content in the SC (27).

Flavonoids have both polar sites from sugar moieties and hydroxy groups, and non-polar sites from the benzene ring backbone. Rutin and isoquercetin have lower logPo/w and are more polar than quercetin as both have more polar regions due to sugar moieties (see **Figure 4-8**).

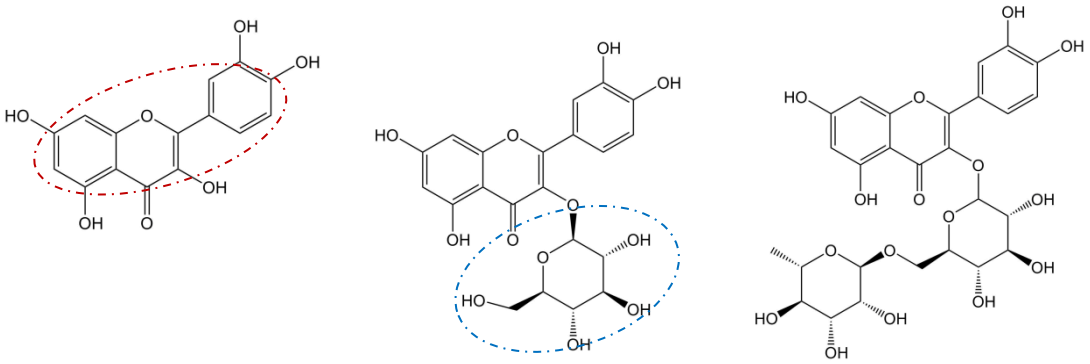

$logP_{o/w}$ 2.02

[1]

logPo/w 0.53

[2]

logPo/w -0.36

[3]

Figure 4-8 Chemical Structures of Flavonoids with their experimental octanol-water partition coefficient, $logP_{o/w}$ [1] Quercetin, [2] Isoquercetin and [3] Rutin. Red dashed circle highlights the benzene ring back-bone of the flavonoids that attribute to the non-polar portion of the molecule, and the blue dashed circle highlights the sugar moieties that attribute to the highly polar region of the flavonoids isoquercetin and rutin.

Flavonoids could be influencing the lipid interactions of the ECM by either disrupting the strength of the hydrogen bonds between the sphingoid bases and bound water, and/or disrupting the Van der Waals bonds between the acyl chains of the lipids. It could be hypothesised that the fatty acids, particularly oleic acid in the vegetable oils are primarily causing lipid disruption, then the flavonoids are passing through the impaired SC barrier.

However, an observation made distinguished in **Figure 4-6** is that there is increased lipid disorder from samples with rutin and isoquercetin compared to quercetin. Hydrophilic polar domains within the ECM could open up due to the sugar moieties present on rutin and isoquercetin, causing increased lipid chain movement. Glucose and rutinose are hydroscopic and will attract water molecules, increasing rutin and

isoquercetin's hydrophilic capacity within the ECM (16) by attracting the unbound water in the SC (27). A study has looked at the location of a hydrophilic active glycerol ($logP_{O/W}$ -1.76) and lipophilic active octyl methoxycinnamate ($logP_{O/W}$ +6.1) within the SC lipids in reconstructed human epidermis (RHE) using Raman spectroscopy (142). They found that glycerol was located in the water rich areas of the lipid matrix, causing swelling of the polar regions leading to an opening up of the lipids chains and increased separation of the lipid chains compared to the untreated samples. This swelling could be occurring in the polar regions due to the sugar moieties on rutin and isoquercietin. The opposite result was seen for octyl methoxycinnamate which was mapped in the lipid domains of the SC, however it did not penetrate far into the SC model compared to glycerol after 15 minutes application. A possible reason for penetration depth difference was not provided, but molecular size of glycerol (92.09 g mol^{-1}) and octyl methoxycinnamate (290.40 g mol^{-1}) should be a factor to consider. Octyl methoxycinnamate may have a higher retention and slower diffusivity with the skin lipids due to its high lipophilic nature RHE however does not have the same water, lipid or natural moisturising factor (NMF) content compared to human skin *in vivo*, which needs to be considered (143).

Due to the their amphiphilic structure these flavonoids can imbed themselves within the SC lipids. Cholesterol and α-tocopherol stabilise lipid membranes and their antioxidant activities are thought to be predominant in preventing reactive oxygen species from migrating within lipid bilayers, thus preventing lipid peroxidation and on set of detrimental effects (144). A study by Arora *et al.* (2000) found that flavonoids and iosflavonoids behave in a similar manner to cholesterol and α-tocopherol (144). Flavonoids were found to imbed themselves within acyl chains and stabilise the fluidity of the lipid membrane model used. In their study they observed rutin, which despite its large molecular size and increased hydrophilic nature due to the rutinose

moiety and hydroxyl groups, permeated and stabilised in the hydrophobic core of the membrane. They comment that this could be because of the strength of hydrophobic interactions between the hydrophobic part of the flavonoids and the phospholipids, in addition to the formation of intramolecular hydrogen bonding between polar regions (144). When flavonoids partition into the lipid matrix membrane, lipid fluidity is decreased and lipid peroxidation inhibited.

In studies previous to this work it was assumed that flavonoids localised at the lipid-water interface of membranes due to their amphiphilic structure.

A more recent study by Sanver *et al.* (2016) investigated flavonoid interactions with a biological membrane model using a Langmuir lipid mono-layer of 1,2-dioleoyl-sn-glycero-3-phosphocholine (DOPC), on a mercury electrode and rapid cyclic voltammetry (145). They found that flavonoid-membrane interactions depended on the planar configuration of the structure; two coplanar rings in the flavonoid structure (*e.g.* quercetin and rutin) showed membrane interaction. Quercetin had a higher interaction with the lipid mono-layer than rutin. With complimentary structure activity relationship (SAR) analysis, this study concluded that due to the rutinose moiety, steric hindrance caused rutin to have less interaction with the membrane than quercetin. Sanver *et al*. 2016 mentioned that results for flavonoid-membrane interactions in the literature are inconsistent as each study uses different model membranes with varying lipid and cholesterol components (145).

Interaction of flavonoids with lipid membranes is pH dependant; quercetin has a deeper partition into lipid membranes at acidic pH when protonated (below the pKa). At alkaline pH when quercetin is deprotonated (above pKa) the negatively charged hydroxyl groups of quercetin will interact with the polar head groups of the lipid membrane, thus partitioning into the hydrophobic regions of the lipids is inhibited (146). All emulsions in this experiment were with the range pH 6.4 – 7.0, above the

pK_a of the flavonoids (rutin pK_a 6.17, isoquercetin 6.17 quercetin 6.31 (51), therefore all flavonoids were deprotonated. Deprotonation increases the flavonoid water solubility, which could lead to ghier disruptive polar bonds within the ECM.

Using ATR-FTIR to observe the changes in lipid conformation of the stratum corneum provides indication of flavonoid-membrane interactions. In **Figure 4-6** on **p146**, comparison between the emulsion and oil type, quercetin has a lesser impact on the CH_2 stretching mode than that of rutin and isoquercetin, as indicated by a smaller wavelength shift from untreated stratum corneum lipids. As previous studies by Sanver et al (21016) have eluted, the aglycone quercetin does have a strong interaction with lipid bio-membranes due to its planar structure (145) and at acidic pH (146). These strong lipid interactions lead to membrane stabilisation, similar to cholesterol and α-tocopherol (144) and reduced movement of the acyl chains within the membrane. However, increased disruption of the acyl chains could occur with rutin and isoquercetin due to reduced flavonoid-lipid interactions and steric hindrance due to the sugar moieties of rutin and isoquercetin. In addition the amphiphilic nature of rutin and isoquercetin can allow them to partition from regions of polar and non-polar domains within the lipid matrix more easily than quercetin.

As far as the author is aware, there is no published literature investigating the flavonoid-membrane interaction specifically of lipids that make up the extracellular matrix (ECM) within the *Stratum corneum*. This missing research is important as the lipids in the stratum corneum are considerably different from cell membrane lipids (16). The ECM is composed of equimolar proportions of ceramides, cholesterol and fatty acids, whereas cell membranes are composed of phospholipids, glycolipids, and cholesterol. There are no phospholipids in the ECM. The formation and self-assembly of the extracellular matrix also differs from that of cell membrane bilayers as there is an absence of proteins in the ECM (16). It is also currently unknown the roles that specific lipids play in the stability and self-assembly of the ECM, which

also make it difficult to determine the exact flavonoid-lipid interaction and permeation behaviour within the SC.

As discussed in the literature review on p**19**, ceramide lipids vary in structure based on the polar sphingoid base and non-polar fatty acid chains and are arranged in changing order. This will effect partitioning of the flavonoids into and through the SC as varying pockets of polar and non-polar regions occur.

Mixtures of key ceramides, fatty acids and cholesterol found in human *Stratum corneum* have been developed to mimic skin lipid organisation investigate the polymorphism of the acyl chains under skin physiological conditions using ATR-FTIR, example model mixtures based on ceramides 2,3,5 and 6 which have different polar head groups and fatty acid chains (31). However, a concern with these models is that they all vary in composition and ratios of ceramides, fatty acids and cholesterol, thus comparability of results between research is reduced (12, 31).

To date there are no studies on flavonoid-membrane interactions on these models. Therefore, although the discussion on the effect of flavonoids on the lipid morphology in SC in this study is led by flavonoid-membrane interactions from cell membrane literature, further research is required without the scope of this project to be conclusive.

Conclusive remarks

Summarising the main findings:

(i) Disruption of the lipids is dependent on oil type and if in combination with flavonoids: almond and coconut oil change lipid morphology more than paraffin oil. Vegetable oils contain fatty acids that can disrupt the lipid morphology, whereas paraffin oil is long chain hydrocarbon that does not penetrate to into the SC, compared to vegetable oils which can penetrate deeper.

(ii) Pickering emulsions had a lesser effect on the lipid chain transition compared to the control emulsions and oil alone, and this is dependent on flavonoid type and oil type. In a PE the oil is trapped by the flavonoid and the oils effect on the lipids is reduced. Therefore Pickering emulsion pose as a controlled release of oil into the skin.

(iii) Bioavailable flavonoids in the control suspensions are having an effect on the lipid packing.

(iv) The structure of the flavonoids and the presence of sugar moieties changes the lipid domains: Rutin and Isoquercetin disrupted the lipid morphology more than quercetin.

It has been observed that the lipid morphology of the extracellular matrix within the *Stratum corneum* , thus barrier function of the SC can be altered both by oil and flavonoid type. Changes in barrier occurs from phase transition of the ECM lipids from orthorhombic to hexagonal/liquid crystal phase transition detectable by ATR-FTIR. The largest disruption of ECM lipids occurred from combination of almond oil, which contains high levels of oleic acid that can fluidise the lipid chains, and from the flavonoids rutin and isoquercetin, of which their amphiphilic structure disrupts the lipids also.

Chapter 5 Skin Delivery and Permeation of Flavonoids from Pickering Emulsions

5.1 Introduction

It is apparent throughout the literature that to achieve successful skin permeation of an active/drug compound, the following key factors need to be thoroughly understood, theoretically and experimentally;

(v) the inherent physiochemical properties of the active and its stability within an application vehicle (formulation),

(vi) the ability for the active to partition from the vehicle onto the stratum corneum,

(vii) the ability of the active to then diffuse through the stratum corneum and epidermal layers to the target site and

(viii) the path length of diffusion of the active within the skin,

all with consideration to anatomical site and temperature of the skin (3, 7, 39, 92).

5.2 Aims and Objectives

1. What is the epidermal permeation release kinetics of these flavonoids from Pickering emulsions using infinite dose technique? Is there a difference between the flavonoids and oil types used?
2. What quantity of flavonoid is delivered through epidermal membrane in 24 hours (from infinite dose) from different oil types?
3. Are Pickering emulsions an effective way to deliver these flavonoids, or do they hinder the penetration for cosmetic purposes?

5.3 Epidermal penetration of flavonoids from Pickering Emulsions

To obtain an understanding of the flavonoid release kinetics and permeation rates, an infinite dose of the flavonoids has to be applied to the membrane, *i.e*. a constant concentration gradient from the surface of the porcine epidermal membrane (split thickness skin) to the receptor chamber. Release kinetics are usually conducted on cellulose membranes, however these are not entirely representable of skin membranes (discussed later in section **2.9.2**)

The results are displayed and discussed in the order of permeation profiles, permeation parameters, release kinetics and finally cumulative amounts.

5.4 Permeation Profiles

The following section displays the permeation profile and mathematical models for release kinetics of the flavonoid form Pickering emulsions and oil types. Plots indicate the amount of flavonoid detected in the receptor phase in µg cm^{-2} against time for a period of 24 hours. Complementary tables display the correlation coefficients (R^2 values) for the fit of linear regression from mathematical models used on the permeation data and corresponding gradient values for release kinetics for initial stages of permeation (first detection to 7 hours).

Linear regression lines were fitted on the data from individual measurements and for mean data points (raw data not shown)

5.4.1 Rutin

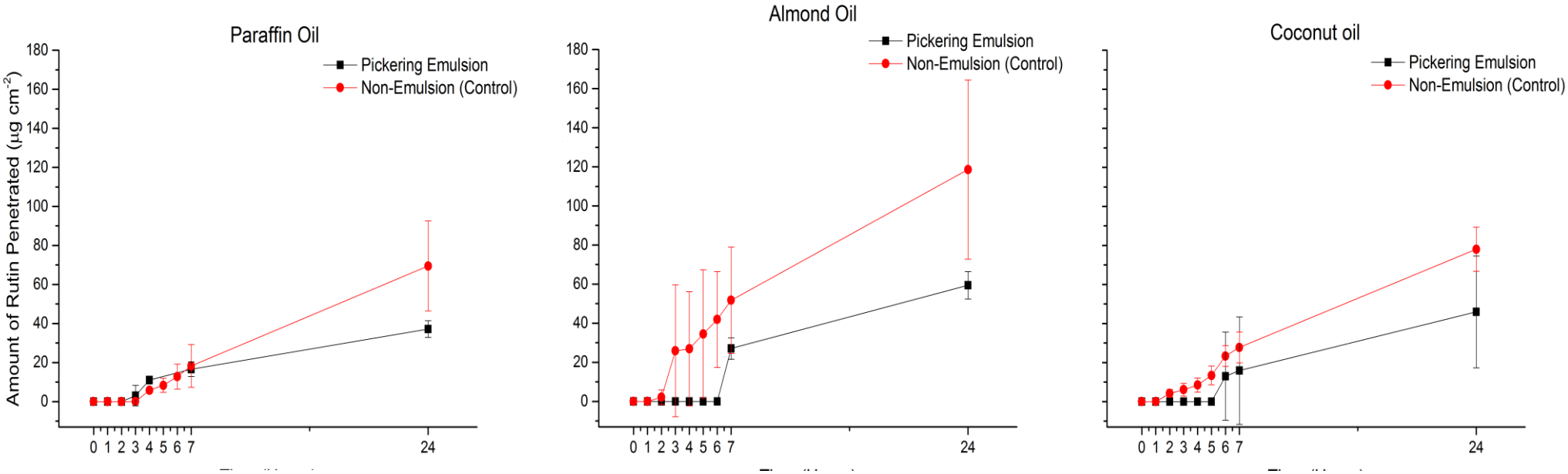

(a) Paraffin Oil (b) Almond Oil (c) Coconut Oil

Figure 5-1 Permeation profiles of rutin through porcine epidermis over 24 hours from Pickering Emulsions and controls made from (a) paraffin oil, (b) almond oil and (c) coconut oil. Based on 3 repeats.

Table XX Mathematical kinetic models on the detected amount of rutin (Q, μg cm^{-2}) over time (t, minutes) from Pickering emulsions and corresponding controls. Models with good correlation (R^2 > 0.95). * 3 or less data points inaccurate for linear regression

1st detection - 7hrs		**Zero order**		**First order**		**Higuchi Model**		**Korsmeyer-Peppas**		
		Q vs t		***ln(Q) vs t***		***Q vs √t***		***ln (Q) vs ln (t)***		
Emulsion Type	*Oil Type*	R^2	*Jss* μg cm^{-2}min^{-1}	R^2	*K*	R^2	*K*	R^2	*n*	*K*
Pickering Emulsion	Paraffin	0.81±0.10	*0.057±0.02*	0.61±0.06	*0.004±0.001*	0.85±0.10	*1.96±0.53*	0.77±0.06	*2.06±0.41*	*0.02±0.02*
	Almond*									
	Coconut*									
Non- Emulsion (Control)	Paraffin	0.96±0.02	*0.073±0.045*	0.83±0.07	*0.005±0.001*	0.99±0.01	*2.87±0.95*	0.95±0.05	*2.44±0.67*	*0.007±0.007*
	Almond	0.79±0.19	*0.14±0.07*	0.72±0.22	*0.004±0.001*	0.78±0.14	*4.53±2.56*	0.81±0.18	*2.07±0.82*	*0.05±0.07*
	Coconut	0.92±0.04	*0.07±0.02*	0.92±0.05	*0.0037±0.0002*	0.76±0.05	*1.39±0.36*	0.92±0.06	*1.37±0.11*	*0.08±0.02*

.

Rutin

From permeation profiles in **Figure 5-1** there was a delay in rutin coming through the skin from Pickering emulsions compared to the controls.

Paraffin oil control had the highest correlation for zero order and Higuchi model with >0.95 and of all the mathematical models. Zero -order and Higuchi models were highest for almond and coconut controls, however < 0.95.

Korsmeyer Peppas model was 0.95 for paraffin oil control, but < 0.95 for almond and coconut.

5.4.2 Isoquercetin

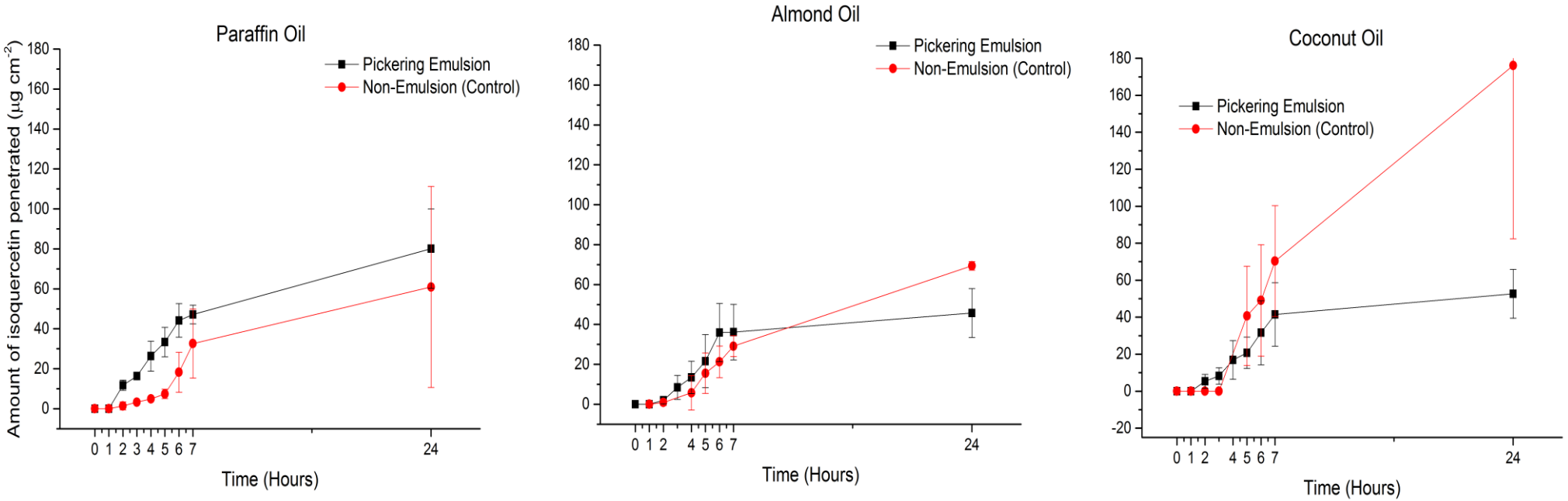

(a) Paraffin (b) Almond Oil (c) Coconut Oil

Figure 5-2 Permeation profiles of isoquercetin through porcine epidermis over 24 hours from Pickering Emulsions and controls made from (a) paraffin oil, (b) almond oil and (c) coconut oil. Based on 3 repeats.

Isoquercetin

Table XXI Mathematical kinetic models on the detected amount of isoquercetin (Q, µg cm-^{2}) permeating porcine epidermal membrane over time (t, minutes) from Pickering emulsions and corresponding control from different oil types. Models with good correlation value R^2 > 0.95).

1st detection - 7hrs		**Zero order**		**First order**		**Higuchi Model**		**Korsmeyer-Peppas**		
		Q vs t		***ln(Q) vs t***		***Q vs √t***		***ln (Q) vs ln (t)***		
Emulsion Type	Oil Type	R^2	*Jss* µg $cm^{-2}min^{-1}$	R^2	*K*	R^2	*K*	R^2	*n*	*K*
Pickering Emulsion	Paraffin	0.96±0.02	*0.13±0.02*	0.74±0.03	0.004±0.0002	0.91±0.02	2.6±0.4	0.95±0.06	*1.6±0.1*	*0.07±0.01*
	Almond*	0.94±0.03	*0.12±0.04*	0.92±0.04	0.0045±0.0004	0.90±0.03	3.4±1.1	0.89±0.05	*1.9±0.4*	*0.03±0.03*
	Coconut*	0.90±0.08	*0.11±0.05*	0.88±0.08	0.0041±0.0002	0.86±0.13	3.1±1.3	0.91±0.07	*1.6±0.2*	*0.06±0.01*
Non- Emulsion (Control)	Paraffin	0.82±0.15	*0.09±0.03*	0.94±0.02	0.0042±7E-05	0.69±0.26	1.7±0.1	0.85±0.17	*1.7±0.3*	*0.03±0.03*
	Almond	0.94±0.06	*0.11±0.01*	0.89±0.03	0.006±0.001	0.92±0.09	3.5±0.9	0.86±0.14	*2.8±1.4*	*0.02±0.02*
	Coconut	0.90±0.01	*0.37±0.15*	0.73±0.08	0.009±0.001	0.91±0.09	13.3±5.5	0.82±0.09	*6.0±0.8*	*2E-6±4E-06*

Isoquercetin

For isoquercetin in Pickering emulsions the best fit mathematical model was zero order kinetics, paraffin oil (R^2 0.96), almond (R^2 0.94) and coconut (R_2 0.90).

For the control systems there was a slight difference. For paraffin oil control the best fit was first order kinetics (R^2 0.94), whereas the vegetable oils followed a zero order kinetics; almond (R^2 0.94) and coconut (R^2 0.90).

Higuchi models R^2 values were >0.90 <0.95 apart from paraffin oil control and coconut PE.

5.4.3 Quercetin

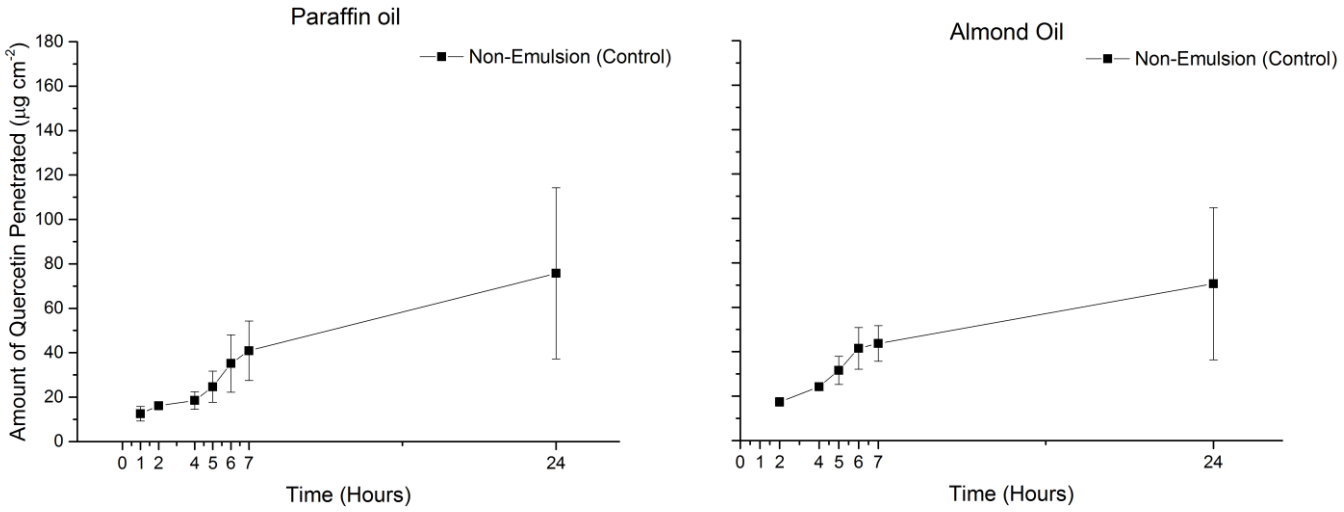

(a) Paraffin Oil (b) Almond Oil

Figure 5-3 Permeation profiles of quercetin through porcine epidermis over 24 hours from non-emulsions made from (a) paraffin oil, (b) almond oil. Based on three repeats. Pickering emulsions with quercetin were not detected in permeation assay.

Quercetin

Table XXII Mathematical kinetic models on the detected amount of quercetin (Q, µg cm-2) permeating porcine epidermal membrane over time (t, minutes) from Pickering emulsions and corresponding control from different oil types. Models with good correlation values (R^2 > 0.95)

1st detection - 24hrs		**Zero order**		**First order**		***ln(Q)***	**Higuchi Model**		**Korsmeyer-Peppas**		
		Q vs t		***vs t***			***Q vs √t***		***ln (Q) vs ln (t)***		
Emulsion Type	*Oil Type*	R^2	*Jss* $\mu g\ cm^{-2}min^{-1}$	R^2	*K*		R^2	*K*	R^2	*n*	*K*
Pickering Emulsion	Paraffin										
	Almond*										
Non- Emulsion (Control)	Paraffin	0.90±0.02	*0.08±0.03*	0.77±0.14	0.002±0.001		0.88±0.04	1.8±0.6	0.96±0.02	*0.47±0.05*	*0.98±0.02*
	Almond	0.92±0.04	*0.11±0.02*	0.68±0.06	0.0037±0.0004		0.94±0.02	3.3±0.8	0.88±0.05	*1.47±0.13*	*0.09±0.02*

Quercetin

The best mathematical model fit for quercetin and paraffin oil control was with the Korsmeyer Peppas model (R^2 0.96), which implies a rapid release kinetic from the membrane. For quercetin and almond oil, the Higuchi model (R^2 0.94) and zero order kinetics (R_2 0.92) were found to be the best mathematical fit of the kinetic data.

5.4.4 Determining steady state flux time frame

The permeation profiles for the flavonoids from first detection to the 24 hour final measurement show two patterns; a partial steady state flux stage (linear gradient, zero-order kinetics gave the highest R^2 values) up to 7 hours followed by a reduction in flux 7 to 24 hours. The complete experimental time up to 24 hours could not be taken as the steady state flux. When zero order kinetics was applied, high R^2 values (>0.95) where achieved, indicative of a linear correlation. However, when the residual plots of the linear fits were analysed, there was x-axis unbalanced pattern which means the data was not trustworthy to be truly linear see attached appendix. When the time frame was reduced to the initial stages of permeation, R^2 values for zero order kinetics were reduced slightly, but still produced the highest linear correlation for rutin and isoquercetin than compared to other mathematical models. The corresponding residual plots showed and even distribution of data, indicating a good linear fit. In addition, it is unrealistic to take the steady state up to 24 hours, as the permeation time frame into the skin from a personal care application is highly unlikely to exceed 7 hours.

5.4.5 Time Lag and Diffusion

By taking within the time frame 1 – 7 hours of permeation as the steady state region, the time lag could be calculated by extrapolating the linear portion of zero-order kinetics to the x-axis. The results for time lag are displayed in **Table XXIII**.

5.5 Permeation parameters and release kinetic data

The following section displays the results for the permeation parameters calculated from the permeation profiles.

Differences between calculated values were investigated using a one tailed students' *t*-test after ANOVA and discussed as significantly different at the P value < 0.05. **Table XXIII** displays the steady state flux (zero order kinetics), permeability coefficient, time lag and the diffusion of the flavonoid within the skin determined by the time lag method. **Table XXIV** displays the initial release coefficient of the flavonoid from the vehicle (Higuchi model), the diffusion coefficient of the flavonoid within the vehicle (derived from Higuchi model), the release exponent and release rate constant (Korsmeyer-Peppas model)

Table XXIII Calculated permeation parameters of flavonoids from Pickering emulsions and controls made with Paraffin Oil (PO), Almond Oil (AO) and Coconut Oil (CO) from the steady state region of permeation, time frame first detection – 7 hours. Mathematical equations described in experimental chapter. RR = rapid release

	Steady state flux, J_{ss}			**Permeability Coefficient. K_p**			**Time Lag**			**Diffusion coefficient within the skin using Time lag, D_s**		
	µg cm^{-2} min^{-1}			**10^{-3} cm min^{-1}**			**MINUTES**			**10^{-6} cm^2 min^{-1}**		
Pickering Emulsions	**PO**	**AO**	**CO**	**PO**	**AO**	**CO**	**PO**	**AO**	**CO**	**PO**	**AO**	**CO**
Rutin	0.06±0.02			0.3±0.08								
Isoquercetin	0.13±0.02	0.12±0.04	0.11±0.05	0.9±0.1	0.8±0.3	0.8±0.3	47±3	104±36	83±27	35±2.5	17±5.0	21±7.5
Non - Emulsion												
Rutin	0.07±0.05	0.14±0.07	0.08±0.02	0.4±0.2	0.8±0.4	0.4±0.1	168±18	107±44	86±12	9.9±1.1	16±7.0	19±2.7
Isoquercetin	0.09±0.03	0.11±0.01	0.37±0.15	0.4±0.4	0.8±0.01	0.3±0.1	132±11	159±83	223±19	13±1.1	13±8.6	0.7±0.07
Quercetin	0.08±0.03	0.11±0.03		0.9±0.4	0.1±0.3		RR	28±21			80.5±59.5	

Table XXIV Calculated release kinetics of flavonoids from Pickering emulsions and non-emulsions made with Paraffin Oil (PO), Almond Oil (AO) and Coconut Oil (CO) from the steady state region of permeation, time frame first detection – 7 hours.

	Higuchi model						Korsmeyer – Peppas model					
	Initial Release coefficient, K_H			Diffusion coefficient within the vehicle, *Dv*			Release Exponent, *n*			Release rate constant, *K*		
	cm $min^{-0.5}$			10^{-3} cm^2 min^{-1}						cm min-1		
Pickering Emulsions	**PO**	**AO**	**CO**	**PO**	**AO**	**CO**	**PO**	**AO**	**CO**	**PO**	**AO**	**CO**
Rutin	1.96±0.53			3.2 ± 1.7			2.1±0.4			0.02±0.02		
Isoquercetin.	2.6±0.4	3.4±1.1	3.1±1.3	5.3 ± 1.7	9.8 ± 6.2	8.7 ± 7.3	1.6±0.1	1.9±0.4	1.6±0.2	0.01±0.01	0.05±0.07	0.08±0.02
Non - Emulsion												
Rutin	2.87±0.95	4.53±2.56	1.39±0.36	6.9 ± 4.9	19.6 ± 16.0	1.6 ± 0.8	2.4±0.7	2.7±0.8	1.4±0.1	0.07±0.01	0.03±0.03	0.06±0.01
Isoquercetin.	1.7±0.1	3.5±0.9	13.3±5.5	1.6 ± 1.4	10.0 ± 5.2	154.2 ± 102.3	1.7±0.3	2.8±1.4	6.0±0.8	0.04±0.03	0.02±0.02	$2E^{-6}$±$4E^{-6}$
Quercetin	1.8±0.6	3.3±0.8		2.8 ± 2.0	8.8 ± 4.3		0.5±0.05	1.5±0.1		1.0±0.02	0.1±0.02	

5.5.1 Permeation Rate (Steady state flux, *Jss*)

Rutin

There was no difference in permeation rate between the emulsion system type with paraffin oil (**Figure 5-4**). No value comparison could be made between emulsion system types for almond and coconut oils as rate could not be determined for these PEs.

Between the three oil types for control systems, rutin delivered with almond oil showed the fastest permeation rate (although not significantly different at $P < 0.05$), with paraffin and coconut being similar.

The rate of rutin delivered through the skin does depend on the oil type, almond showing preferential increased rate from the control.

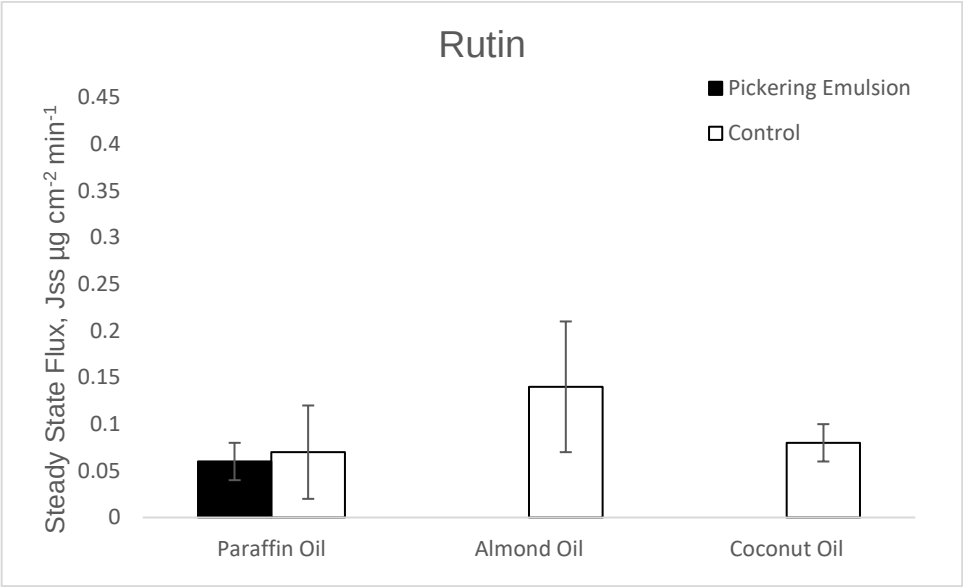

Figure 5-4 Comparison of permeation rates, expressed as flux, of rutin through porcine epidermis over 7 hours.

Isoquercetin

Permeation rate of isoquercetin was not different between oil types for Pickering emulsions, whereas for controls the permeation rate increased in the order of oil type paraffin < almond < coconut (coconut delivering isoquercetin significantly faster with P < 0.05), **Figure 5-5**. These results could indicate that isoquercetin permeation rate is affected by the location of isoquercetin in the system, and the exposure of the oil to the skin membrane.

The flux of isoquercetin in a paraffin oil Pickering Emulsion was twice as fast as PE with rutin and paraffin oil (compare **Figure 5-4** and **Figure 5-5** (significantly different at $P < 0.05$). Control systems for isoquercetin were similar to rutin for paraffin and almond oil, apart from coconut oil which had a higher flux.

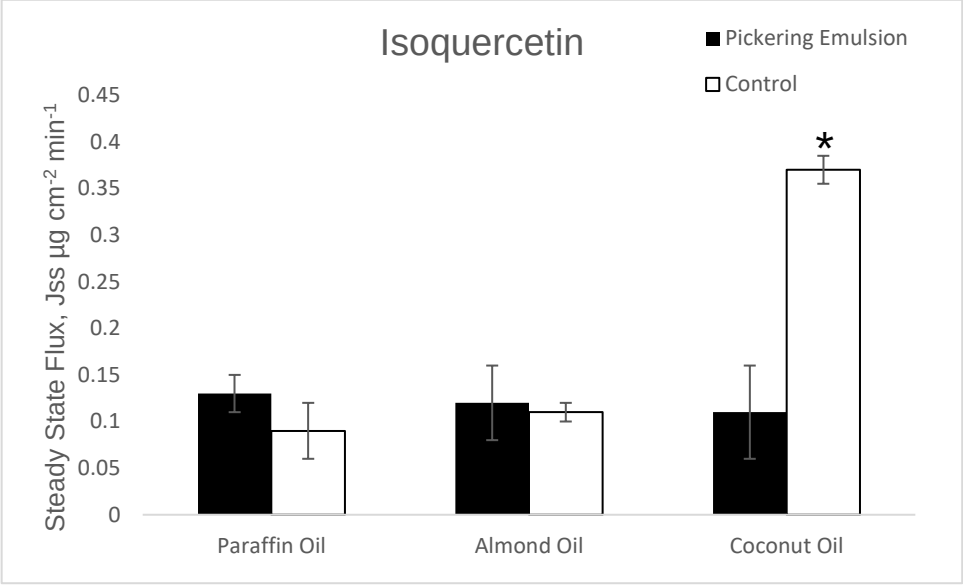

Figure 5-5 Comparison of permeation rates, expressed as flux, of isoquercetin through porcine epidermis over 7 hours. * denotes significantly different from other permeation rates at *P* < 0.05)

Quercetin

Steady state for Pickering emulsions could not be determined for quercetin as there was no detection of the flavonoid in the receptor phase during experimentation. For control systems, quercetin permeation rate with paraffin oil was slower than almond oil, although not significantly different, **Figure 5-6**. The permeation rate was similar to that of rutin and isoquercetin in control systems, indicating that physiochemical properties of the flavonoids may not have a significant impact on permeation rate.

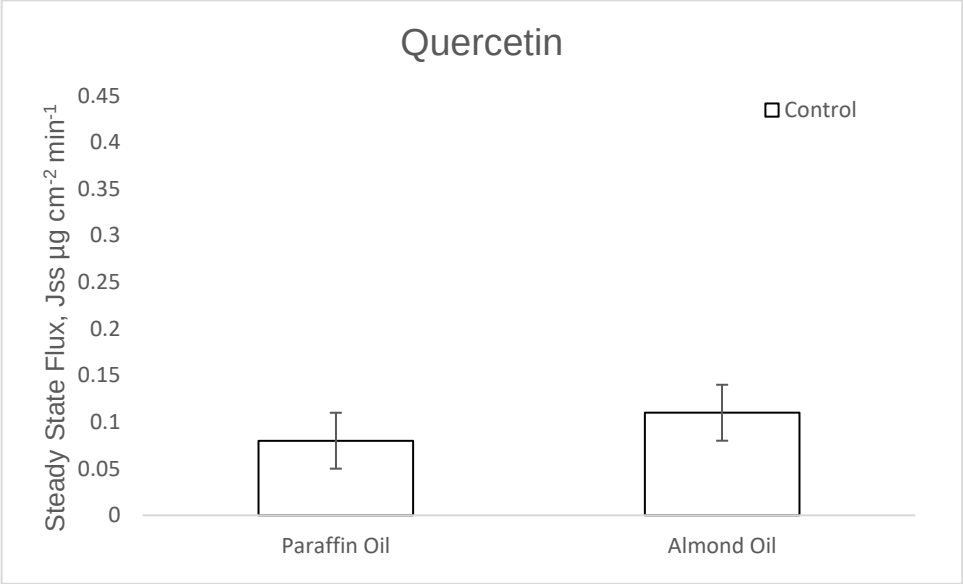

Figure 5-6 Comparison of permeation rates, expressed as flux, of quercetin through porcine epidermis over 7 hours.

5.5.2 Diffusion coefficient within the membrane (time lag method)

Rutin

Diffusivity within the membrane could not be determined for rutin from Pickering Emulsions using the time lag method. For the control systems diffusivity within the membrane increased in the order of paraffin < almond < coconut oils, with only coconut being significantly different from paraffin oil ($P < 0.05$), **Figure 5-7**. The vegetable oils can change the lipid morphology of the extracellular matrix that may be enhancing the diffusion of rutin through the membrane (see chapter **4** for the disruption of lipids). As oils in the control system are not coated with flavonoid as with PEs, the stratum corneum is exposed to these oils allowing lipid chains to become fluidized, in turn increasing the diffusion rutin through the membrane. As rutin particles are coating the oil droplets in the PE it is further evidence that that oil is primarily having an effect on the lipid morphology of the SC.

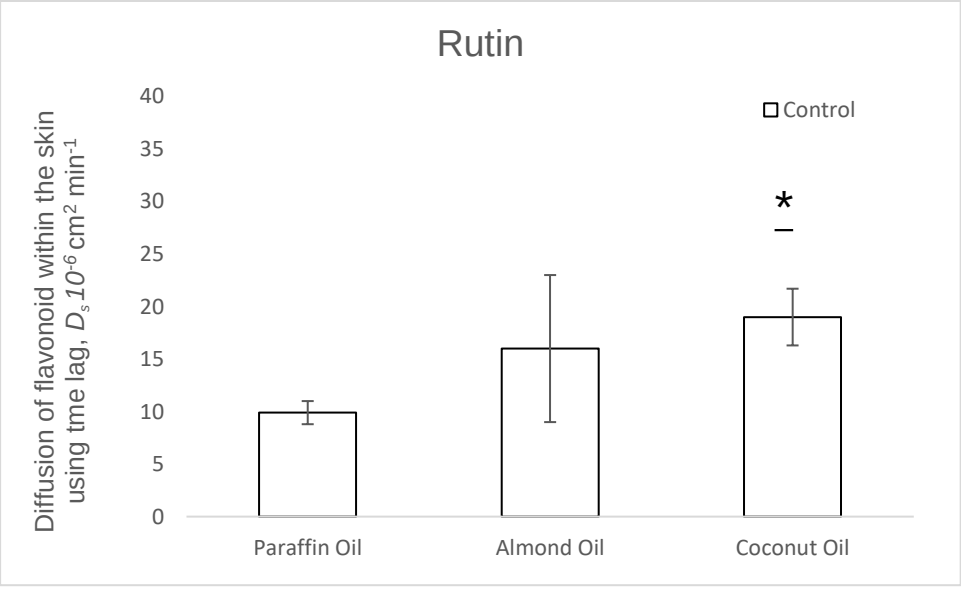

Figure 5-7 Diffusion of rutin within the porcine membrane calculated from the time lag method in 7 hours. * denotes diffusion within the skin from a coconut oil control emulsion significantly higher than than using paraffin oil ($P < 0.05$).

Isoquercetin

The diffusivity of isoquercetin within the membrane was different from the results seen with rutin. Significantly higher diffusion of isoquercetin through the skin was from a Pickering emulsion with paraffin oil, compared to the vegetable oils Pickering emulsions and corresponding controls.

The control systems for isoquercetin were in the order paraffin ≈ almond > coconut oils, diffusion coefficient of isoquercetin in coconut control emulsions was significantly lower compared to paraffin and almond oil which were similar.

All diffusion coefficients for isoquercetin from control systems were lower than the corresponding PE (significantly for paraffin and coconut oil only). isoquercetin had higher diffusivity within the skin from PE than the control.

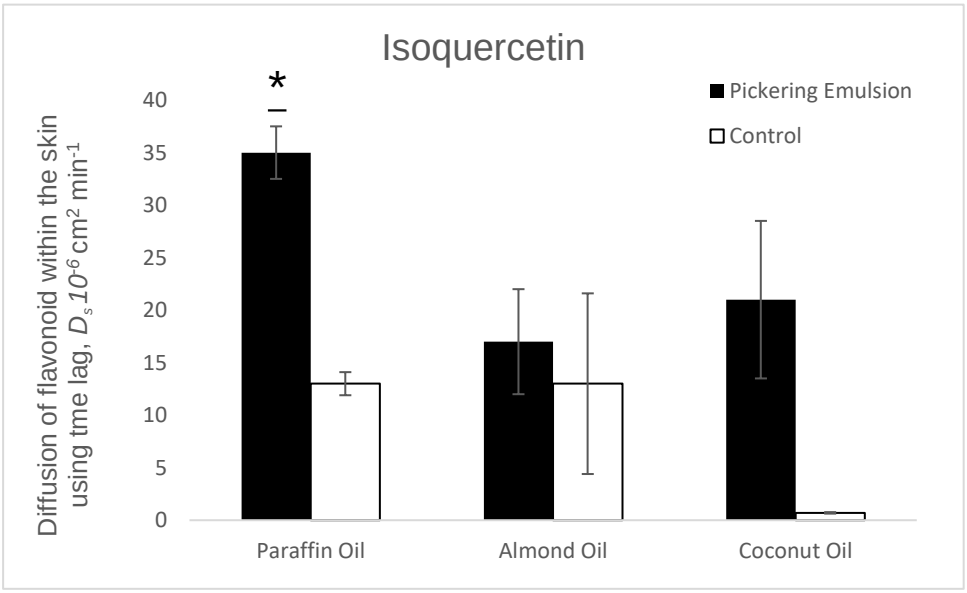

Figure 5-8 Diffusion of isoquercetin within the porcine membrane calculated from the time lag method in 7 hours. * denotes diffusion within the skin from a paraffin oil control emulsion significantly higher (*P* < 0.05).

Quercetin

Diffusivity within the membrane for quercetin in Pickering emulsions could not be determined. As there was rapid release from the membrane for paraffin control system, using the time lag method to determine the diffusion coefficient could not be used. However, for almond oil control results did provide a time lag which produced the highest diffusion coefficient between flavonoids, although with large error. The higher diffusivity of quercetin compared to rutin and isoquercetin within could be due to physiochemical properties; quercetin being more polar ($logP_{o/w}$ 2.20), compared to the more hydrophilic isoquercetin (0.53) and rutin (-0.36). Quercetin is also the smallest of the flavonoids at 330.27 g mol^{-1}, whereas isoquercetin and rutin are 464.38 g mol^{-1} and 610.15 g mol^{-1} respectively. These molecular weights are of the molecules, and not of flavonoid particle sizes that may have formed crystals.

5.6 Release Kinetics

5.6.1 Higuchi coefficient K_H (Initial release

The Higuchi coefficient, K_H, describes the initial release rate of a permeant from a matrix membrane (147). It is worth noting that the membrane is used in other release kinetic studies is polymeric, *e.g.* cellulose, which does not swell or undergo physical change during drug release, as this would affect the release kinetics (148). In this study, viable tissue has been used instead of polymeric membrane as the former provides kinetic information from a real-life model akin to human skin, and so that lipid conformation analysis could be done post-permeation assay. Oils have been found to cause swelling of the *Stratum corneum*

Rutin

The non-initial release rate of rutin was lower from the Pickering emulsion than the control with paraffin oil, suggesting that the rutin in a Pickering emulsion has a slow

release. It could not be determined for rutin from Pickering Emulsion with almond coconut oil. A slow release of rutin from the membrane correlates with low diffusion within the membrane (**Figure 5-7**) and diffusion of rutin within the Pickering emulsion (**Figure 5-12** on p**187**)

For control systems, the non-initial release rate showed to be higher for almond > paraffin > coconut oil (**Figure 5-9**), suggesting the oil type could be having an enhancement the release from the epidermal membrane. Coconut oil was significantly slower in release rate from the emulsion in control than paraffin oil and almond oil.

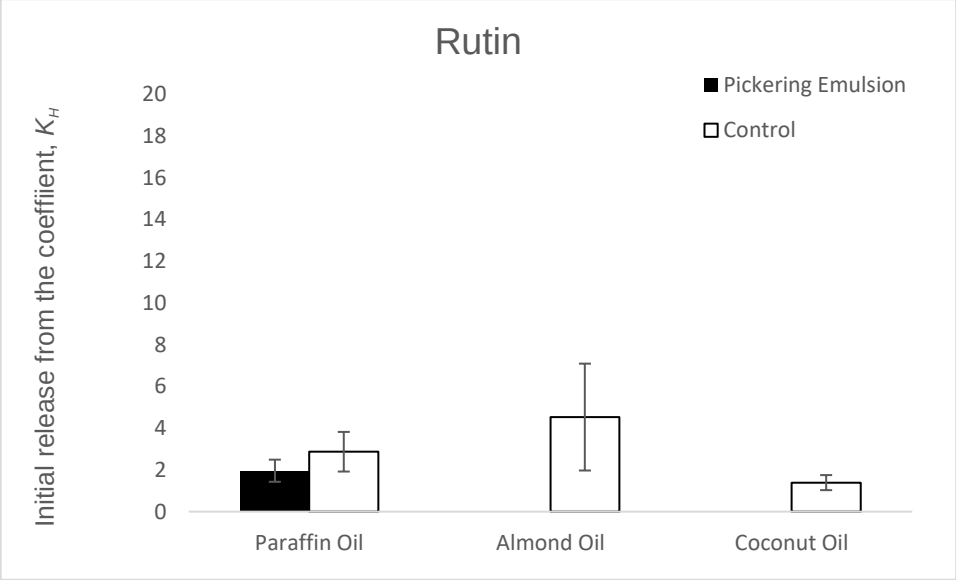

Figure 5-9 Release coefficient of Rutin from the membrane matrix, Higuchi Principle

The non-initial release rate of rutin was slower than isoquercetin in Pickering emulsions, possibly attributed to the difference in physiochemical properties of the flavonoids. Isoquercetin is smaller than rutin therefore the former permeates the stratum corneum easily, and rutin has a higher water solubility that isoquercetin, thus remaining more preferentially at the O/W interface *i.e.* a slower collapse of the emulsion.

Isoquercetin

From **Figure 5-10**, the initial release of isoquercetin from PE with paraffin oil was higher than the paraffin control (although not significantly different). K_H increased from controls increase in the order paraffin ≈ almond < coconut oil, indicating oil type in combination of the location of isoquercetin crystals in the emulsions changed the release. Initial release of isoquercetin was higher than rutin for paraffin Pickering Emulsion, but not different across the 3 oil types for PE.

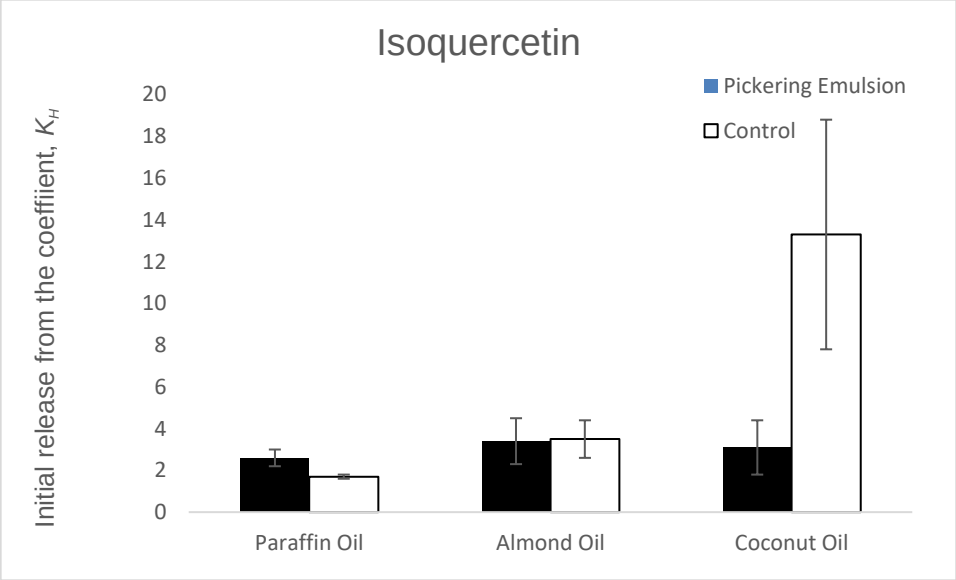

Figure 5-10 Release coefficient of Isoquercetin from the membrane matrix, Higuchi Principle

By comparing **Figure 5-9** and **Figure 5-10,** initial release of isoquercetin was higher than rutin for paraffin Pickering Emulsion, but not different across the 3 oil types for PE. Isoquercetin control for coconut oil had a higher release coefficient than rutin for all rutin control oil types.

Quercetin

Initial release for quercetin from PE could not be determined. Quercetin could have been partially dissolved into the oil phases and been retained within the upper layers

of the epidermis with the oils. Analysis of the oil phases after homogenisation should be carried out in future experiments to investigate this possibility. From **Figure 5-11** it can be seen that quercetin had a higher release in combination with almond oil than with paraffin oil, however not significantly different.

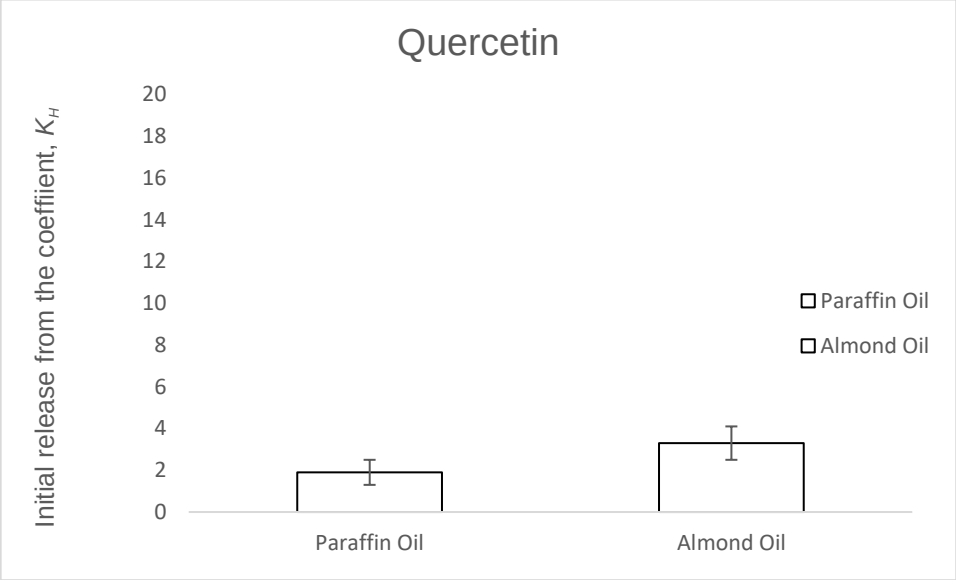

Figure 5-11 Release coefficient of Quercetin from the membrane matrix, Higuchi Principle

The initial release of quercetin from controls was not significantly different between paraffin oil and almond oil, and not different from the other flavonoids.

5.6.2 Diffusion coefficient, *Dv* (Higuchi model) – diffusion from vehicle

Information on the diffusivity of the flavonoid within the vehicle can be deduced from the Higuchi principle and provides insight to the behaviour of the flavonoids within the formula. This is important as the thermodynamics of a permeant within a formula affect the skin permeation because of availability to the skin surface.

Rutin

Diffusion of rutin within the control systems is higher than within the Pickering emulsion for paraffin oil, **Figure 5-12.** This is due to the thermodynamic activity of rutin being reduced when at the O/W interface in a PE compared to a aqueous suspension of rutin. Diffusivity for rutin from the PE emulsions could not be determined for almond and coconut oil.

Diffusion of rutin within the almond oil control was higher compared to paraffin oil, which could be attributed to the lipophilivity of the oil; paraffin oil being more hydrophobic than almond oil. However for coconut oil, which would have the same possible affect as almond oil (*i.e.* higher diffusivity than paraffin oil) the diffusivity was significantly lower than almond and paraffin oil. An explanation could be due to the possible solidification of coconut oil that hinders the thermodynamics of rutin when in the Franz diffusion cell. The jacketed Franz cell is controlled at 37 ˚C, however centre of the membrane away from the warmed cell could be cooler therefore solidification of coconut oil occurring.

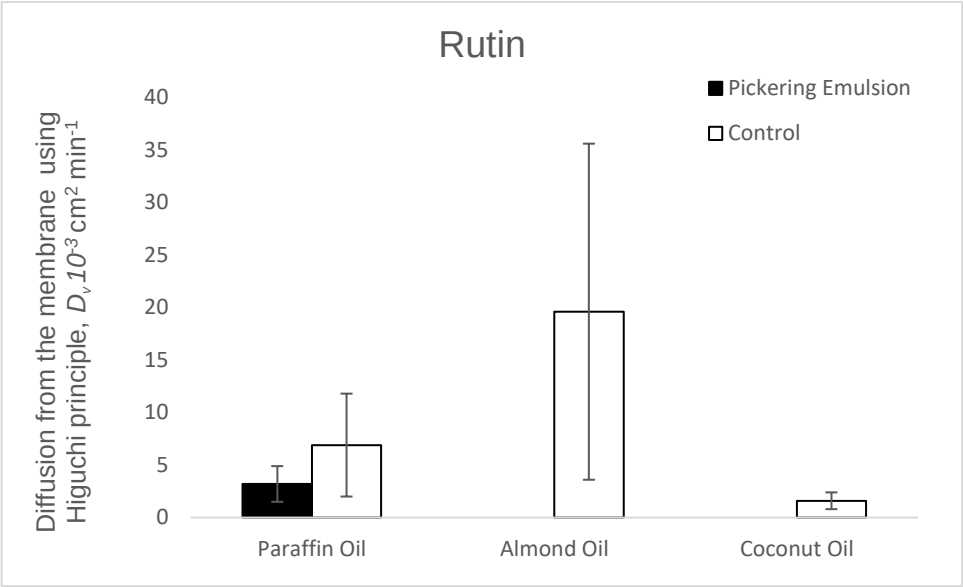

Figure 5-12 Diffusion of rutin within the vehicle of Pickering Emulsion of Control

An interesting observation is that the diffusivity of rutin within the paraffin and almond oil control systems was higher than the other flavonoids (refer to **Table XXIV** on **p176** for comparison), however not for coconut oil. The higher diffusivity in paraffin and almond oil could be due to the increased water solubility of rutin due to the extra sugar group on the structure of rutin, which effects the polarity of the molecule ($LogP_{O/W}$ - 0.34, isoquercetin 0.53 quercetin 2.02), which will be discussed further on in section x.

Isoquercetin

Diffusivity of isoquercetin within paraffin oil was lower than almond and coconut oil for the Pickering emulsions, **Figure 5-13**. This suggests that isoquercetin is held more preferentially at the O/W interface with a hydrocarbon oil than with the vegetable oil. This can be due to the presence of naturally occurring fatty acids and glycerols within the almond and coconut oil that displace the flavonoid from the O/W interface.

Diffusivity with the control system of isoquercetin increased from paraffin to almond to coconut oil which follows the same pattern as rutin, apart from coconut oil, which for isoquercetin increased the diffusivity significantly ($P < 0.05$).

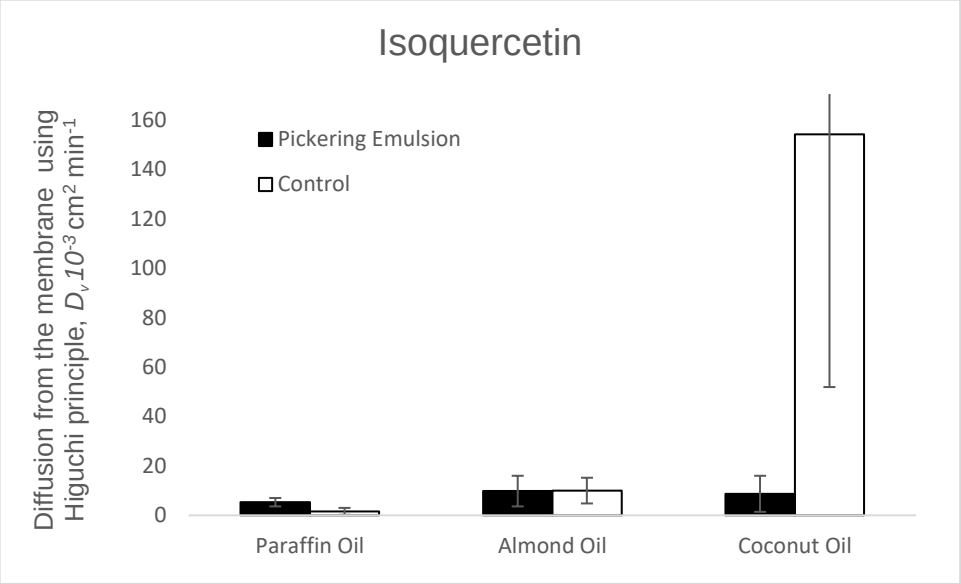

Figure 5-13 Diffusion of isoquercetin within the vehicle of Pickering Emulsion of Control

Quercetin

Diffusivity of quercetin within the Pickering emulsions could not be determined. For controls, quercetin increased in diffusivity in order paraffin < almond oil, which was similar to isoquercetin. For paraffin oil, diffusivity was overall higher for rutin compared to the two other flavonoids.

5.6.3 Korsmeyer-Peppas *n* component

This release model is used to characterise different release mechanisms from cylindrical membranes (149).

For all flavonoids from PE and controls (bar quercetin control with paraffin oil), the n component >1 (range 1.5 – 2.8) indicating super case II transport mechanism or erosion controlled release. However the R_2 values for the mathematical models was lower compared to zero-order and Higuchi models.

The best fit for the Korsmeyer-Peppas model was quercetin control system with paraffin oil, providing a *n* value of 0.5, indicating Fickian diffusion (127).

5.7 Cumulative amounts of flavonoids penetrating through epidermis

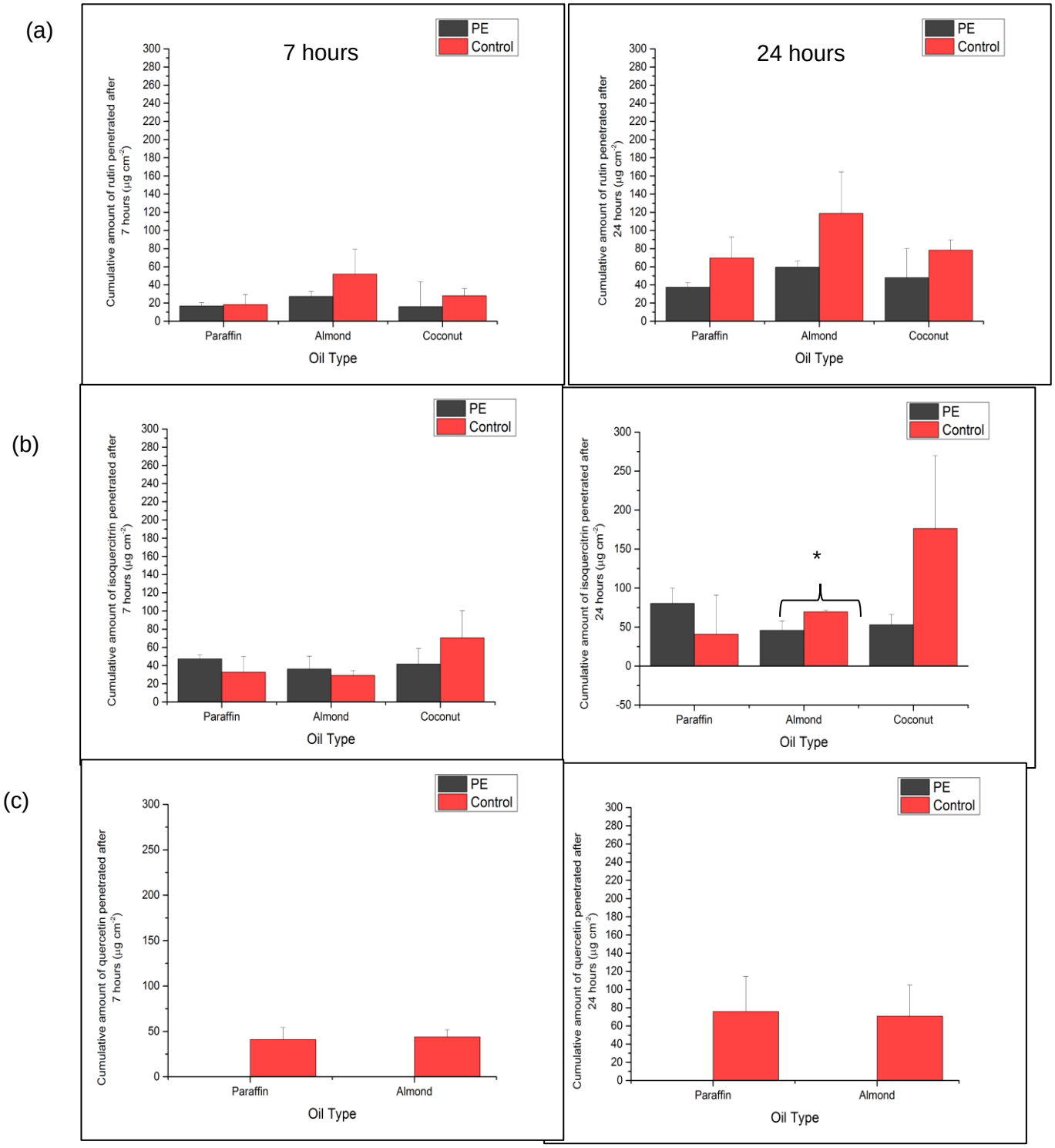

Figure 5-14 The cumulative amounts of flavonoids penetrating porcine epidermis membrane in 7 and 24 hours. (a) rutin (b) isoquercetin and (c) quercetin. * denotes significant differences at P < 0.05 after a one-tailed students *t*-test with a P-value < 0.05

The cumulative amount of flavonoids permeating the porcine epidermis are displayed in **Figure 5-14** and discussed in turn:

Rutin

After 7 hours there is no significant difference between the amount of rutin penetrating the epidermal membrane from Pickering emulsions with paraffin, almond and coconut oil, nor from the control. However, trend across all oils indicates that the controls deliver higher amounts of rutin compared to the PE.

After 24hours there are significant differences of the amount of rutin penetrating the epidermis. Rutin delivered from the control was significantly higher than from Pickering emulsion for paraffin and almond oils.

Rutin was also delivered in higher quantity from PE made with almond oil than PE made with paraffin oil. Coconut oil PE and control was found not to be significantly different from the other oils and between emulsion types.

Isoquercetin

After 7 hours there is no significant difference in the amount of isoquercetin delivered from Pickering emulsions form the three oil types. The coconut oil control was higher in trend than the paraffin oil control emulsion.

After 24hours the cumulative amount of isoquercetin was found to be significantly more from control from almond and coconut oils compared to the corresponding Pickering emulsions. No significant difference was found comparing PE or controls to paraffin oil.

Quercetin

Quercetin was only detected in the receptor phase after application to the donor side of the epidermal membrane from controls, not from Pickering emulsions. Out of the

three flavonoids investigated, quercetin is the least water soluble. However the receptor medium contain 50% v/v ethanol to ensure the solubility of all flavonoids. As mentioned previously in chapter 3, quercetin did not form any emulsion with coconut oil, and separation of water-oil was instant after homogenisation.

There was found to be no difference between the amount of quercetin penetrating the epidermal membrane at 7 hours or 24 hours from controls.

5.7.1.1 Flavonoids penetrating the membrane expressed as 'Percentage (%) of initial Applied Dose'

An alternative analysis into quantifying the amount of flavonoids penetrating the membrane is to express the amount penetrated as a percentage of the initial applied dose. This was done for all flavonoids and emulsion systems and is displayed in **Table XXV** on p**193**.

When expressed as a percentage of applied dose (**Table XXV**), it is clear that flavonoids permeate in the order quercetin > isoquercetin > rutin, which is the order of lipophilicity $LogP_{O/W}$ 2.02, 0.53, -0.34 respectively and of increasing molecular weight; 330.27 g mol^{-1}, 464.38 g mol^{-1} and 610.15 g mol^{-1} respectively. More isoquercetin was released from all oil types in a PE and control when compared to rutin after 7 hours (significantly for paraffin oil PE and coconut control $P < 0.05$) and more quercetin was released from a control from all oil types compared to rutin and isoquercetin (significantly more compared to rutin from paraffin oil, $P < 0.05$).

Table XXV Cumulative amounts and percentage (%) of applied dose of flavonoids at 7 and 24 hours after permeation assay from Pickering emulsions and control emulsions using different oil types.

Flavonoid	Pickering Emulsion	Time interval (hours)	Average cumulative amount µg cm^{-2}	Standard deviation	% of applied dose	Standard deviation	Flavonoid	Control emulsion	Time interval (hours)	Average cumulative amount µg cm^{-2} cm^{-2}	Standard deviation	% of applied dose	Standard deviation
Rutin	Paraffin	7	16.6	3.7	8.85	1.97	Rutin	Paraffin	7	18.3	10.9	9.76	5.81
		24	37.4	4.7	19.95	2.51			24	69.5	23.1	37.07	12.32
	Almond	7	27.1	5.5	14.45	2.93		Almond	7	51.8	27.2	27.63	14.51
		24	59.4	7	31.68	3.73			24	118.6	45.8	63.25	24.43
	Coconut	7	15.9	27.5	8.48	14.67		Coconut	7	27.8	7.9	14.83	4.21
		24	46.0	28.7	24.53	14.93			24	78.1	11.3	41.65	6.03
Isoquercetin	Paraffin	7	47.2	4.6	32.52	3.17	Isoquercetin	Paraffin	7	32.6	17.3	22.46	11.92
		24	80.2	19.8	55.26	13.64			24	60.9	50.3	41.96	34.66
	Almond	7	36.2	13.9	24.94	9.58		Almond	7	29.1	5.2	20.05	3.58
		24	45.7	12.2	31.49	8.41			24	69.4	2.1	47.82	1.45
	Coconut	7	41.5	17.2	28.60	11.85		Coconut	7	70.3	29.9	48.44	20.60
		24	52.7	13.2	36.31	9.10			24	176.1	93.7	121.35	64.57
Quercetin	Paraffin	7	*		-	-	Quercetin	Paraffin	7	43.0	18.4	45.50	19.31
		24	*		-	-			24	59.0	35.8	62.43	37.93
	Almond	7	*		-	-		Almond	7	43.5	11.4	46.06	12.07
		24	*						24	68.9	48.3	72.95	51.14

* No release of quercetin was detected from epidermis membrane during permeation assays, therefore % quercetin delivered as applied dose could not be determined.

5.7.2 Trans epidermal water loss

The trans-epidermal water loss (TEWL) measurement was taken before and after permeation assay to assess if a skin barrier for normal healthy skin was in place. Skin samples with a normal TEWL value were used indicating an intact and unimpaired *Stratum corneum* barrier. Measurements were taken afterwards to assess whether the barrier had altered during the permeation assay or by the Pickering emulsions/control. TEWL values were in the range for“ healthy to normal skin condition” (values10-25) set out by the manufacturer guidelines Courage & Khazaka (116). All skin samples showed a reduced value in TEWL after 24 hours from the initial TEWL value, indicating an improved barrier (**Table XXVI**), apart from the sample of rutin with coconut oil PE.

Table XXVI Trans epidermal water loss (TEWL) values of porcine skin epidermis before and after skin permeation assays (a) rutin (b) isoquercetin and (c) quercetin.

(a)	**Trans Epidermal Water Loss (TEWL) for Rutin Samples**	
Pickering Emulsions	**Pre-permeation (T0)**	**Post-permeation (T24)**
Paraffin Oil	23.5 ± 3.9	8.5 ± 1.7
Almond Oil	15.9 ± 2.3	7.3 ± 1.1
Coconut Oil	17.7 ± 1.2	34.1 ± 4.2
Control (Non-emulsion)		
Paraffin Oil	23.9 ± 5.3	7.0 ± 6.2
Almond Oil	22.1 ± 6.4	8.5 ± 4.5
Coconut Oil	21.4 ± 6.8	8.4 ± 4.3
(b)	**Trans Epidermal Water Loss (TEWL) for Isoquercetin Samples**	
Pickering Emulsions	**Pre-permeation (T0)**	**Post-permeation (T24)**
Paraffin Oil	19.4 ± 3.5	18.1 ± 2.4
Almond Oil	23.0 ± 2.6	13.8 ± 1.2
Coconut Oil	23.9 ± 8.3	21.3 ± 2.9
Control (Non-emulsion)		
Paraffin Oil	23.7 ± 5.6	4.2 ± 3.2
Almond Oil	18.5 ± 4.2	7.0 ± 3.6
Coconut Oil	27.0 ± 0.9	13.7 ± 4.8

(c)

(c)	Trans Epidermal Water Loss (TEWL) for Quercetin samples	
Pickering Emulsions	**Pre-permeation (T0)**	**Post-permeation (T24)**
Paraffin Oil	26.0 ± 3.8	14.6 ± 0.5
Almond Oil	17.4 ± 5.5	11.2 ± 5.1
Control (Non-emulsion)		
Paraffin Oil	23.3 ± 4.3	14.1 ± 7.1
Almond Oil	24.8 ± 2.2	12.4 ± 6.2

5.8 Discussion

As the Pickering emulsion and control systems were the same in ingredient and ratio composition (oil + water + flavonoid), there are several factors that can affect the permeation of the flavonoids through split-thickness skin:

1. the location of the flavonoid within the system, *i.e.* at the O/W interface or as a partial solution in the aqueous phase,
2. Flavonoid physiochemistry
3. Oil type used in the system (hydrocarbon or vegetable oil)
4. Availability of that oil (suspended/encapsulated by the flavonoid in an emulsion or “free” and not in an emulsion)
5. Barrier properties and skin membrane condition

5.8.1 Location of the flavonoid within the system

In a Pickering emulsion the flavonoid particles aggregate at the oil-water interface under shear, coating and stabilising oil droplets suspended in the external aqueous phase. This study used a 1 mM concertation of flavonoid in the aqueous phase to stabilise a 20 % oil fraction as previous studies have demonstrated (49, 150). At this concentration, the solubility limit of the flavonoid in water is passed and the flavonoid is in excess in the system. In a PE the flavonoid is at the oil-water interface which reduces the amount of flavonoid suspended in the external aqueous phase. This is illustrated in **Figure 5-15**.

In control mixtures where the aqueous and oil phases are mixed without high energy input (no use of the jet homogeniser), no emulsion has formed (view chapter **3** visually demonstrating no emulsion formed). Flavonoids remain as a particle suspension in the aqueous external phase, possible slight solubilisation in the oil phase, and with sedimentation of the flavonoid particles and creaming of the oil

occurring after mixing in test vials. Therefore, there is a higher concentration of flavonoid in the external aqueous phase of the control mixtures than the aqueous phase of the PE. Solubility of flavonoids is the oil should be investigated for confirmation. As previously discussed in Chapter 3, the flavonoids are ionsed in these PEs and suspensions, increasing their water solubility.

In both Pickering emulsion and controls the aqueous phase is 80 % of the applied formula into the donor compartment and will have a higher surface contact area to the *Stratum corneum* (SC), therefore any flavonoid remaining in the aqueous phase will have preferential contact with the skin than bound flavonoid at the O/W interface. The thermodynamic activity of the flavonoids in the external aqueous phase is higher than flavonoids bound at the O/W interface, changing permeation kinetics (115).

Due to the presence of excess flavonoids available in the aqueous phase in the control, it is suggested that more of rutin, isoquercetin and quercetin are available to penetrate the *Stratum corneum* within an aqueous medium over 24 hours, compared to the Pickering emulsions for all oil types. This is demonstrated in a higher % dose of flavonoids delivered from the controls than compared to Pickering emulsions at 24 hours (**Table XXV**). Whereas for Pickering emulsions, the amount of flavonoid available to penetrate the SC is time dependant on the rate of water evaporation and the structural collapse of the Pickering emulsion. This is graphically represented as a basic cartoon in **Figure 5-15** when an infinite dose is applied.

(a)

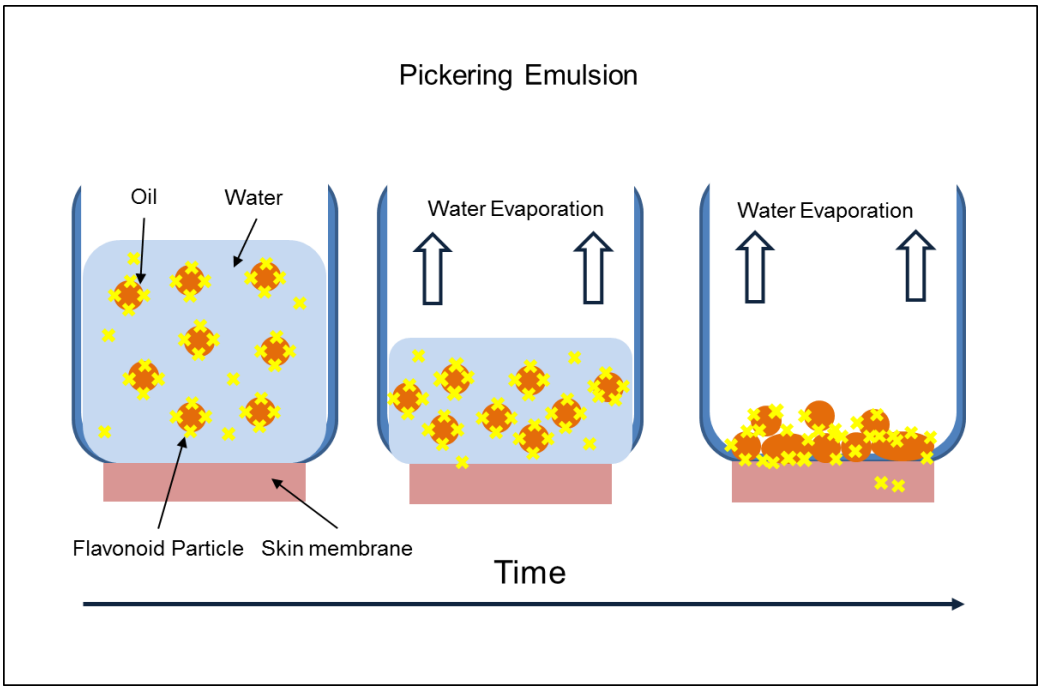

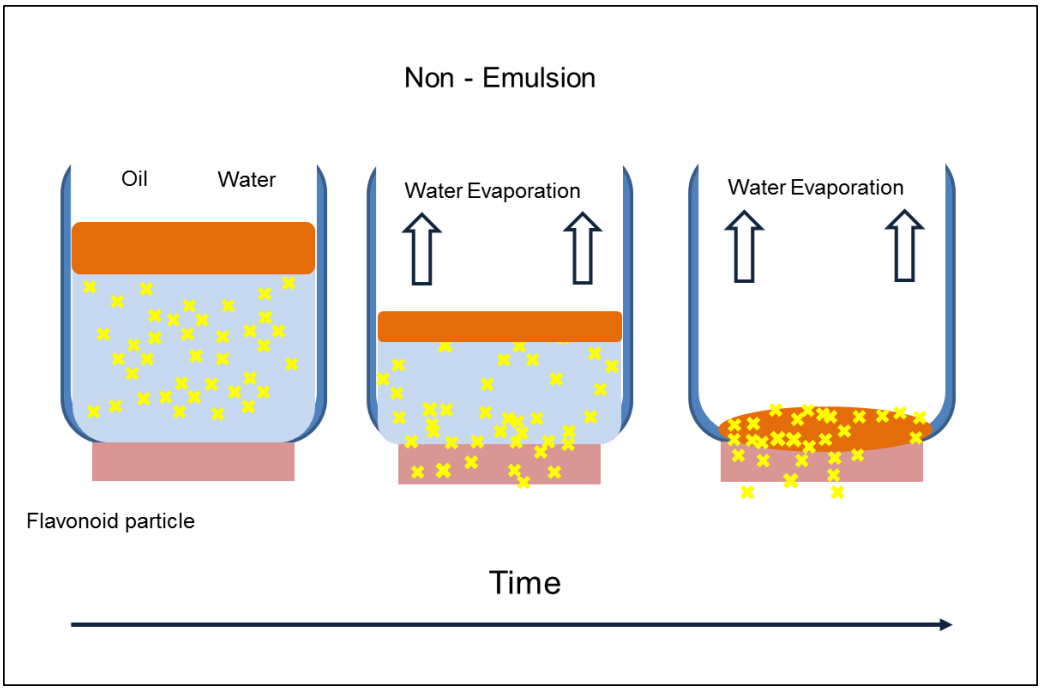

(b)

Figure 5-15 Schematic representation of structural differences in emulsion formation and possible scenario of the flavonoid particle/crystal location and skin penetration in (a) Pickering emulsions and (b) non-emulsion

Skin permeation is seen as a passive process of diffusion. When there is a higher concentration of suspended flavonoid particles in the external aqueous phase it pertains to an increase in thermodynamic activity of the flavonoid and a is driving force through the skin membrane, whereas when the flavonoid is held at the O/W interface in a PE the thermodynamic activity of the flavonoid is reduced (115). Supersaturation of a formula in which the concentration in the permeant surpasses its solubility limit and is in excess. Supersaturation is seen as a technique to enhance skin permeation of a molecule (72).

Excess or “free” flavonoid must traverse through the external phase to the skin surface. A few nm into the external phase at the skin surface, the water molecules are more ordered and the diffusion of the flavonoids here would be slower than in the bulk vehicle. This film layer can be rate limiting for sorption of molecules to a surface in aqueous bulk mediums, but not when the bulk medium has been mixed (151). Considering this, a reason why rutin has slightly higher or similar release coefficient (**Table XXIV**) than isoquercetin and quercetin, despite it being larger in MW (610.15 g mol^{-1} comparative to quercetin at 338.27 g mol^{-1}), could be do due the increased water solubility of the rutin molecule to traverse polar and non-polar regions between the ceramide chains with the extracellular matrix (ECM) of the SC. It is pertinent to note that this reasoning is based on the physiochemical properties of the rutin molecule, and not of a particle or crystal size of µm.

After the initial release rate their comes a slightly slower release of rutin and isoquercetin form PE than with the controls over the 24 hour period (permeation profiles **Figure 5-1 and Figure 5-2**). This could be suggestive of a time dependant destabilisation of the emulsion that increases the bioavailability of these flavonoids to penetrate the SC. Consideration to the location of actives within an emulsion has been investigated in literature and it is concluded that the location and emulsion type greatly effects permeation delivery (115). It is also important to consider the

dosing in permeation experiments; finite vs infinite dosing as occlusive affects can occur in the latter changing thermodynamic activity of applied actives. Thermodynamic activity is dependent on the evaporation of the external phase and collapse of the internal phase (115).

No detection of quercetin from Pickering Emulsions

No detection of quercetin was found in the receptor phase of the permeation assays during the time period up to 24 hours, with a total of six repetitions. However, quercetin was detected from the controls.

The difference between the PE and the control is the use of high pressure jet homogenisation. From photographs of emulsion and the Confocal Scanning Laser Microscopy (CSLM) images (chapter 3) quercetin appears to form an emulsion and quercetin to be located at the O/W interface, although in aggregated crystals surrounding oil droplet formation It is possible that quercetin under high pressure is dissolved preferentially into the oil phase of the emulsion (log$P_{o/w}$ of quercetion 2.02). Paraffin and almond oil do not penetrate the skin deeper than the *Stratum corneum* (136-139) therefore quercetin could be retained within the upper layers of the SC in with the oils. Further investigation into the skin retention and location of flavonoids in the skin would provide conclusive results on this.

5.8.1.1 Flavonoid physiochemistry

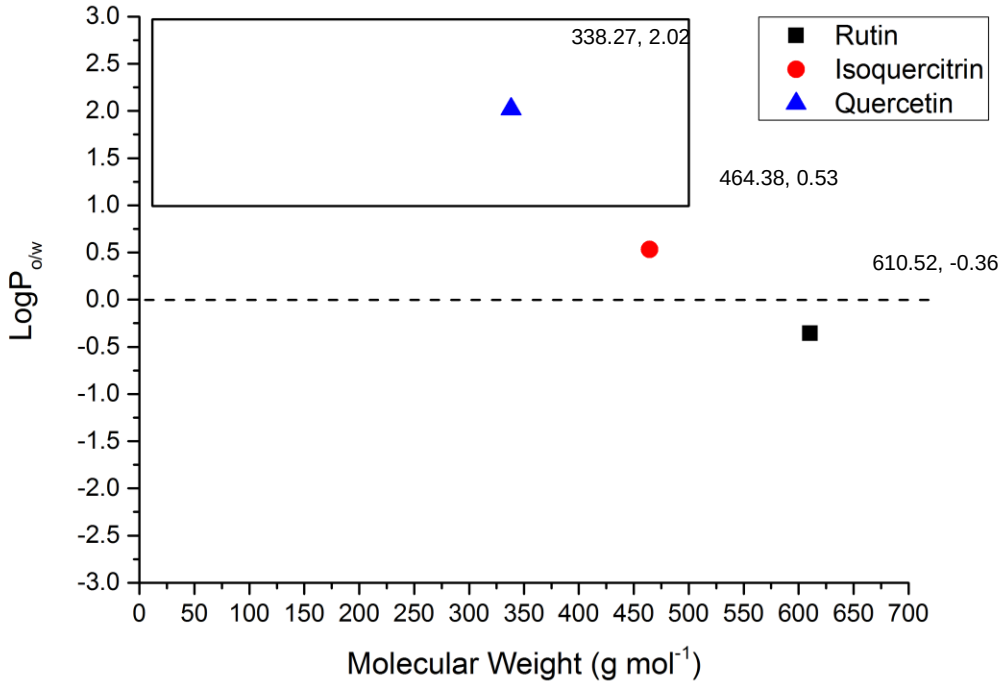

Figure 5-16 Physiochemical properties of flavonoids; partition coefficient between octanol and water ($LogP_{O/W}$) and molecular weight. Rectangle box indicates prefere,tial physiochemical properties for a skin permeant

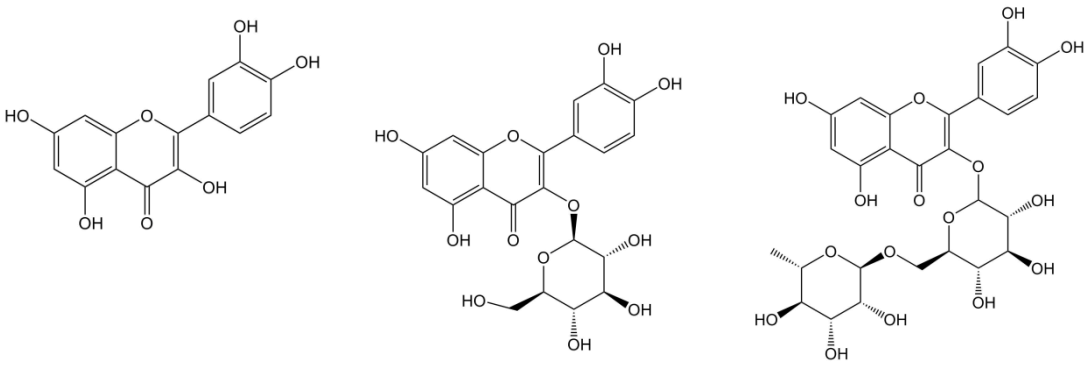

[1] **[2]** **[3]**

Figure 5-17 Chemical structures of quercetin [1], isoquercetin [2], and rutin [3]

A comparison of the physiochemical properties of rutin, isoquercetin and quercetin are shown in **Figure 5-16 and Figure 5-17**. It is clear that these three flavonoids have a correlation of molecular weight and lipophilicity. The molecular weight of the flavonoids varies due to the sugar moieties at the 3-OH position. The lipophilic portion of these flavonoids comes from the conjugated aromatic rings in the parent aglycone structure and the hydrophilic portion comes from the sugar moieties. As quercetin does not possess any sugar moieties, quercetin has a higher lipophilic $\log P_{O/W}$ of 2.02 compared to both isoquercetin and rutin. Isoquercetin possess one sugar moiety (glucose) which lower the partition coefficient to 0.53 and rutin has two sugar moieties (rhamnose and glucose) which reduces its partition coefficient further to -0.36, compared to the aglycone.

Most recognised physiochemical properties for membrane permeation is the molecular weight and lipophilicity; molecules < 500 g mol^{-1} and a $\log P_{O/W}$ between 1-3 being ideal as the skin is predominantly lipid based (93).The box in **Figure 5-16** represents this area for an ideal physiochemical properties for a molecule to permeate the *stratum corneum*. This demonstrates that isoquercetin and rutin fall out of this ideal category, and quercetin molecule has the ideal properties.

5.8.1.2 Permeability into the skin

Permeability is based on the partition coefficient of the molecule and the diffusivity into the *Stratum corneum*, which is reliant on the physiochemical properties of the molecule. Potts and Guy developed an equation based on the physiochemical properties of a molecule to theoretically ascertain its permeability through the SC from an aqueous medium (112); (Equation 15)

$$\log Kp = 0.71 \cdot \log P_{o/w} - 0.0061 \cdot \mathrm{MW} - 6.3$$

Equation 15

Where log$P_{o/w}$ is the octanol-water partition coefficient and MW is the molecular weight. Using this equation and the physiochemical properties of rutin, isoquercetin and quercetin in **Figure 5-16**, the theoretical permeability of the flavonoids were determined and are displayed **Figure 5-18** plotted alongside the experimentally determined log*Kp* of flavonoids from Pickering emulsions with different oil types using the permeation rate, J_{ss}. The estimated results from the Potts and Guy model show that quercetin has the highest permeability, followed by isoquercetin and lastly rutin, with linear correlation (R^2 = 0.99). However, experimentally the permeability coefficient for all three flavonoid was found to be similar, independent of the oil type used in the Pickering emulsions or from the controls. This may imply that the Potts and Guy model is not necessarily a good indication of the prediction of skin permeability of a flavonoid crystals in experimentation in combination with other components such as oils, as Potts and Guy model determines the permeability of individual molecules. It could be dependent on the applied concentration and availability of the active, dosing quantity or the structure of the molecule.

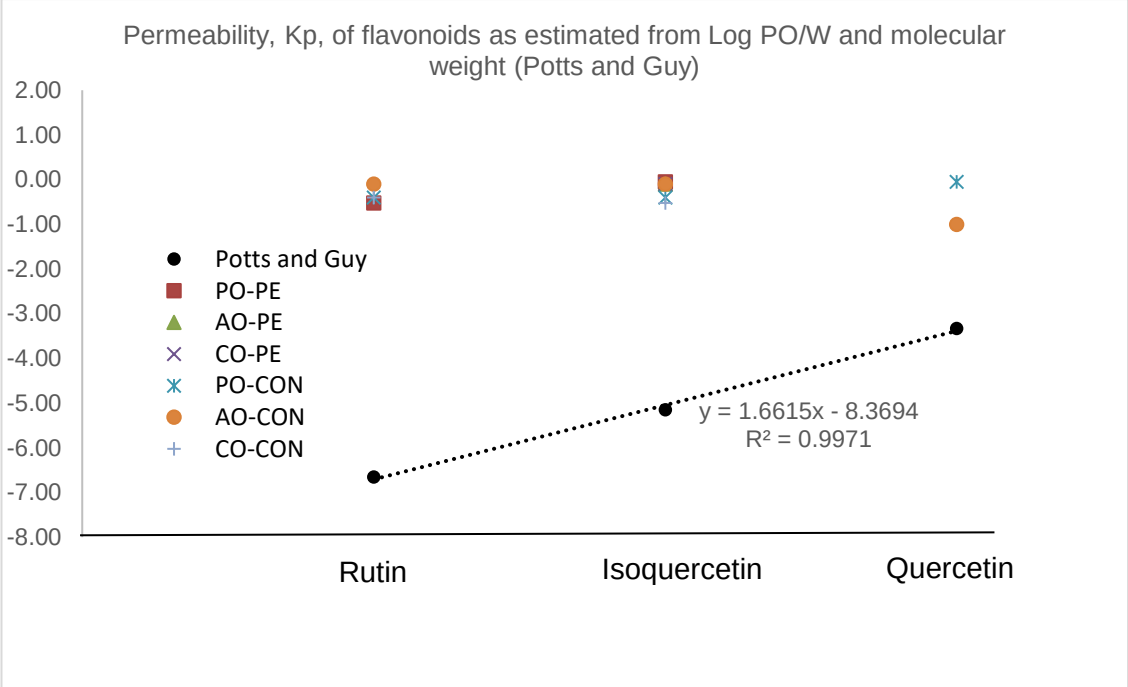

Figure 5-18 Estimated permeability of flavonoids from physiochemical properties of using the Potts and Guy model (equation 15) alongside the experimentally determined permeability, K_p from permeation data. PE = Pickering emulsion, PO = Paraffin Oil, AO = Almond Oil, CO = Coconut Oil, CON = control. Raw data in Table XXVII

Table XXVII Experimentally determined permeability of flavonoids through porcine epidermis and theoretically determined permeability

Permeability, LogKp	Rutin	Isoquercetin	Quercetin
Predicted (Potts and Guy)	-6.66	-5.15	*-3.33*
Pickering emulsions			
Paraffin Oil	-0.52	-0.05	
Almond Oil		*-0.1*	
Coconut Oil		*-0.1*	
Control Emulsions / Suspensions			
Paraffin Oil	-0.4	-0.4	-0.05
Almond Oil	-0.1	-0.1	-1
Coconut Oil	-0.4	-0.52	

Permeability between the flavonoids and emulsions was similar for flavonoids. Based on physiochemical properties of the flavonoid molecule alone, quercetin is the most likely flavonoid in this studied set to permeate the skin more easily due to its high lipophilicity and low molecular weight. The ability of rutin and isoquercetin to permeate the membrane as a similar permeability to quercetin could be due to their chemical structure; by having both polar and non-polar regions of the molecule they are able to traverse through the lipid membrane of the matrix. This polar and non-polar locations within the chemical molecule are not taken into account for the Potts and Guy model, nor is the permeability of larger aggregated particles.

Flavonoid particle did aggregate into crystals as seen visually and from Confocal Scanning Laser Microscopy (Chapter **3**) and how these crystals influence the permeation through the lipid matrix is unclear, although crystallisation of a permeant on the skin surface after solvent evaporation does perturb the percutaneous permeation of flavonoids (39, 55) .

Permeation of a molecule through the skin will go through polar and non-polar lipid regions in the ECM. It has been discussed that there are pockets of polar regions within the lipid matrix of the SC because of the sphingoid bases of the ceramides (28). Therefore permeating actives that possess both polar and non-polar components in their chemical structure, in this reasearch, rutin and isoquercetin, could partition through the polar pockets as well as the non-polar lipid chains within the ECM (refer to **Figure 5-17** p**202** to observe structural differences between flavonoids, particularly glucose and rutinose moieties on the structure of isoquercetin and quercetin, respectively). This could explain the permeation of these flavonoids despite their size; ≥ 500 g mol^{-1} (**Figure 5-16** p**202**) of which goes out the guidelines of Lipinski's rule for a suitable membrane permeant (93). As quercetin

does not contain sugar moieties which contribute to hydrophilicity, quercetin remains partitioned in the non-polar regions of the lipids and becomes "trapped" in the SC layers with the oils, rather than penetrating further. This suggests why no quercetin was measured to permeate the epidermal membrane in (**Figure 5-3** p**170)** as it is retained within the lipid matrix, or is preferentially adsorbed in the oil phase of the emulsion, retained within the upper layers of the SC. This result is opposite to when quercetin is in the suspension control mixture; it was shown by permeation assays to penetrate the epidermal membrane in the highest percentage dose (**Table XXV** p**193**) and have a rapid release rate as determined by the Korsmeyer-Peppas model (refer to **Table XXII** p**171** and **Table XXIV** p**176**); both sets of data higher than rutin and isoquercetin. This can be explained by both the lipophilicity and the molecular size of quercetin; more polar and smaller than the other flavonoids which allow quercetin to permeate more easily through the ECM of the *Stratum corneum* and epidermal layers. These two opposing results conclude that the location of the flavonoid, and permeant in an emulsion or formulation, is important not only for partitioning into the SC, but additionally for permeating through the skin.

5.8.2 Oil type used in the system (hydrocarbon or vegetable oil)

Significantly more rutin penetrated through the skin with almond oil in a Pickering emulsion than in a PE with paraffin after 24 hours ($P < 0.05$) (**Figure 5-1** p**164**). The control emulsions of paraffin and almond oils to deliver rutin were not significantly different, although the almond was higher in trend. This could be because the PE droplets formed with oil types could vary in uniform particle coating of the flavonoids, leading to a porous coating. Leaching of oil can be occurring, leading to collapse of the emulsion as the water phase evaporates off the skin. Therefore exposing the oil to disrupt the *Stratum corneum* lipids to promote rutin through the skin. There is no significant difference in rutin penetrated at 7 hours between PE with paraffin oil and almond oil. There could be a delayed response in permeation as the collapse of the emulsions and vegetable oils can disrupt the lipid chains of the ECM over time.

5.8.2.1 Diffusivity within the vehicle; Pickering emulsion and oils

Rutin diffused from the emulsion to the skin faster in the control emulsion for paraffin oil than the PE – a reason for this could be due to the majority of the rutin being held at the interface within the emulsion. When rutin is not in a Pickering emulsion, it's thermodynamic activity is higher therefore the driving force for rutin to diffuse from the aqueous medium to the skin surface is higher. This is also reflected in the rutin diffusing faster from the almond control compared to the paraffin control. Almond oil contains oleic acid that can change the packing order for the lipids in the matrix, which could disrupt them enough to allow for the rutin to diffuse into the SC greater than paraffin oil. As paraffin is a straight chain hydrocarbon that has no polar head groups, it will not disrupt the lipid packing. This is also the result with isoquercetin and quercetin: the diffusivity to the skin of the flavonoids is greater for the vegetable oils than the hydrocarbon oil. The diffusivity of isoquercetin from Pickering emulsions was also in the order of vegetable oils faster than the

hydrocarbon oil however not significantly different. Again, the oil type is influencing the lipid packing conformation of the SC. In a PE, the coating of the flavonoid prevents the oil from disrupting the lipid chain packing. Oil fraction was used at 20 % and serves as a comparison to previous flavonoid Pickering emulsions (49), requires less stabilisation and emulsions which possess a lower oil content have been found to increase the skin permeation of polyphenols (39). However, it would be a consideration of future work to enhance this oil content and repeat experimentation to build the understanding oil type has on the skin permeation of flavonoids.

5.8.3 Availability of oil (suspended/encapsulated by the flavonoid in an emulsion or "free" and not in an emulsion)

Pickering emulsions made with silica particles have been studied; a concern of using solid silica particles is what is the fate of the silica; does it remain in the upper layers of the epidermis or permeate into deeper layers? (83).

Chapter 6 Further research discussion

6.1.1 Formation of Pickering emulsions with flavonoids and oil.

In this study, the concentration of rutin, isoquercetin and quercetin used to form Pickering emulsions with 20 % oil fraction was 1 mM. This concentration surpasses the aqueous solubility of each of the flavonoids and the aqueous phase can be described as being saturated. This aturation will affect the bioavailability, thermodynamic activity and skin penetration behaviour of the flavonoids. A problem that arises with an excess concertation of the flavonoids is aggregation and crystal formation of the flavonoids within the oil phase of the emulsion. This aggregation could lead to clumping of oil droplets rather than a uniform dispersed emulsion and large crystal formation will hinder skin penetration.

Reducing the concentration of flavonoids in the emulsion system needs to be conducted because this may i) prevent flavonoid aggregation and crystal formation, ii) change the Pickering emulsion formation and stability and ii) change the thermodynamic activity and skin penetrating behaviour of the flavonoids.

It is not known what the minimum nor maximum concentration of flavonoid is required to stabilise a Pickering emulsion with a 20 % oil fraction. However, a lower or concentration less than 1 mM could change the stability of the emulsion by preventing aggregation and crystallisation of the flavonoids. As observed in the Confocal Scanning Laser Microscopy images in chapter 3, the flavonoids, particularly rutin and isoquercetin adsorb at the O/W interface and also form clusters entrapping oil droplets. A uniform layer of flavonoids at the O/W interface may form if less aggregatiion occurs.

Another method to ensure aggregation of the flavonoids does not occur is to ensure adequate dispersion in the aqueous phase prior to the jet homogenisation. In this study a high sheer mixer was used for 2 minutes to disperse the flavonoids,

however this step may need to be longer to break up crystals. The use of a sonicator may be used to break up crystals.

suggested experiments include forming Pickering emulsions with consecutive flavonoid concentrations, *e.g.* 0.1, 0.2, 0.4, 0.6, 0.8 up to 2 mM with a 20 % oil fraction of paraffin, almond and coconut oil. Evaluation analysis using CSLM for location of flavonoids, particle size distribution visual stability evaluation and permeation assays using infinite dose.

A knowledge gap is the flavonoids solubility within the oils and where the flavonoids migrate to the emulsion over time and what happens during emulsion collapse on the skin. Further experiments should analyse the oil fraction over time to see the migration and quantify the flavonoid being depleted from the emulsion during skin permeation assays and the location of quercetin in the oil droplets. Future work should also incorporate chemical analysis of the aqueous phases of the two systems.

6.2 Permeation assays

6.2.1 Infinite vs finite dosing

Skin permeation assays done in this study used an infinite (excess) dose loading in the Franz diffusion cells. Infinite loading is necessary to provide the determination of release kinetics and thermodynamic activity properties of the actives in the emulsion and how this changes when the flavonoids are incorporated into a Pickering emulsion. However, the draw backs of this are that the constant contact and the occlusive nature of the formulation on the skin which will over time change the barrier properties of the *Stratum corneum e.g.* becoming super hydrated.

The opposite of this would be to use a finite dose; more representable of real life conditions of the end user using the formulation. This amount had been quoted as 2 mg cm^{-3} (89). The differences between finite and infinite dosing are highlighted in the literature in chapter 1. Future experiment recommendations are to use a finite dose loading on skin membrane in permeation studies. Requirement for the substantiation of skin permeation in cosmetic dose is to obtain at least 8 repetitions of skin permeation assays, ideally on human cadaver skin (152). After finite dosing FT-IR analysis should be conducted as finite dosing changes the barrier properties of the *Stratum corneum* and should be analysed in comparison with the infinite study results.

6.2.2 Using cellulose membrane for permeation controls

A cellulose membrane should be used in future research as a standard control membrane. This may be a solution to reducing the variability of error seen in the results. As cellulose membranes will be homogeneous, for permeation release kinetics the results would have higher accuracy than with a biological membrane. Biological tissue it will have uncontrolled variabilities; such as protein, lipid and structural formation that can change the permeation of molecules. Biological membranes can become dehydrated when exposed to the receptor fluid, changing the hydration and the barrier properties of the membrane.

6.2.3 In vivo analysis

Franz diffusion cells do not completely represent human physiological conditions, therefore future research should include *in vitro* analyses of skin permeation; paired with tape stripping, infrared or Raman spectroscopy for depth profiling of skin permeation actives.

6.3 Depth profiling of flavonoids within the skin membrane

6.3.1 Tape stripping – removal of skin layers by tape.

An important knowledge gap is the location and migration of the flavonoids within the *Stratum corneum* and epidermis after skin permeation. This can commonly be done by tape stripping layers of the skin with adhesive tape and then determining the concentration of active by back extraction and HPLC analysis. However, this technique is not accurate as the pressure to apply the tape on the skin surface must be the same each time a strip is taken, and each strip can have varying amounts of skin cells not attributed to a single planar layer. In tape stripping the membranes in the samples are destroyed and cannot be further analysed.

6.3.2 Raman Spectroscopy

Another technique is Raman spectroscopy which can be used for depth profiling of actives within a skin membrane and does not destroy the skin sample. Raman spectroscopy can provide information on the chemical moieties present on a compound, giving a distinctive fingerprint that can be used to identify substances in the upper layers of the skin. Symmetrical vibrations of non-polar groups are often best identified by Raman spectroscopy, whereas asymmetric vibrations of polar groups are best identified by IR spectroscopy (129).

Raman spectroscopy has been used in studies to determine the spatial distribution of drug molecules within skin biopsies and to monitor the biotransformation of the pro-drug into the active molecule. (153, 154). By using a technique such as this it provides useful information about the location of the biotransformation *e.g.* in the epidermis or dermis, and thus where best the activity of this drug molecule will occur. As these techniques do not require touching the sample they are deemed non-invasive and non-destructive. Advantages of these techniques include that monitored compounds do not require labelling with fluorescence or spin labels to be

detectable, the sample to be measured is not limited by size and the atomic vibrations are detected instantaneously providing a snap shot of all molecular conformations (155). The technique can also be combined with confocal microscopy to determine depth morphology of skin samples, and to what depth actives are reaching in the skin (156, 157).The use of Raman spectroscopy has been used as a method to determine the penetration profile of flavonoids (153, 158), for the determination of antioxidant stability of cosmetic formulations (159) and can be combined with confocal microscopy to determine depth profile.

6.4 Additional ingredients to the emulsion

In these preliminary experiments the Pickering emulsions and controls were purposely kept simple with only the omission of the jet homogeniser, which has been concluded as necessary to form the Pickering emulsions. If other ingredients such as an emulsifier were to be incorporated in the controls, the emulsion stability and the skin permeation of the flavonoids would have been altered and not directly comparable to the Pickering emulsions. Questions that arise during this research are how does the delivery change of multiple actives with multiple lipophilicities. Future studies should include a mixture of flavonoids *e.g.* rutin and isoquercetin combined in a Pickering emulsion and stability and skin permeation repeated. The inclusion of an aqueous thickener could be the next stage in development, such as xanthan gum.

Additional future studies is to reduce the pH of the emulsions to acidic pH 4-5 to below the pKa of the flavonoids and observe Pickering emulsion stability and skin permeation. As previously mentioned, below their pKa flavonoids will be protonated which will increase their lipid solubility and could effect their permeation through the lipid membrane of the *Stratum corneum.*

6.5 Detailed stability testing of Pickering emulsions

Time constraints and resources did not allow a full comprehensive stability test of the Pickering emulsions; monitoring pH, viscosity and location of flavonoids by CSLM over time in different environmental conditions (heat, freeze thaw and UV exposure). This would enhance the knowledge of further stability of flavonoids for Pickering emulsions for cosmetic formulations.

The purpose of this research was to improve the formula stability of flavonoids and to observe the skin permeation release kinetics when these flavonoids had enhanced formula stability. Looking beyond this is to develop on a formula with consumer and market acceptability as a topical cosmetic product with antioxidant actives in for therapeutic benefits to the skin.

Chapter 7 Summary and Conclusions of Research

This research had several focal points: to re-engineer formulation design for personal care applications, choosing flavonoids as skin actives, improving their formulation stability by incorporation into Pickering emulsions, evaluation of skin permeation and *Stratum corneum* lipid morphology and barrier properties after topical treatment.

Unlike other studies that have investigated the penetration enhancement of actives through the skin encapsulated within the solid coated particles (80) the active in the Pickering emulsions in this study is the stabilising agent of the oil droplet, rather than the flavonoids being encapsulated within the oil droplet. This could lead the way to multi-component formulas as a technique to deliver multiple actives; soluble in the oil phase and the coating of the oil droplets. It also increases the use of multi-functional ingredients and reduces emulsifiers in the formulation that can cause skin irritancy.

Chapter 3 demonstrated that flavonoids rutin, isoquercetin and quercetin can be made into Pickering emulsions with various oil types, although the strength of the stability is dependent on oil type; inert paraffin oil proving to form stable PE than natural vegetable oils almond and coconut. The rate of de-adsorption of flavonoids from the surface of the PE is high, therefore they form stable emulsions, which was demonstrated after 6 months of storage.

Chapter 4 demonstrated interesting results; lipid changes which change the barrier properties of the SC allowing for changes in skin permeation, and is a balance between the oil type and the flavonoid type. There is evidence that quercetin could be dissolving in the lipids of the SC which allows for enhanced permeation into the skin from the topical emulsions, but then is retained within the SC lipids, not causing too much disruption as to impair barrier function, but not to penetrate further into the

skin layers. Quercetin was not observed to penetrate the epidermal layers when made into a Pickering emulsion, however in suspension it did.

Results in changes in lipid morphology of the extracellular matrix by rutin and isoquercitrin were highly interesting. The primary reason for selecting these flavonoids was for their ability to form Pickering emulsions at the O/W interface due to their amphiphilic structure, however surprisingly their surface active nature also disrupted acyl chain packing of the ceramides which form the skin's barrier. This result demonstrates that flavonoids – with the correct structure – are unique multi-functional personal care "active" ingredients; antioxidant capactiy, emulsion stabilising (which improves their formulation solubility) and as a potential mild permeation enhancer to the *Stratum corneum.*

Chapter 5 evaluated the skin permeation and came to the following conclusions that the location of the flavonoid crystals has proven to be a key component in the permeation and release kinetics.It has become clear from comparison of results between Pickering emulsions formed with flavonoids, and flavonoid suspensions – "non-emulsion" controls, the location of the flavonoids with the emulsion changes their availability to partition into the *Stratum corneum* as their thermodynamic activity is changed, thus altering their membrane permeation. Pickering emulsions therefore can have potential use as a controlled release system.

The research has shown an interesting approach to formulation design and has proved that incorporating rutin, isoquercetin and quercetin into Pickering emulsions does change the behaviour of permeation from the emulsion into the *Stratum corneum*, and further influences the penetration through the skin. In addition, the difference in oil type used influences the permeation and penetration into the skin, and is dependent on fatty acid content. The barrier properties of the lipids in the SC are rate limiting for any permeant penetrating the skin, and a change in these lipids

to impair the barrier has been observed both by oil (almond and coconut) and flavonoid type (rutin and isoquercetin). A combination of the polarity of the flavonoids, the oil and the position of the flavonoids in the emulsion system are important to effective formulation design, and this study provides the basis for future research in this field.

Chapter 8 References

1. Boncheva M, Damien F, Normand V. Molecular organization of the lipid matrix in intact Stratum corneum using ATR-FTIR spectroscopy. Biochimica et Biophysica Acta (BBA) - Biomembranes. 2008;1778(5):1344-55.
2. Dufton E. Efficacy and Optimal Skin-Delivery of Plant-Derived Antioxidant Compounds via Cosmetic Formulation: University of Leeds; 2014.
3. Wiechers JW, Watkinson AC, Cross SE, Roberts MS. Predicitng the Skin Penetration of Actives from Complex Cosmetic Formulations: An Evaluation of inter Formulation and inter Active Effects During Formulation Optimization for Transdermal Delivery. International Journal of Cosmetic Science. 2012;34:525-35.
4. Abbot S. How the "Stuff" in Formulations Impacts the Delivery of Actives Cosmetics & Toiletires 2013:116-23.
5. Otto A, Plessis Jd, Wiechers JW. Formulation Effects of Topical Emulsions on Transdermal and Dermal Delivery. International Journal of Cosmetic Science. 2009;31:1-19.
6. Lane ME, Hadgraft J, Oliveira G, Vieira R, Mohammed D, Hirata K. Rational Formulation Design. Int J Cosmet Sci. 2012;34(6):496-501.
7. Wooi Ng K, Man Lau W. Skin Deep: The Basics of Human Skin Structure and Drug Penetration. In: Dragicevic N, Maibach H, editors. Percutaneous Penetration Enhancers: Chemical Methods in Penetration Enhancement. NY: Springer; 2015. p. 3-12.
8. MacNeil S. Progress and opportunities for tissue-engineered skin. Nature. 2007;445(7130):874-80.
9. Wickett RR, Visscher MO. Structure and function of the epidermal barrier. American Journal of Infection Control. 2006;34(10):S98-S110.
10. Priestley G. An Introduction to the Skin and Diseases. In: Priestley G, editor. Molecular Aspects of Dermatology. UK: John Wiley & Sons; 1993. p. 1-17.
11. Carter E, Edwards H. Biological Applications of Raman Spectroscopy. In: Gremlich H-U, Yan B, editors. Infrared and Raman Spectroscopy of Biological Materials. Practical Spectroscopy. New York: Marcel Dekker, Inc; 2001. p. 421-75.
12. Garidel P, Fölting B, Schaller I, Kerth A. The microstructure of the stratum corneum lipid barrier: Mid-infrared spectroscopic studies of hydrated ceramide:palmitic acid:cholesterol model systems. Biophysical Chemistry. 2010;150(1):144-56.
13. Critchley P. Skin Lipids. In: Priestley GC, editor. Molecular Aspects of Dermatology: John Wiley & Sons Ltd; 1993. p. 147-69.
14. Wertz P, Downing D. Ceramides of pig epidermis: structure determination Journal of Lipid Research. 1983;24(6):759-65.

15. Motta S, Monti M, Sesana S, Caputo R, Carelli S, Ghidoni R. Ceramide composition of the psoriatic scale. Biochimica et Biophysica Acta (BBA) - Molecular Basis of Disease. 1993;1182(2):147-51.
16. Boncheva M. The physical chemistry of the stratum corneum lipids. International Journal of Cosmetic Science. 2014;36(6):505-15.
17. Maurice Gray G, White RJ. Glycosphingolipids and Ceramides in Human and Pig Epidermis. Journal of Investigative Dermatology. 1978;70(6):336-41.
18. Hansen HS, Jensen B. Essential function of linoleic acid esterified in acylglucosylceramide and acylceramide in maintaining the epidermal water permeability barrier. Evidence from feeding studies with oleate, linoleate, arachidonate, columbinate and α-linolenate. Biochimica et Biophysica Acta (BBA) - Lipids and Lipid Metabolism. 1985;834(3):357-63.
19. Forslind BO. Forslind B. A domain mosaic model of the skin barrier. Acta Derm Venereol74: 1-61994. 1-6 p.
20. Ohta N, Ban S, Tanaka H, Nakata S, Hatta I. Swelling of intercellular lipid lamellar structure with short repeat distance in hairless mouse stratum corneum as studied by X-ray diffraction. Chemistry and Physics of Lipids. 2003;123(1):1-8.
21. Abraham W, Downing DT. Lamellar Structures Formed by Stratum Corneum Lipids in Vitro: A Deuterium Nuclear Magnetic Resonance (NMR) Study. Pharm Res. 1992;9(11):1415-21.
22. Laugel C, Yagoubi N, Baillet A. ATR-FTIR spectroscopy: a chemometric approach for studying the lipid organisation of the stratum corneum. Chemistry and Physics of Lipids. 2005;135(1):55-68.
23. Levin J, Maibach H. The Correlation Between Transepidermal Water Loss and Percutaneous Absorption. In: Dragicevic N, Maibach H, editors. Percutaneous Penetration Enhancers: Chemical Methods in Penetration Enhancement Drug Manipulation Strategies and Vehicle Effects: Springer; 2015.
24. Rogers J, Harding C, Mayo A, Banks J, Rawlings A. Stratum corneum lipids: the effect of ageing and the seasons. Archives of Dermatological Research. 1996;288(12):765-70.
25. Choe C, Lademann J, Darvin ME. Depth profiles of hydrogen bound water molecule types and their relation to lipid and protein interaction in the human stratum corneum in vivo. Analyst. 2016;141(22):6329-37.
26. Alonso A, Meirelles NC, Tabak M. Effect of hydration upon the fluidity of intercellular membranes of stratum corneum: an EPR study. Biochimica et Biophysica Acta (BBA) - Biomembranes. 1995;1237(1):6-15.
27. Imokawa G, Kuno H, Kawai M. Stratum corneum lipids serve as a bound-water modulator. Journal of Investigative Dermatology. 1991;96(6):845-51.
28. Schroeter A, Eichner A, J M, Neubert RH. The Importance of Stratum Corneum Lipid Organization for Proper Barrier Function. In: Dragicevic N, Maibach H, editors. Percutaneous Penetration Enhancers: Chemical Methods in Penetration Enhncement - Drug Manipulation Strategies and Vehicle Effects: Springer-Verlag 2015. p. 19-38.

29. Bradley M. Curve Fitting in Raman and IR Spectroscopy: Basic Theory of Line Shaper and Applications. Application Note: 50733. Thermo Fisher Scientific Inc.; 2007.
30. Wartewig S. Basic Principles of Vibrational Spectroscopy. IR asnd Raman Spectroscopy : Fundamental Processing: Wiley-VCH GmbH & Co. KGaA; 2003. p. 27-30.
31. Corbe E, Laugel C, Yagoubi N, Baillet A. Role of ceramide structure and its microenvironment on the conformational order of model stratum corneum lipids mixtures: an approach by FTIR spectroscopy. Chemistry and Physics of Lipids. 2007;146(2):67-75.
32. Chen L, Hu JY, Wang SQ. The role of antioxidants in photoprotection: a critical review. Journal of the American Academy of Dermatology. 2012;67(5):1013-24.
33. Gonzalez-Paredes A, Clares-Naveros B, Ruiz-Martinez MA, Durban-Fornieles JJ, Ramos-Cormenzana A, Monteoliva-Sanchez M. Delivery systems for natural antioxidant compounds: Archaeosomes and archaeosomal hydrogels characterization and release study. Int J Pharm. 2011;421(2):321-31.
34. Oresajo C, Pillai S, Manco M, Yatskayer M, McDaniel D. Antioxidants and the Skin: Understanding Formulation and Efficacy. Dermatologic Therapy. 2012;25:252-9.
35. Yotsawimonwat S, Rattanadechsakul J, Rattanadechsakul P, Okonogi S. Skin Improvement and Stability of *Echinacea purpurea* Dermatological Formulations. International Journal of Cosmetic Science. 2010;32:340-6.
36. Iacopini P, Baldi M, Storchi P, Sebastiani L. Catechin, epicatechin, quercetin, rutin and resveratrol in red grape: Content, *in vitro* antioxidant activity and interactions. Journal of Food Composition and Analysis. 2008;21:289-98.
37. Seeram NP, Adams LS, Hardy ML, Heber D. Total Cranberry Extract versus its Phytochemical Constituents: Antiproliferative and Synergistic Effects against Human Tumor Cell Lines. Journal of Agricultural and Food Chemistry. 2004;52:2512-7.
38. Perde-Schrepler M, Chereches G, Brie I, Tatomir C, Postescu ID, Soran L, et al. Grape seed extract as photochemopreventive agent against UVB-induced skin cancer. Journal of photochemistry and photobiology B, Biology. 2013;118:16-21.
39. Zillich OV, Schweiggert-Weisz U, Hasenkopf K, Eisner P, Kerscher M. Release and in vitro skin permeation of polyphenols from cosmetic emulsions. Int J Cosmet Sci. 2013;35(5):491-501.
40. Rice-Evans CA, Miller NJ, Paganga G. Structure-Antioxidant Activity Relationships of Flavonoids and Phenolic Acids. Free Radical Biology & Medicine. 1996;20(7):933-56.
41. Wright JS, Johnson ER, DiLabio GA. Predicting the Activity of Phenolic Antioxidants: Theoretical Method, Analysis of substituent Effects and Application to Major Families of Antioxidants. Journal of the American Chemistry Society. 2001;123:1173-83.
42. Vagánek A, Rimarčik J, Lukeš V, Klein E. On the Energetics of Homolytic and Heterolytic O-H Bond Cleavage in Flavonoids. Computational and Theoretical Chemistry. 2012;991:192-200.

43. Zhang G, Flach CR, Mendelsohn R. Tracking the dephosphorylation of resveratrol triphosphate in skin by confocal Raman microscopy. Journal of controlled release : official journal of the Controlled Release Society. 2007;123(2):141-7.
44. Markham K, Bloor S. Analysis and Identification of Flavonoids in Practice. In: Rice-Evans C, Packer L, editors. Flavonoids in Health and Disease. NY: Marcel Dekker Inc.; 1998.
45. López-Nicolás JM, García-Carmona F. Aggregation State and pK_a Values of (*E*)-Resveratrol as Determined by Fluorescence Spectroscopy and UV-Visible Absorption Journal of Agricultural and Food Chemistry. 2008;56:7600-5.
46. Valentová K, Vrba J, Bancířová M, Ulrichová J, Křen V. Isoquercitrin: Pharmacology, toxicology, and metabolism. Food and Chemical Toxicology. 2014;68:267-82.
47. de Araújo MEMB, Moreira Franco YE, Alberto TG, Sobreiro MA, Conrado MA, Priolli DG, et al. Enzymatic de-glycosylation of rutin improves its antioxidant and antiproliferative activities. Food Chemistry. 2013;141(1):266-73.
48. Das MK, Kalita B. Design and Evaluation of Phyto-Phospholipid Complexes (Phytosomes) of Rutin for Transdermal Application. Journal of Applied Pharmaceutical Science. 2014;4(10):51-7.
49. Luo Z, Murray BS, Yusoff A, Morgan MR, Povey MJ, Day AJ. Particle-Stabilizing Effects of Flavonoids at the Oil-Water Interface. Journal of agricultural and food chemistry. 2011;59(6):2636-45.
50. Michaels AS, Chandrasekaran SK, Shaw JE. Drug permeation through human skin: Theory and invitro experimental measurement. AIChE Journal. 1975;21(5):985-96.
51. SciFinder. Predicted pKa values Calculated using Advanced Chemistry Development (ACD/Labs) Software V11.02 (© 1994-2018 ACD/Labs). 2018.
52. Tfayli A, Guillard E, Manfait M, Baillet-Guffroy A. Molecular interactions of penetration enhancers within ceramides organization: a Raman spectroscopy approach. Analyst. 2012;137(21):5002-10.
53. EuropeanComission. Substance : 2-(2-ethoxyethoxy)ethanol Diethylene Glycol Monoethyl Ether (DEGEE), Ethoxydiglycol 2018. Available from: http://ec.europa.eu/growth/tools-databases/cosing/index.cfm?fuseaction=search.details_v2&id=93861.
54. O'Lenick A, Price S. Surfactants. In: Schlossman M, editor. The Chemistry and Manufacture of Cosmetics. III: Ingredients Book Two: Allured Publishing Corporation; 2002. p. 967-98.
55. Zillich OV, Schweiggert-Weisz U, Eisner P, Kerscher M. Polyphenols as Active Ingredients for Cosmetic Products. International Journal of Cosmetic Science. 2015;37(5):455-64.
56. Cumming KI, Winfield AJ. In vitro evaluation of a series of sodium carboxylates as dermal penetration enhancers. International Journal of Pharmaceutics. 1994;108(2):141-8.
57. Nara B, Ivy L, Hongbo Z, I. MH. Long-term repetitive sodium lauryl sulfate-induced irritation of the skin: an in vivo study. Contact Dermatitis. 2005;53(5):278-84.

58. Puglia C, Rizza L, Offerta A, Gasparri F, Giannini V, Bonina F. Formulation Strategies to Modulate the Topical Delivery of Anti-Inflammatory Compounds. Journal of the Society of Cosmetic Chemists. 2013;64(5):341-54.
59. Todorova P, Grant-Ross P, Tamburic S. Biomimetic vs. Traditional Skin Moisturization: An In Vivo Comparison. IFSCC Congress; Paris: IFSCC; 2015.
60. Baby A, Haroutiounian-Filhoa C, Sarrufa F, Sales de Oliveira Pintoa C, Kanekoa T, Velasco M. Influence of Urea, Isopropanol, and Propylene Glycol on Rutin In Vitro Release from Cosmetic Semisolid Systems Estimated by Factorial Design. Drug Development and Industrial Pharmacy. 2009;35:272-82.
61. Pantzaris TP, Basiron Y. The Lauric (coconut and palmkernal) Oils. In: Gunstone FD, editor. Vegetable Oils In Food Technology: Composition, Properties and Uses: Blackwell Publishing; 2002. p. 157-202.
62. Roncero JM, Álvarez-Ortí M, Pardo-Giménez A, Gómez R, Rabadán A, Pardo JE. Virgin almond oil: Extraction methods and composition. 2016. 2016;67(3).
63. Kandimalla K, Kanikkannan N, Andega S, Singh M. Effect of Fatty acids on the Permeation of Melatonin across Rat and Pig Skin In-vitro and on the Transepidermal Water Loss in Rats In-vivo. Journal of Pharmacy and Pharmacology. 1999;51(7):783-90.
64. Roussel L, Abdayem R, Gilbert E, Pirot F, Haftek M. Influence of Excipients on Two Elements of the *Stratum Corneum* Barrier: Intercellular Lipids and Epidermal Tight Junctions. In: Dragicevic N, Maibach H, editors. Percutaneous Penetration Enhancers: Chemical Methods in Penetration Enhancement. NY: Springer; 2014. p. 69-90.
65. Naik A, Pechtold LARM, Potts RO, Guy RH. Mechanism of oleic acid-induced skin penetration enhancement in vivo in humans. Journal of Controlled Release. 1995;37(3):299-306.
66. Koyama Y, Bando H, Yamashita F, Takakura Y, Sezaki H, Hashida M. Comparative Analysis of Percutaneous Absorption Enhancement by d-Limonene and Oleic Acid Based on a Skin Diffusion Model. Pharm Res. 1994;11(3):377-83.
67. Rossetti FC, Lopes LB, Carollo AR, Thomazini JA, Tedesco AC, Bentley MV. A delivery system to avoid self-aggregation and to improve in vitro and in vivo skin delivery of a phthalocyanine derivative used in the photodynamic therapy. Journal of controlled release : official journal of the Controlled Release Society. 2011;155(3):400-8.
68. Wiechers JW, Kelly CL, Blease TG, Dederen JC. Formulation for efficacy. International Journal of Cosmetic Science. 2004;26:173-82.
69. Hirata K, Helal F, Hadgraft J, Lane ME. Formulation of carbenoxolone for delivery to the skin. Int J Pharm. 2013;448(2):360-5.
70. Liu J, Guo Y, Zhang J, Qi Y, Jia X, Gao G, et al. Systematic chemical analysis of flavonoids in the Nelumbinis stamen. Phytomedicine : international journal of phytotherapy and phytopharmacology. 2014;21(13):1753-8.
71. Alonso C, Marti M, Martinez V, Rubio L, Parra JL, Coderch L. Antioxidant cosmeto-textiles: skin assessment. European journal of

pharmaceutics and biopharmaceutics : official journal of Arbeitsgemeinschaft fur Pharmazeutische Verfahrenstechnik eV. 2013;84(1):192-9.
72. Rai V, Raghavan L. Transdermal Drug Delivery Systems Using Supersaturation. In: Dragicevic N, Maibach H, editors. Percutaneous Penetration Enhancers: Chemical Methods in Penetration Enhancement: Springer; 2015. p. 151-62.
73. Leveque N, Raghavan SL, Lane ME, Hadgraft J. Use of a molecular form technique for the penetration of supersaturated solutions of salicylic acid across silicone membranes and human skin in vitro. International Journal of Pharmaceutics. 2006;318(1):49-54.
74. Brooks G. Cosmetic Emulsions - Creams and Liquids. In: Schlossman M, editor. The Chemistry and Manufacture of Cosmetics: Allured Publishing; 2000.
75. Yutani R, Morita S-y, Teraoka R, Kitagawa S. Distribution of Polyphenols and a Surfactant Component in Skin during Aerosol OT Microemulsion-Enhanced Intradermal Delivery. Chemical and Pharmaceutical Bulletin. 2012;60(8):989-94.
76. Yutani R, Kikuchi T, Teraoka R, Kitagawa S. Efficient Delivery and Distribution in Skin of Chlorogenic Acid and Resveratrol Induced by Microemulsion Using Sucrose Laurate. Chemical and Pharmaceutical Bulletin. 2014;62(3):274-80.
77. Vicentini FTMC, Fonseca YM, Pitol DL, Iyomasa MM, Bentley MVLB, Fonseca MJV. Evaluation of Protective Effect of a Water-In-Oil Microemulsion Incorporating Quercetin Against UVB-Induced Damage in Hairless Mice Skin Journal of Pharmacy and Pharmaceutical Sciences. 2010; 13(2):274-85.
78. Kitagawa S, Yoshii K, Morita S-y, Teraoka R. Efficient Topical Delivery of Chlorogenic Acid by an Oil-in-Water Microemulsion to Protect Skin against UV-Induced Damage. Chemical and Pharmaceutical Bulletin. 2011;59(6):793-6.
79. Kitagawa S, Tanaka Y, Tanaka M, Endo K, Yoshii A. Enhanced skin delivery of quercetin by microemulsion. Journal of Pharmacy and Pharmacology. 2009;61(7):855-60.
80. Frelichowska J, Bolzinger M-A, Valour J-P, Mouaziz H, Pelletier J, Chevalier Y. Pickering w/o emulsions: Drug release and topical delivery. International Journal of Pharmaceutics. 2009;368(1):7-15.
81. Marto J, Ascenso A, Simoes S, Almeida AJ, Ribeiro HM. Pickering emulsions: challenges and opportunities in topical delivery. Expert Opinion on Drug Delivery. 2016:1-15.
82. Duffus LJ, Norton JE, Smith P, Norton IT, Spyropoulos F. A comparative study on the capacity of a range of food-grade particles to form stable O/W and W/O Pickering emulsions. Journal of Colloid and Interface Science. 2016;473:9-21.
83. Chevalier Y, Bolzinger M-A, Briancon S. Pickering Emulsions for Controlled Drug Release Delivery to the Skin. In: Dragicevic N, Maibach H, editors. Percutaneous Penetration Enhancers: Chemical Methods in Penetration Enhancement2015. p. 267-84.

84. Hu J-W, Yen M-W, Wang A-J, Chu IM. Effect of oil structure on cyclodextrin-based Pickering emulsions for bupivacaine topical application. Colloids and Surfaces B: Biointerfaces. 2018;161:51-8.
85. Luo Z, Murray BS, Ross A-L, Povey MJW, Morgan MRA, Day AJ. Effects of pH on the ability of flavonoids to act as Pickering emulsion stabilizers. Colloids and Surfaces B: Biointerfaces. 2012;92:84-90.
86. CTPA. Definition of a Cosmetic 2015 [cited 2015]. Available from: http://www.ctpa.org.uk/content.aspx?pageid=304.
87. MHRA. Definition of Boarderline Medicinal Product 2018. Available from: https://www.gov.uk/guidance/decide-if-your-product-is-a-medicine-or-a-medical-device.
88. Ghafourian T, Samaras EG, Brooks JD, Riviere JE. Modelling the Effect of Mixture Components on Permeation Through Skin. Int J Pharm. 2010;398(1-2):28-32.
89. Wiechers JW, Watkinson AC, Cross SE, Roberts MS. Predicting skin penetration of actives from complex cosmetic formulations: an evaluation of inter formulation and inter active effects during formulation optimization for transdermal delivery. Int J Cosmet Sci. 2012;34(6):525-35.
90. Shah JC, Kaka I, Tenjarla S, Lau SWJ, Chow D. Analysis of percutaneous permeation data: II. Evaluation of the lag time method. International Journal of Pharmaceutics. 1994;109(3):283-90.
91. Hadgraft J, Lane ME. Skin Permeation: The Years of Enlightenment. International Journal of Pharmaceutics. 2005;305:2-12.
92. Hadgraft JW, Somers GF. Percutaneous Absorption: A Review. Journal of Pharmacy and Pharmacology. 1956;8:625-34.
93. Lipinski C, Lombardo F, Dominy B, Feeney P. Experimental and Computational Approaches to Estimate Solubility and Permeability in Drug Discovery and Development Settings. Advanced Drug Delivery Reviews. 1997;23:3-25.
94. Leeson P. Drug Discovery: Chemical Beauty Contest. Nature. 2012;481:455-6.
95. Lin CF, Leu YL, Al-Suwayeh SA, Ku MC, Hwang TL, Fang JY. Anti-inflammatory activity and percutaneous absorption of quercetin and its polymethoxylated compound and glycosides: the relationships to chemical structures. European journal of pharmaceutical sciences : official journal of the European Federation for Pharmaceutical Sciences. 2012;47(5):857-64.
96. Abla MJ, Banga AK. Quantification of Skin Penetration of Antioxidants of varying Lipophilicity. International Journal of Cosmetic Science. 2013;35:19-26.
97. Rothwell JA, Day A, Morgan M. Experimental determination of octanol-water partition coefficients of quercetin and related flavonoids. Journal of Agricultural and Food Chemistry. 2005;53:4355-60.
98. Roleira FM, Siquet C, Orru E, Garrido EM, Garrido J, Milhazes N, et al. Lipophilic phenolic antioxidants: correlation between antioxidant profile, partition coefficients and redox properties. Bioorganic & medicinal chemistry. 2010;18(16):5816-25.
99. Pallicer JM, Pous-Torres S, Sales J, Roses M, Rafols C, Bosch E. Determination of the hydrophobicity of organic compounds measured as

logP(o/w) through a new chromatographic method. Journal of chromatography A. 2010;1217(18):3026-37.
100. Otberg N, Richter H, Schaefer H, Blume-Peytavi U, Sterry W, Lademann J. Variations of Hair Follicle Size and Distribution in Different Body Sites. Journal of Investigative Dermatology. 2004;122:14-9.
101. Lademann J, Meinke MC, Schanzer S, Richter H, Darvin ME, Haag SF, et al. *In vivo* Methods for the Analysis of the Penetration of Topically Applied Substances in and through the Skin Barrier. International Journal of Cosmetic Science. 2012;34:551-9.
102. Zhang Q, Saad P, Mao G, Walters R, Mack Correa M, Mendelsohn R, et al. Infrared Spectroscopic Imaging Tracks Lateral Distribution in Human Stratum Corneum. Pharm Res. 2014;31(10):2762-73.
103. PermaGear. PermaGear Inc Franz Diffusion Cells 2017. Available from: http://permegear.com/franz-cells/.
104. O.V. Zillich US-W, K. Hasenkopf, P. Eisner and M. Kerscher. Release and *in vitro* skin permeation of polyphenols from cosmetic emulsions. International Journal of Cosmetic Science. 2013;35:491-501.
105. Kong R, Bhargava R. Characterization of porcine skin as a model for human skin studies using infrared spectroscopic imaging. Analyst. 2011;136(11):2359-66.
106. Li N, Su Q, Tan F, Zhang J. Effect of 1,4-cyclohexanediol on percutaneous absorption and penetration of azelaic acid. Int J Pharm. 2010;387(1-2):167-71.
107. Tanji N, Okamoto M, Katayama Y, Hosokawa M, Takahata N, Sano Y. Investigation of the cosmetic ingredient distribution in the stratum corneum using NanoSIMS imaging. Applied Surface Science. 2008;255(4):1116-8.
108. Organisation_for_Economic_Co-operation_and_Development. Guidance Notes On Dermal Absorption: Series on Testing and Assessment No. 156. 2018.
109. OECD. OECD Environmental Health and Safety Publications: Guidance Document for the Conduct of Skin Absorption Studies No. 28. In: Publications OEHaS, editor. No. 28 ed. Paris, France2004.
110. Lian G, Chen L, Han L. An evaluation of mathematical models for predicting skin permeability. Journal of Pharmaceutical Sciences. 2008;97(1):584-98.
111. Mitragotri S, Anissimov YG, Bunge AL, Frasch HF, Guy RH, Hadgraft J, et al. Mathematical models of skin permeability: An overview. International Journal of Pharmaceutics. 2011;418(1):115-29.
112. Potts RO, Guy RH. Predicting Skin Permeability. Pharm Res. 1992;9(5):663-9.
113. Sinko P. Diffusion. In: Sinko PJ, editor. Martin's Physical Pharmacy and Pharmaceutical Sciences: Physical Chemical and Biopharmaceutical Principles in the Pharmaceutical Sciences. 6th ed: Lippincott Williams & Wilkins; 2011. p. 223-57.
114. Flynn GL, Stewart B. Percutaneous drug penetration: Choosing candidates for transdermal development. Drug Development Research. 1988;13(2-3):169-85.
115. Otto A, du Plessis J. The Effects of Emulsifiers and Emulsion Formulation Types on Dermal and Transdermal Drug Delivery. In: Dragicevic

N, Maibach H, editors. Percutaneous Penetration Enhancers: Chemical MEthods in Penetration Enhancement Drug Manipulation Strategies and Vehicle Effects: Springer; 2015. p. 223-42.
116. Courage&Khazaka. Tewameter TM 300 2018. Available from: https://www.courage-khazaka.de/en/16-wissenschaftliche-produkte/alle-produkte/172-tewameter-e.
117. Korsmeyer RW, Gurny R, Doelker E, Buri P, Peppas NA. Mechanisms of solute release from porous hydrophilic polymers. International Journal of Pharmaceutics. 1983;15(1):25-35.
118. de Sousa Neto D, Gooris G, Bouwstra J. Effect of the ω-acylceramides on the lipid organization of stratum corneum model membranes evaluated by X-ray diffraction and FTIR studies (Part I). Chemistry and Physics of Lipids. 2011;164(3):184-95.
119. Školová B, Janůšová B, Zbytovská J, Gooris G, Bouwstra J, Slepička P, et al. Ceramides in the Skin Lipid Membranes: Length Matters. Langmuir. 2013;29(50):15624-33.
120. Oguri M, Gooris GS, Bito K, Bouwstra JA. The effect of the chain length distribution of free fatty acids on the mixing properties of stratum corneum model membranes. Biochimica et Biophysica Acta (BBA) - Biomembranes. 2014;1838(7):1851-61.
121. Uchiyama M, Oguri M, Mojumdar EH, Gooris GS, Bouwstra JA. Free fatty acids chain length distribution affects the permeability of skin lipid model membranes. Biochimica et Biophysica Acta (BBA) - Biomembranes. 2016;1858(9):2050-9.
122. Cross SE, Roberts MS, Jiang R, Benson HAE. Can Increasing the Viscosity of Formulations be used to Reduce the Human Skin Penetration of the Sunscreen Oxybenzone? Journal of Investigative Dermatology. 2001;117(1):147-50.
123. Selzer D, Abdel-Mottaleb MMA, Hahn T, Schaefer UF, Neumann D. Finite and infinite dosing: Difficulties in measurements, evaluations and predictions. Advanced Drug Delivery Reviews. 2013;65(2):278-94.
124. Jacobi U, Kaiser M, Toll R, Mangelsdorf S, Audring H, Otberg N, et al. Porcine ear skin: an in vitro model for human skin. Skin Research and Technology. 2007;13(1):19-24.
125. Abd E, Yousef SA, Pastore MN, Telaprolu K, Mohammed YH, Namjoshi S, et al. Skin models for the testing of transdermal drugs. Clinical Pharmacology : Advances and Applications. 2016;8:163-76.
126. Papadopoulou A, Green RJ, Frazier RA. Interaction of Flavonoids with Bovine Serum Albumin: A Fluorescence Quenching Study. Journal of agricultural and food chemistry. 2005;53(1):158-63.
127. Dyja R, Jankowski A. The effect of additives on release and in vitro skin retention of flavonoids from emulsion and gel semisolid formulations. International Journal of Cosmetic Science. 2017;39(4):442-9.
128. Dickinson E. Food emulsions and foams: Stabilization by particles. Current Opinion in Colloid & Interface Science. 2010;15(1):40-9.
129. Larkin P. Chapter 1 - Introduction: Infrared and Raman Spectroscopy. In: Larkin P, editor. Infrared and Raman Spectroscopy. Oxford: Elsevier; 2011. p. 1-5.

130. Gray GM, Yardely H. Lipid compositions of cells isolated from pig, human, and rat epidermis. Journal of Lipid Research. 1975;16(6):434-40.
131. Gray GM, White RJ, Williams RH, Yardleymrc HJ. Lipid composition of the superficial stratum corneum cells of pig epidermis. British Journal of Dermatology. 1982;106(1):59-63.
132. Caussin J, Gooris GS, Janssens M, Bouwstra JA. Lipid organization in human and porcine stratum corneum differs widely, while lipid mixtures with porcine ceramides model human stratum corneum lipid organization very closely. Biochimica et Biophysica Acta (BBA) - Biomembranes. 2008;1778(6):1472-82.
133. Shintani M, Ogiso T. Mechanism for the Enhancement Effect of Fatty Acids on the Percutaneous Absorption of Propranolol. Journal of Pharmaceutical Sciences. 1990;79(12):1065-71.
134. Tanojo H, Bouwstra JA, Junginger H, Boddé H. In Vitro Human Skin Barrier Modulation by Fatty Acids: Skin Permeation and Thermal Analysis Studies. Pharm Res. 1997;14(1):42-9.
135. Aungst BJ. Structure/Effect Studies of Fatty Acid Isomers as Skin Penetration Enhancers and Skin Irritants. Pharm Res. 1989;6(3):244-7.
136. Intarakumhaeng R, Shi Z, Wanasathop A, Stella QC, Wei KS, Styczynski PB, et al. In vitro skin penetration of petrolatum and soybean oil and effects of glyceryl monooleate. International Journal of Cosmetic Science. 2018;40(4):367-76.
137. Patzelt A, Lademann J, Richter H, Darvin ME, Schanzer S, Thiede G, et al. In vivo investigations on the penetration of various oils and their influence on the skin barrier. Skin Research and Technology. 2012;18(3):364-9.
138. Petry T, Bury D, Fautz R, Hauser M, Huber B, Markowetz A, et al. Review of data on the dermal penetration of mineral oils and waxes used in cosmetic applications. Toxicology Letters. 2017;280:70-8.
139. Choe C, Lademann J, Darvin ME. Analysis of Human and Porcine Skin in vivo/ex vivo for Penetration of Selected Oils by Confocal Raman Microscopy. Skin Pharmacology and Physiology. 2015;28(6):318-30.
140. Choe C, Lademann J, Darvin ME. A depth-dependent profile of the lipid conformation and lateral packing order of the stratum corneum in vivo measured using Raman microscopy. Analyst. 2016;141(6):1981-7.
141. Stamatas GN, de Sterke J, Hauser M, von Stetten O, van der Pol A. Lipid uptake and skin occlusion following topical application of oils on adult and infant skin. Journal of Dermatological Science. 2008;50(2):135-42.
142. Fleischli FD, Mathes S, Adlhart C. Label free non-invasive imaging of topically applied actives in reconstructed human epidermis by confocal Raman spectroscopy. Vibrational Spectroscopy. 2013;68(0):29-33.
143. Fleischli FD, Morf F, Adlhart C. Skin Concentrations of Topically Applied Substances in Reconstructed Human Epidermis (RHE) Compared with Human Skin Using in vivo Confocal Raman Microscopy. CHIMIA International Journal for Chemistry. 2015;69(3):147-51.
144. Arora A, Byrem TM, Nair MG, Strasburg GM. Modulation of Liposomal Membrane Fluidity by Flavonoids and Isoflavonoids. Archives of Biochemistry and Biophysics. 2000;373(1):102-9.

145. Sanver D, Murray BS, Sadeghpour A, Rappolt M, Nelson AL. Experimental Modeling of Flavonoid–Biomembrane Interactions. Langmuir. 2016;32(49):13234-43.
146. Movileanu L, Neagoe I, Flonta ML. Interaction of the antioxidant flavonoid quercetin with planar lipid bilayers. International Journal of Pharmaceutics. 2000;205(1):135-46.
147. Higuchi T. Rate of release of medicaments from ointment bases containing drugs in suspension. Journal of Pharmaceutical Sciences. 1961;50(10):874-5.
148. Paul DR. Elaborations on the Higuchi model for drug delivery. International Journal of Pharmaceutics. 2011;418(1):13-7.
149. Dash S, Murthy P, Nath L, Chowdry P. Kinetic Modeling On Drug Release From Controlled Drug Delivery Systems. Acta Poloniae Pharmaceutica - Drug Research. 2010;67(3):217-23.
150. Luo Z, Murray BS, Ross AL, Povey MJ, Morgan MR, Day AJ. Effects of pH on the ability of flavonoids to act as Pickering emulsion stabilizers. Colloids and surfaces B, Biointerfaces. 2012;92:84-90.
151. Pignatello JJ, Xing B. Mechanisms of Slow Sorption of Organic Chemicals to Natural Particles. Environmental Science & Technology. 1996;30(1):1-11.
152. EuropeanComission. THE SCCS NOTES OF GUIDANCE FOR THE TESTING OF COSMETIC INGREDIENTS AND THEIR SAFETY EVALUATION. 2015.
153. Zhang G, Flach CR, Mendelsohn R. Tracking the dephosphorylation of resveratrol triphosphate in skin by confocal Raman microscopy. Journal of Controlled Release. 2007;123(2):141-7.
154. Zhang G, Moore DJ, Sloan KB, Flach CR, Mendelsohn R. Imaging the Prodrug-to-Drug Transformation of a 5-Fluorouracil Derivative in Skin by Confocal Raman Microscopy. J Invest Dermatol. 2007;127(5):1205-9.
155. Mantsch H. Historical Survey of Infrared and Raman Spectroscopy of Biological Materials. In: Gremlich H-U, Yan B, editors. Infrared and Raman Spectroscopy of Biological Materials Practical Spectroscopy. New York, USA: Marcel Dekker, Inc; 2001. p. 1-14.
156. Caspers P, Lucassen G, Puppels G. Combinded *in vivo* Confocal Raman Spectroscopy and Confocal Microscopy of Human Skin. Biophysical Journal. 2003;85:572-80.
157. Franzen L, Selzer D, Fluhr JW, Schaefer UF, Windbergs M. Towards drug quantification in human skin with confocal Raman microscopy. European Journal of Pharmaceutics and Biopharmaceutics. 2013;84(2):437-44.
158. Tfaili S, Josse G, Angiboust J-F, Manfait M, Piot O. Monitoring caffeine and resveratrol cutaneous permeation by confocal Raman microspectroscopy. Journal of Biophotonics. 2014;7(9):676-81.
159. Darvin ME, Sterry W, Lademann J. Resonance Raman spectroscopy as an effective tool for the determination of antioxidative stability of cosmetic formulations. Journal of Biophotonics. 2010;3(1-2):82-8.